



**Universitat de les
Illes Balears**

**DOCTORAL THESIS
2015**

**MEDICANES: METEOROLOGICAL
ENVIRONMENTS AND RISK ASSESSMENT IN
THE PRESENT AND FUTURE CLIMATE**

Maria Tous Nadal



**Universitat de les
Illes Balears**

**DOCTORAL THESIS
2015**

Doctoral Programme of Physics

**MEDICANES: METEOROLOGICAL
ENVIRONMENTS AND RISK ASSESSMENT IN
THE PRESENT AND FUTURE CLIMATE**

Maria Tous Nadal

Thesis Supervisor: Prof. Romualdo Romero

Doctor by the Universitat de les Illes Balears

*Whether the weather be fine,
Or whether the weather be not,
Whether the weather be cold,
Or whether the weather be hot,
We'll weather the weather
Whatever the weather,
Whether we like it or not!*

"Weather", unknown author

Agraïments

Voldria expressar els meus sincers agraïments a totes aquelles persones que, d'una o altra manera, han fet possible la realització d'aquesta tesi.

En primer lloc i de manera molt especial, al Prof. Romualdo Romero, director d'aquesta tesi, per haver-me donat l'oportunitat d'endinsar-me en l'increïble i fascinant món de la meteorologia. Va començar ja fa un bon grapat d'anys essent el meu tutor de diverses beques de col·laboració i del treball acadèmicament dirigit, i després, del màster i del doctorat. A més de ser un molt bon cap que m'ha sabut guiar i ajudar, també m'ha recolzat i donat ànims en els moments necessaris, mostrant la seva gran qualitat humana. Per tots aquests anys, moltes gràcies Romu!

Aquest agraïment el voldria estendre a altres membres del Grup de Meteorologia amb qui sempre he pogut comptar, tant a nivell investigador com a nivell personal. En especial, m'agradaria fer referència al Prof. Climent Ramis i al Dr. Víctor Homar, sense l'ajuda dels quals, al llarg de moltes hores d'enriquidors comentaris i suport tècnic i moral, tota la feina d'aquests anys no hauria estat possible. Al Prof. Sergio Alonso, la confiança que ha dipositat en mi i les seves paraules d'ànim que sempre m'ha donat, com també ha fet el Dr. Joan Cuxart. Per suposat, agrair als "becaris" (que a dia d'avui ja han progressat en les seves respectives carreres) i administradors del sistema, per la seva gran ajuda tant en els moments d'inicialització com durant tota la trajectòria, i per les bones estones no laborals que hem passat plegats.

També als companys de despatx, amb els quals el tracte diari ha estat molt senzill, creant un molt bon ambient de treball i de companyonia, compartint riures, dubtes i moments d'estrès i, en general, creant una bona pinya que ha traspassat les parets de la universitat. I a tots aquells amics, de la facultat i de la universitat, que he anat fent durant aquests anys. Dins aquest grup d'amics voldria remarcar el grup de molt bons d'amics que he fet en el grup de Física Aplicada (o Materials, com els acostum a anomenar), sempre disposats a ajudar-me, donar-me ànims i suport, i que durant el pas dels anys s'ha anat reforçant i incrementant. Sou genials!

Gràcies també a les amistats de “large time scale”. No sé si puc dir que tenc molts o pocs amics en la vida, però el que sí sé és que són molt bons amics. A tots voltros, gràcies per ser com sou. De les amistats que vaig fer durant la carrera voldria destacar na Marga, que tot i que cada una està seguint el seu camí en la vida, mantenim aquell vincle d’amistat que esper segueixi existint per molts i molts d’anys. I a tu, Marina, amiga meva... Què més et puc dir? T’he repetit anys i anys lo agraïda que t’estic per permetre’m ser la teva amiga, ja des de ben petites. És que fas tan fàcil ser amiga teva! Moltes gràcies per ser-hi SEMPRE.

I would like to thank Prof. Kerry A. Emanuel for allowing me to visit and learn from his work team at MIT, and Prof. Pier Luigi Vidale and Dr. Len C. Shaffrey at University of Reading. From this last university, I am also grateful to Dr. Giuseppe Zappa for his help and patience, and all the PhD students who welcomed me, with a special mention to Roberto and Mike.

Agraïments també per a la família Riutort: al pare, en Miquel, per haver-me fet estimar la física i alimentar el cuquet de la curiositat científica, i a la seva filla Guida, física, membre del Grup de Meteorologia, companya i amiga.

A la gent de l’AEMET, també moltes gràcies, en especial a n’Ana Genovés, Joan Campins, Maria Àngels Picornell i José Antonio Guijarro. I molt especialment, al Dr. Agustí Jansà, qui sempre m’ha ajudat a entendre millor els fenòmens meteorològics, amb paciència i un somriure a la cara, tant quan ell estava fent feina allà com ara que està més aprop, compartint el mateix despatx a la universitat.

Francesc, moltes gràcies. Has estat i segueixes essent més que un amic. M’has vist riure i m’has vist plorar, i hem compartit molts moments de tota mena. Moltes gràcies per seguir estant al meu costat.

Pel final m’he guardat els qui tenc més prop de tot en el cor: la meva família. A alguns de vosaltres ja no vos tenc aquí prop per poder celebrar aquesta tesi amb una abraçada i mirades i somriures de complicitat, però sapiguen que vos tenc molt, però que molt molt presents en els meus pensaments. Vau veure com la començava però no l’heu pogut veure acabar. Em sap greu. Mon pare, padrí Joan “de Murillo” i padrines Maria (“de Murillo” i “de Sa Cabaneta”): una abraçada i una besada ben forta allà on sigueu. Ma mare, Joan, padrí Pep i família en general: gràcies de veritat. Gràcies per la paciència que heu tingut i haver-me animat sempre a seguir endavant, donant-me suport a totes les decisions que he anat prenent durant la meva vida i fent-me sentir que sí podia fer-ho, fins i tot en els projectes més ambiciosos.

Gràcies a tots per haver-me donat sempre ànims. Gràcies, moltes gràcies de tot cor.

Preface: What is all this about?

Meteorology influences our life. That is obvious. When the sun shines, people seem happy, go outside for a walk, play in parks or they want just lay and relax close to the sea. When it rains, children use their wellies and splash. When it is windy, sailors go out to the sea and feel their freedom in the middle of nowhere...

There is a proverb in Catalan, my native language, which says “totes les masses fan mal”. It means that when you have a lot of something, even if it is good “a priori”, it could become bad, dangerous and not as funny as you expected. That is what severe weather is in this context. Depending on the area you consider, severe weather could be defined as heavy precipitations, strong winds, droughts, etc.

Due to (or thanks to) new technologies, the world is better connected nowadays. In fact, sometimes you know more about what happens in other countries than in the street next to yours. News usually show political events and catastrophes and, sometimes, good moments and big parties from around the world. A century ago, when people did not travel as much as today, Mediterranean people had never heard about hurricanes. In some books there were references about great storms over the tropical oceans, but that was all. Few years later, when the meteorological research improved, some particularities on storms were discovered and they became cataloged as tropical cyclones, calling hurricanes to the most intense ones. Well, I have named these maritime storms tropical cyclones, but they have different names depending on the area where they occur, like “typhoons” in the west of the Indian Ocean, “Willy-Willy” in Australia or “Baguio” in Philippine.

All of them seem to occur far from here, though, as the area around the Mediterranean Sea is often advertised as perfect for its calming and relaxing weather. Mediterranean climate is mainly characterized by hot dry summers and wet cool winters, but has also very

interesting weather phenomena as torrential downpours or episodes of high wind. But, wait a minute! Not far in the past, it was possible to identify some kinds of Mediterranean cyclones that, to some point, possess certain tropical cyclone features. Does it mean “tropical” cyclones can also develop over the Mediterranean Sea? Even they are not very frequent and do not exhibit the degree of severity as common tropical cyclones, yes, they are possible. For this reason, the first goal of this thesis is to check how many tropical-like cyclones we have, how they look like and how the meteorological conditions affect their development and characteristics.

In addition, recently, interest and concern about how human-induced climate change would affect extreme events are increasing. Ten years ago, in 2005, hurricane Katrina made landfall in southern United States and it became the deadliest US hurricane since 1928. In 2012, hurricane Sandy threatened New York citizens. They thought they were in too high latitudes to host a tropical cyclone, so their warning systems were not well-suited. As the cyclone was approaching, the chaos took place. Why such an intense tropical cyclone could reach these high latitudes? How often will this happen? Does it mean tropical cyclones can develop in areas were they did not use to? In this context, we are also curious about how Mediterranean tropical-like cyclones will be affected in future climate scenarios, so this thesis pursues to evaluate the magnitude of the expected changes in intensity, frequency and location of these storms.

Summary

Medicanes are a rare and physically unique type of Mediterranean cyclone. They show similarities with tropical cyclones with regard to their development (based on the thermodynamical disequilibrium between the warm sea and the overlying troposphere) and the kinematic and thermodynamical properties (medicanes are intense vortices with a warm core and even a cloud-free-eye). Although medicanes are smaller and the characteristic wind speeds are lower, the severity of the winds can cause substantial damage on islands and coastal areas.

The special characteristics of medicanes make their detection difficult: only with high resolution meteorological analyses and dense maritime observations that task would be possible. For this reason, an alternative method using satellite images and restricted criteria about the disturbance symmetry, size and lifespan, has been applied leading to the detection of 12 medicanes from 1982 to 2003.

To improve the medicane forecast capability or even to assess the potential risk of these storms in future climates, it is necessary to characterize the special conditions of the synoptic-scale meteorological environments that are needed for their development and maintenance. By comparing these environments against the bulk of intense Mediterranean cyclonic situations, high values of mid-tropospheric relative humidity, significant diabatic contribution to the surface level equivalent potential temperature tendency, and low values of tropospheric wind shear, are revealed as important parameters involved in medicane genesis, as in tropical cyclones. An empirical genesis index previously derived for the tropical regions is also tested in this thesis, and it is revealed as a possible discriminative parameter of the precursor environments.

Despite their small size, mesoscale runs of medicane situations at moderate horizontal resolutions (7.5 km) made with MM5 are able to simulate the formation of a subsynoptic cyclone and the general trajectory of the disturbance, and for most of the cases a warm-core axi-symmetrical structure becomes evident in the simulations. In addition, a sensitivity analysis examining the role of the sea surface heat fluxes is conducted: latent and sensible heat fluxes from the Mediterranean are switched off during the simulations

to explore the effects of these factors on the medicane trajectories and deepening rate. Results show different roles of the surface heat fluxes on medicane properties (intensification and track) depending on their magnitude and spatial distribution over the Mediterranean Sea. In this way, three distinct evolution patterns have been identified using the database of twelve events.

In the context of the growing concern about how climate change will affect the number and intensity of hurricanes, two different analysis for medicanes have been conducted in this thesis: an oriented dynamical downscaling and a direct detection of storms in a high-resolution global climate model. On one hand, the oriented dynamical downscaling consists in projecting the previous empirical genesis index into four different global climate models, with spatial resolutions about 200 km, and analyze (simulate) just the areas with elevated medicane risk values. On the other hand, an independent study using a direct detection and tracking of warm-core cyclones is applied to a high resolution global climate model (spatial resolution about 25 km). Both methods predict a decreasing trend in medicane occurrence, and indicate the south-east of Italy and the Gulf of Lion as the areas with higher probability of medicane development in future scenarios. With regard to future changes in medicane intensity, there seems to be signs of an enhanced risk of violent storms.

Resum

Els medicanes són un tipus de cicló poc freqüent, i amb certes particularitats, que es dona al Mediterrani. Els medicanes tenen similituds amb els ciclons tropicals referents al seu desenvolupament (basat en el desequilibri termodinàmic entre mar-atmosfera) i les propietats cinemàtiques i termodinàmiques (els medicanes són vòrtexs intensos amb nucli càlid i, algunes vegades, fins i tot poden tenir un ull lliure de núvols). Malgrat els medicanes són més petits i els seus vents associats són més febles que als ciclons tropicals, la força dels seus vents poden causar importants danys a illes i zones costeres.

Les característiques especials dels medicanes fan que la seva detecció sia difícil: sols disposant de dades d'anàlisi meteorològiques a molta alta resolució i una xarxa densa d'observacions marítimes, aquesta tasca es podria dur a terme. Per aquest motiu, en aquesta tesi s'ha utilitzat un mètode alternatiu utilitzant imatges de satèl·lit i aplicant criteris restrictius basats en la simetria de la pertorbació, la mida i la durada. D'aquesta manera s'han detectat 12 medicanes durant el període comprès des de 1982 a 2003.

Una bona caracterització dels ambients meteorològics precursors dels medicanes ens pot ajudar a entendre els mecanismes de gènesi i millorar les prediccions. En aquesta tesi es comparen els valors de diverses variables meteorològiques d'interès en els medicanes amb els ambients d'altres ciclons intensos sobre la Mediterrània. En aquest sentit, valors elevats de la humitat relativa a nivells mitjos, la contribució diabàtica a la tendència local de temperatura potencial equivalent superficial, i valors baixos de la cisalla de vent entre nivells baixos i alts, pareixen paràmetres importants relacionats amb la gènesi dels medicanes, com també ho són dels ciclons tropicals. Un índex empíric de gènesi, provinent d'estudis sobre les regions tropicals, també ha estat avaluat en aquesta tesi i es presenta com un possible paràmetre discriminant dels ambients precursors.

Malgrat la mida petita dels medicanes, s'ha comprovat que simulacions amb l'MM5 amb resolucions espacials de 7.5 km poden representar la formació de ciclons subsinòptics i les seves trajectòries, i per a la majoria dels casos també l'estructura simètrica amb nucli càlid. A més, s'ha realitzat una anàlisi de sensibilitat examinant el paper dels fluxos de calor en la superfície de la mar: s'han desactivat l'intercanvi de calor latent i sensible

sobre la Mediterrània durant les simulacions per estudiar els efectes d'aquests factors sobre les trajectòries i la intensificació dels medicanes. Els resultats mostren tres patrons de comportament diferents sobre aquestes propietats dels medicanes identificats prèviament, depenent de la magnitud i la distribució espacial dels fluxos.

En relació a la creixent preocupació sobre com afectarà el canvi climàtic a la freqüència i intensitat dels huracans, s'han realitzat dues anàlisis independents referent als medicanes: regionalitzacions dinàmiques de manera dirigida, i detecció directa sobre un model climàtic global a alta resolució. Per una part, les regionalitzacions dinàmiques consisteixen en determinar les zones d'alt risc mitjançant l'índex empíric descrit anteriorment i simular sols aquests ambients amb un model de mesoscala (aquest es força amb quatre models climàtics globals de resolucions espacials de l'ordre de 200 km). Per altra part, la detecció directa es realitza sobre un model climàtic global a una resolució aproximada de 25 km. En ambdós casos, els resultats mostren una reducció en la freqüència dels medicanes i assenyalen el sud-est d'Itàlia i el golf de Lleó com les zones amb major probabilitat de desenvolupament de medicanes en escenaris de clima futur. Referent als canvis d'intensitat en el futur, pareix que hi ha indicis d'augment del risc de tempestes violentes.

Publication list of the Author related with the Thesis

Tous, M., G. Zappa, R. Romero, L. Shaffrey, P.-L. Vidale, 2015, Projected changes in medicanes in the HadGEM3 N512 high-resolution global climate model. *Clim. Dyn.* (Conditionally accepted).

Ramis, C., M. Tous, V. Homar, R. Romero and S. Alonso. Medicanes: quasi-tropical mesoscale cyclones in the Mediterranean. 2013. C. García-Legaz and F. Valero (Eds.). *Adverse Weather in Spain*. 44-50. ISBN: 978-84-96709-43-0

Tous, M., R. Romero and C. Ramis. 2013. Surface heat fluxes influence on medicane trajectories and intensification. *Atmos. Res.* 123: 400-411. DOI: 10.1016/j.atmosres.2012.05.022

Tous, M., and R. Romero. 2013. Meteorological environments associated with medicane development. *Int. J. Climatol.* 33: 1-14. DOI: 10.1002/joc.3428

Tous, M., and R. Romero. 2011. Medicanes: cataloging criteria and exploration of meteorological environments. *Tethys.* 8: 55-63. DOI:10.3369/tethys.2011.8.06

Contents

Preface: What is all this about?	ii
Summary (English)	iii
Resum (Català)	v
Publication list of the Author related with the Thesis	vii
I MEDICANES: THE SUBJECT OF THIS THESIS	1
1 Introduction	3
1.1 Previous medicanes	4
1.2 Other medicane studies	8
1.3 Background on tropical cyclones	9
1.4 Tropical cyclones and climate change	14
1.5 Objectives and outline of the thesis	16
2 Creating a database of events	17
2.1 Introduction	17
2.2 Use of Meteosat	19
2.3 Criteria establishment	21
2.4 Medicane spatial and temporal distributions	25

II EXPLORING THE METEOROLOGICAL ENVIRONMENTS	29
3 Meteorological environments characterization	31
3.1 Introduction	31
3.2 Selected parameters	33
3.3 M06 parameter sequence	36
3.4 Comparison against MEDEX intense cyclones	39
3.5 Conclusions	43
4 Sensitivity to surface heat fluxes	45
4.1 Introduction	45
4.2 Capability of the MM5 model to simulate medicane events	48
4.3 Surface heat fluxes influence	53
4.3.1 Surface heat fluxes influence on medicane trajectories	53
4.3.2 Surface heat fluxes influence on medicane intensification	55
4.3.3 Interpretation in terms of precipitable water and SurFlux distributions	57
4.4 Conclusions	61
III ASSESSING MEDICANE RISK UNDER CLIMATE CHANGE	63
5 Oriented dynamical downscaling	65
5.1 Introduction	65
5.2 First climatological analyses	66
5.3 Capability of the MM5 model to simulate medicanes using low resolution inputs	71
5.4 Guiding the downscaling	75
5.5 Results for the present and future climate	81
5.6 Conclusions	83

6	High-resolution global climate model	85
6.1	Data and methodology	85
6.1.1	The HadGEM3 climate model	85
6.1.2	Cyclone tracking algorithm	87
6.2	Climatology of mesocyclones in the Mediterranean	88
6.3	Medicane assessment: present climate	90
6.4	Medicane assessment: future climate	95
6.5	Conclusions	98
IV	CONCLUSIONS AND FURTHER WORK	101
7	Conclusions	103
8	Further work	107
	APPENDIX	111
A:	Synthetic generation of medicanes	113
	Nomenclature	119
	Bibliography	125

Part I

MEDICANES: THE SUBJECT OF THIS THESIS

Chapter 1

Introduction

Medicane is an acronym of Mediterranean hurricane. Although it is not well known who/when/where was the term adopted for the first time, it became of occasional use during the first lustrum of this century. Since that time on, this word has slowly gained ground in research studies.

Medicane term is not referring to a real hurricane over the Mediterranean area, but to a type of cyclone that, when it is fully developed, has similar features to tropical cyclones (TC). Owing to the large geographical differences between the Mediterranean Sea and the tropical oceans, medicanes are smaller and weaker than TC, but they also put in danger the islands and coastal regions.

The Mediterranean basin is recognized as one of the main cyclogenetic areas in the world (Pettersen, 1956; Hoskins and Hodges, 2002; Wernli and Schwierz, 2006), and much of the high impact weather affecting the Mediterranean countries (notably strong winds and heavy precipitations) have been statistically associated with the near presence of a distinct cyclonic signature (e.g. Jansà et al., 2001). Cyclones can range from synoptic to mesoscale in size, and from pure baroclinic systems to orographically or diabatically modulated disturbances in type. Their peak occurrences and notorious consequences have been clearly linked to the presence of prominent orographic systems surrounding the Mediterranean Sea (Reiter, 1975; Buzzi and Tibaldi, 1978; Speranza et al., 1985; Genovés and Jansà, 1991; Martín et al., 2007). Most of these kind of cyclones are well understood, typically being lee baroclinic disturbances. The spatial distribution of these cyclones is

not uniform and there are two preferred regions for cyclogenesis: Cyprus area and the gulf of Genoa (Alpert et al., 1990; Campins et al., 2011). In spite of the high frequency of cyclones over the Mediterranean Sea and the large number of studies devoted to them, small cyclones as medicanes are generally not well represented and detected by usual methodologies.

Medicanes develop over the sea. This fact complicates the task of acquiring observed data during its development. The density of buoys over the Mediterranean Sea is very coarse and ships avoid to cross these storms for safety reasons. Satellite images and re-analysis data are the only available material to study these events, but they tend to fall within the spatial and temporal gaps of the observing network. In addition to this, the few number of medicanes per year makes its analysis difficult, specially from a statistical point of view.

Nevertheless, due to their parallelism, we can lean on TC studies to guide our medicane understanding. It is well known medicane genesis process starts with a cold air intrusion in altitude which overlaps with a relatively warm ocean on the bottom. This contrast makes the ideal scenario for the environment working like a Carnot engine, similarly to the proposed theory to explain how TC are sustained by surface heat fluxes.

1.1 Previous medicanes

From 1960's, when some satellite images became available, it has been possible to identify vortices in the Mediterranean basin with similar characteristics to TC. Warning signs of these possible events were usually based on registers of abrupt pressure drops and high values of wind speed.

Ernest and Matson (1983) studied a cyclone dated on January 26th, 1982 (Fig. 1.1.1). It was the first Mediterranean tropical storm detected over the Mediterranean Sea, close to Libya's waters. The cyclone reached its peak intensity at 1800 UTC maintaining an atmospheric pressure of 992 mbar and was succeeded by a period of gradual weakening, with the system pressure eventually rising to 1009 mbar. The cyclone slightly reintensified, however, for a six-hour period. Ship reports indicated winds of 93 km/h were present, i.e. tropical storm-force winds on the Saffir-Simpson hurricane wind scale (Table 1.1), likely near the eye-wall of the cyclone, which features the highest winds in a tropical cyclone.

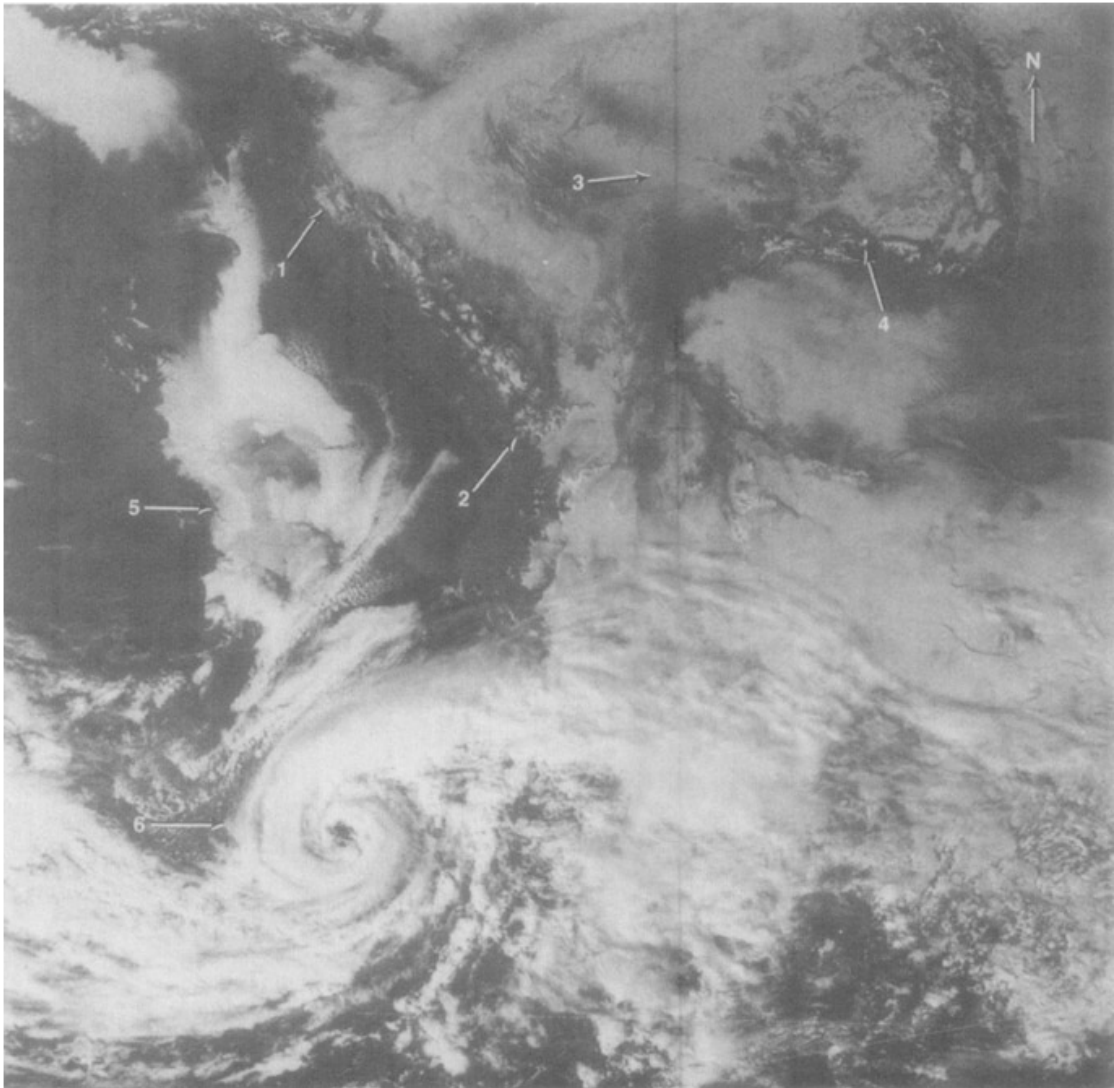


Figure 1.1.1: NOAA-7 visible band satellite image of the eastern Mediterranean Sea area taken on 26 January 1982 at 1236 GMT. Resolution is 1.1 km. Ernest and Matson (1983)

Its acquired tropical cyclone characteristics made the authors to entitle their article “A Mediterranean Tropical Storm?”. Just a bit later, Businger and Reed (1989), whose study was centered in polar lows, accepted some violent cyclonic windstorms over the Mediterranean Sea, with some tropical cyclone characteristics, as a subclass of polar lows. These sub-synoptic warm-core vortices are very notorious for inducing sudden changes in pressure and wind over the affected areas, although the winds do not normally attain hurricane intensity.

Thereafter, physical and structural parallelism between TC and this kind of cyclones over the Mediterranean Sea have been accepted. More examples are Pytharoulis et al. (1999) presenting a “Study of the Hurricane-Like Mediterranean Cyclone of January 1995” and Homar et al. (2003), studying another remarkable medicane occurred in September 1996. In the first one, a numerical simulation using the mesoscale version of the Unified model in a special run over central and eastern Mediterranean reproduced many of the observed features of the cyclone successfully. The hypothesis that the system was hurricane-like was supported by the presence of a warm core structure and the influence of strong surface fluxes of heat and moisture on its development. In the second one, the role of the convective activity in that cyclone genesis was also proved in contrast to baroclinic development using a factor-separation technique.

In November 2011, the National Oceanic and Atmospheric Administration (NOAA) designates officially the first Mediterranean tropical cyclone (Fig. 1.1.2). This event was called with two different names: “01M” by the NOAA Satellite Analysis Branch and “Rolf” by the Free University of Berlin (FU Berlin). On November 7 at 12 UTC, NOAA services warned against a tropical disturbance over the Mediterranean Sea. After that, the disturbance transformed and strengthened into a tropical depression off the Gulf of Lion and upgraded to tropical storm status. At peak intensity, the storm was situated close to the coast of France. It had a minimum low pressure of 991 Pa and estimated wind speeds reaching 45 knots according to various satellite analysis techniques. It caused economical damages and two fatalities.

At the time of writing this thesis, the last cyclone considered as a medicane by EUMETSAT occurred on November 7, 2014. This storm first hit Lampedusa on the island of Linosa, then Malta and finally the eastern coast of Sicily before it disappeared to the east. Gusts of 135 km/h were recorded at Lampedusa and up to 154 km/h in Malta.

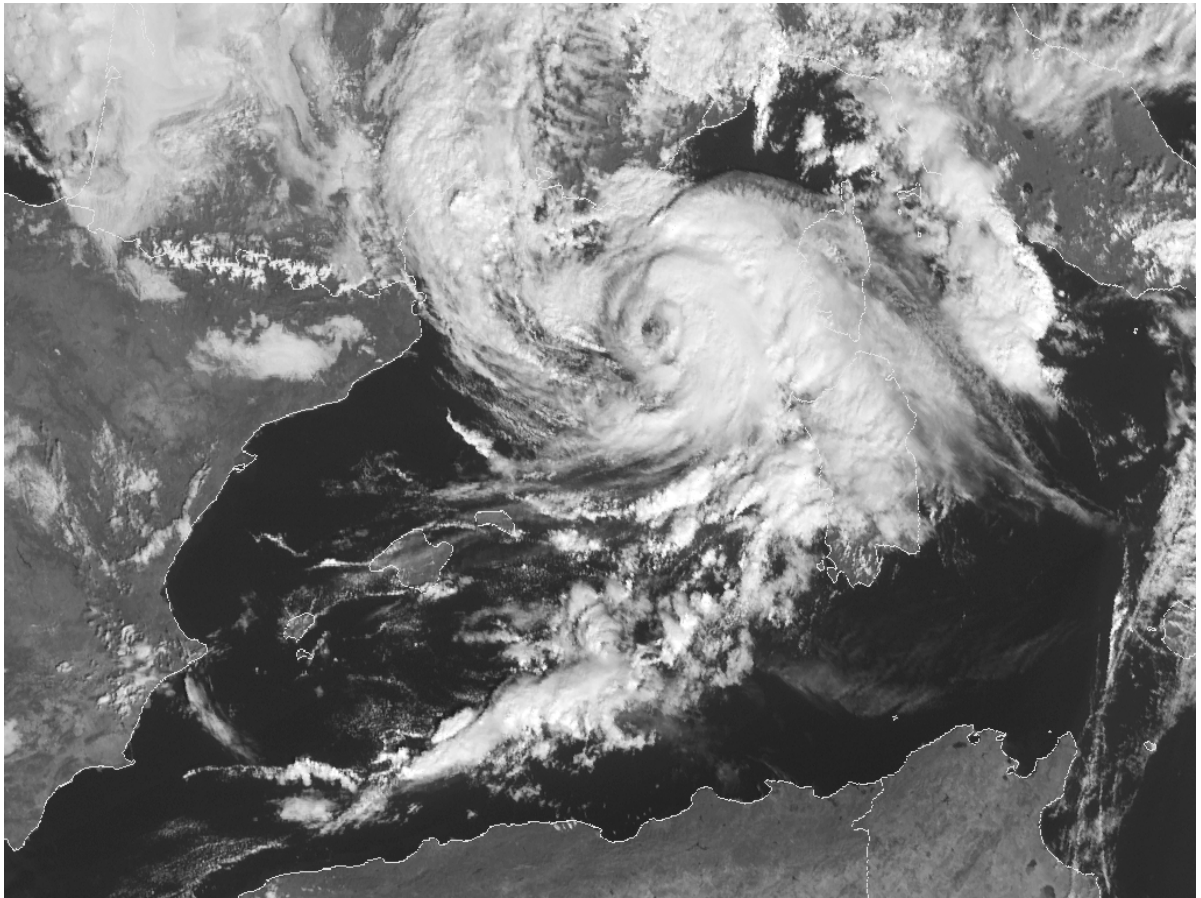


Figure 1.1.2: Meteosat-8 HRV image (Rapid Scans) on November 8th, 2011.

In order to study general meteorological patterns behind medicane development and maintenance, it would be necessary to collect all existing cases and create a database of events. Fita et al. (2007) analyzed seven medicane environments exhibiting different intensities and behaviors. A larger list of possible events is available at <http://meteo.uib.es/medicanes>. To build this list of events it was not applied a clear discriminative criteria. Actually, medicane detection and classification is not well databased because there is not any official agency responsible for monitoring “tropical” cyclone activity over the Mediterranean. Objective and subjective thresholds for the classification are not clear and there has been much debate about if some cyclones should be labeled as medicanes or not.

1.2 Other medicane studies

Leaving aside particular event studies, there has been an increase of efforts to investigate different aspects of medicanes. On one hand, there is interest to evaluate the particularities of the environments able to generate medicanes in spite the Mediterranean Sea is not prone to these extreme phenomena. For example, in Fita et al. (2007), an axisymmetric numerical model was used to analyze the characteristics and behavior of tropical-like Mediterranean storms, and Romero and Emanuel (2006) introduced an empirical genesis index, also used for tropical cyclone studies, to evaluate the areas with higher probability of medicane genesis. On the other hand, it is useful to define objective criteria in order to discriminate medicanes from other Mediterranean cyclones. Cavicchia et al. (2014a) and Picornell et al. (2014) use adaptations of the Hart’s cyclone phase diagram (Hart, 2003) to examine medicane thermal structure and impose different conditions for their effective detection. In Cavicchia et al. (2014a), a downscaling methodology applied to six decades of NCEP/NCAR reanalyses data-set is explored, exploiting the added value of high-resolution atmospheric fields and a detection algorithm designed specifically for medicanes, to analyze the climatology of past medicanes in a systematic way. Picornell et al. (2014) is focused to adapt the cyclone phase diagram to small and intense cyclonic structures, in particular medicanes, from NWP model outputs, testing procedures and parameter values in four well-known medicane events.

Studies like Gaertner et al. (2007), Cavicchia and von Storch (2011), Cavicchia et al. (2014a), Romero and Emanuel (2013) and Walsh et al. (2014), focus on medicanes from a

climatological point of view using different techniques. Gaertner et al. use a multimodel ensemble of nine RCMs with horizontal resolution between 50 and 55 km. They find an enhanced future risk of tropical cyclone development over the Mediterranean Sea, although these results are limited by the used horizontal resolutions, which do not allow the RCMs to resolve the vast majority of medicanes as we know them today (i.e. small-scale, warm core vortices). As mentioned previously, Cavicchia et al.'s works are centered in downscaling methodologies to resolutions about 10 km. They found that the projected effect of climate change on Mediterranean tropical-like cyclones is a decreased frequency (about 40%) at the end of the century and a tendency toward a moderate increase of intensity. Romero and Emanuel use a collection of synthetically generated events (see Appendix A), showing fewer medicanes (reduction of 10-40%) but a higher number of violent storms at the end of the 21st century, compared to present. Finally, Walsh et al. use Regional Climate Models (RCM) simulations using a storm detection and tracking algorithm specifically designed to identify warm core systems, as in Cavicchia's studies, and the results suggest that the number of warm core cyclones over the Mediterranean Sea will decrease in future projections.

1.3 Background on tropical cyclones

NOAA/ National Weather Service defines tropical cyclone (TC) as a rotating, organized system of clouds and thunderstorms that originates over tropical or subtropical waters and has a closed low-level circulation. Tropical cyclones rotate counterclockwise in the Northern Hemisphere. These warm-core, non-frontal low pressure systems have some common structural elements: 1) boundary layer inflow; 2) eyewall; 3) cirrus shield; 4) rainbands; 5) upper tropospheric outflow. As these storms become more intense, a clear central eye becomes visible from satellite (Fig. 1.3.1).

Tropical cyclones are classified on their maximum sustained winds at surface as "tropical depressions" (<17 m/s), "tropical storms" (17-33 m/s) or "hurricanes" (>33 m/s). Hurricanes are subdivided in categories from 1 to 5, being 5 the one with highest sustained winds and most catastrophic damages (Table 1.1). This name, "hurricane", is just used when it is formed over the North Atlantic (including Caribbean and Gulf of Mexico) and the eastern and central North Pacific. In other areas, they are called by different names: "Typhoons" in western Northern Pacific; "Willy-Willy" in southwest Australia;

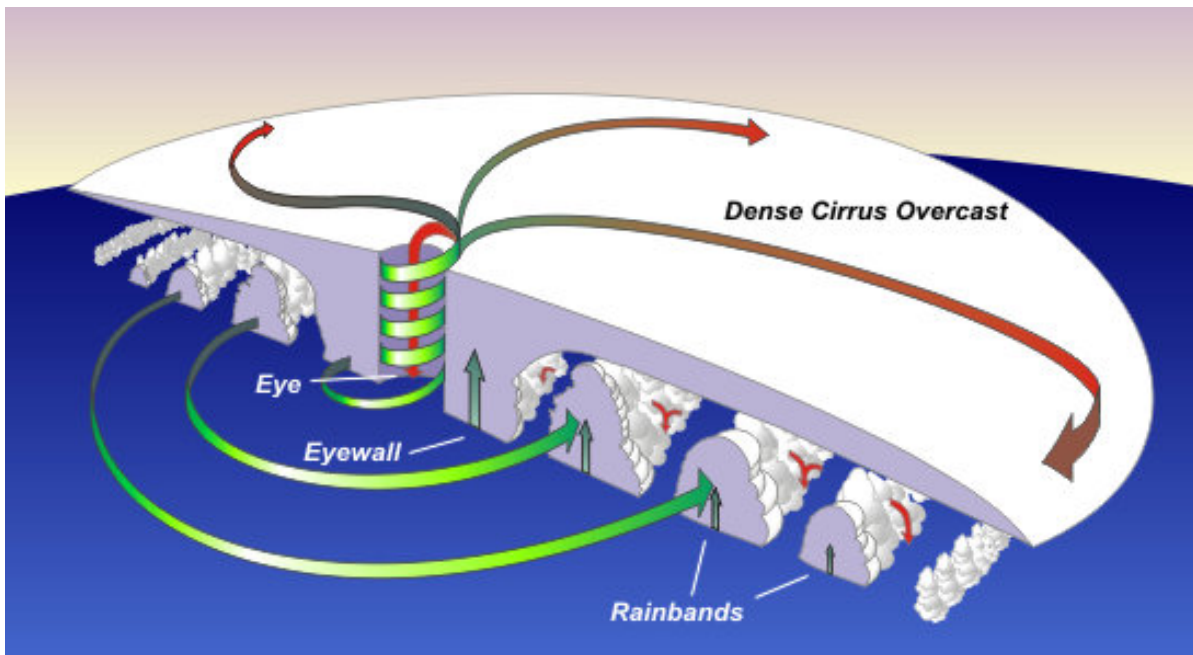


Figure 1.3.1: The main parts of a tropical cyclone are the rainbands, the eye, and the eyewall (image from NOAA website).

and “Tropical Cyclones” in the rest of South Indian Ocean, Arabian Sea/Northern Indian Ocean and Coral Sea/South Pacific.

If the environment conditions are favorable, an incipient disturbance can become a tropical storm. The warm ocean waters of the tropics provide the energy source for the tropical cyclone development and maintenance, warming and moistening the tropical storm boundary layer by evaporation (latent heat flux) and heat transfer (sensible heat flux) processes. This energy (moist static energy) is converted to kinetic energy during the tropical cyclone intensification. Theories for the potential intensity (PI) possible for a storm are based on this mechanism, as we will see later.

Palmén (1948) fixed the 26-27°C lower sea surface temperature (SST) bound requisite for tropical storm formation. He related this threshold with the boundary layer equivalent potential temperature (θ_e) needed to sustain tropical deep convection. Under these values, there is not risk for tropical cyclone development. Afterwards, Gray (1968) added other necessary (but not sufficient) conditions for tropical genesis based on large-scale parameters, summarized as:

Category	Wind Speed	Storm Surge
	km/h (mph) m/s	m (ft)
5	≥ 250 (156) 69	> 5.5 (18)
4	210-249 (131-155) 58-69	3.8-5.5 (13-18)
3	178-209 (111-130) 49-58	2.6-3.8 (9-12)
2	154-177 (96-110) 42-49	1.7-2.6 (6-8)
1	119-153 (74-95) 33-42	1-1.7 (4-5)
Tropical Storm	63-118 (39-73) 17-33	0-1 (0-3)
Tropical Depression	0-62 (0-38) 0-17	0 (0)

Table 1.1: Saffir-Simpson hurricane wind scale.

- sufficient ocean thermal energy (SST $> 26^{\circ}\text{C}$ to a depth of 60 m).
- enhanced mid-troposphere (700 hPa) relative humidity.
- conditional instability.
- enhanced lower troposphere relative vorticity.
- weak vertical shear of the horizontal winds at the genesis site.
- displacement by at least 5° latitude away from equator.

The first three conditions (thermodynamic parameters) are related with the deep convection criteria and can be indicators of seasonal genesis potential. The last three (dynamical parameters) are associated to daily probability of genesis. However, some tropical cyclones have been detected within 5° latitude of the equator recently, suggesting the last requirement to be relaxed.

In addition, the variable called ‘‘Potential Intensity’’ (PI) is defined in order to set the maximum possible surface wind speed. For this goal, there are two alternative theories. The first ideas are based on Miller (1958), who related the minimum pressure of the hurricane with the temperature of the sea surface over which it moves. Afterwards,

Ooyama, 1964; Charney and Eliassen, 1964 proposed a theory for tropical cyclone maintenance and intensification: the Conditional Instability of the Second Kind (CISK). According to CISK, the low-level convergence in the wind field produces convection and cumulus formation, thereby releasing latent heat. This enhances the convergence and further increases convection, creating a positive feedback. Then, this energy is converted into mechanical energy, which means the winds of the TC.

But CISK theory have two deficiencies: The tropical atmosphere is usually near neutral to moist convection instead to conditional unstable, and latent heating does not directly transfer to an increase in kinetic energy. For these reasons, an alternative theory to calculate PI is to consider the tropical cyclone as a closed system, that is a Carnot engine (Emanuel, 1986), in which all heat energy is converted to mechanical energy. This theory is called the Wind-Induced Surface Heat Exchange (WISHE). By this view, the energy cycle of a mature TC follows a process of isothermal expansion (with addition of enthalpy), adiabatic expansion, isothermal compression and adiabatic compression. Taking Fig. 1.3.2 as reference, the air of the tropical cyclone begins to move along a spiral path from the outside (point a in the figure) towards the center of the depression. Then, it experiences a decrease in pressure and its entropy increases obeying the transfer of enthalpy from the sea surface (mostly in the form of evaporation) and the dissipation of the kinetic energy in the planetary boundary layer. At the same time, its angular momentum decreases due to friction with the surface. The temperature in this section (a-b) remains almost unchanged. On the walls of the eye of the TC (point b), the flow turns upward approximately along surfaces of constant entropy and angular momentum, while the pressure obviously decreases. This stretch is approximately adiabatic and free of friction. Later, on the periphery of the system, the air turns downward (stretch o-o') and the entropy gained in the initial convergent stretch is lost to the space by thermal radiation, while it acquires angular momentum by mixing with the environment. This stretch is largely isothermal. Finally, the circuit is closed between the points o' and a, keeping the angular momentum and without much entropy available for the production of kinetic energy. The main difference between the theoretical engine and real a TC is that, in the latter case, heat absorption occurs mainly in the form of latent heat of vaporization, acquired from the surface of the sea by the converging air currents. The other key difference is that the energy available in the traditional Carnot cycle is used to perform work on its environment, while in TC the work is consumed in turbulent dissipation at the boundary layer.

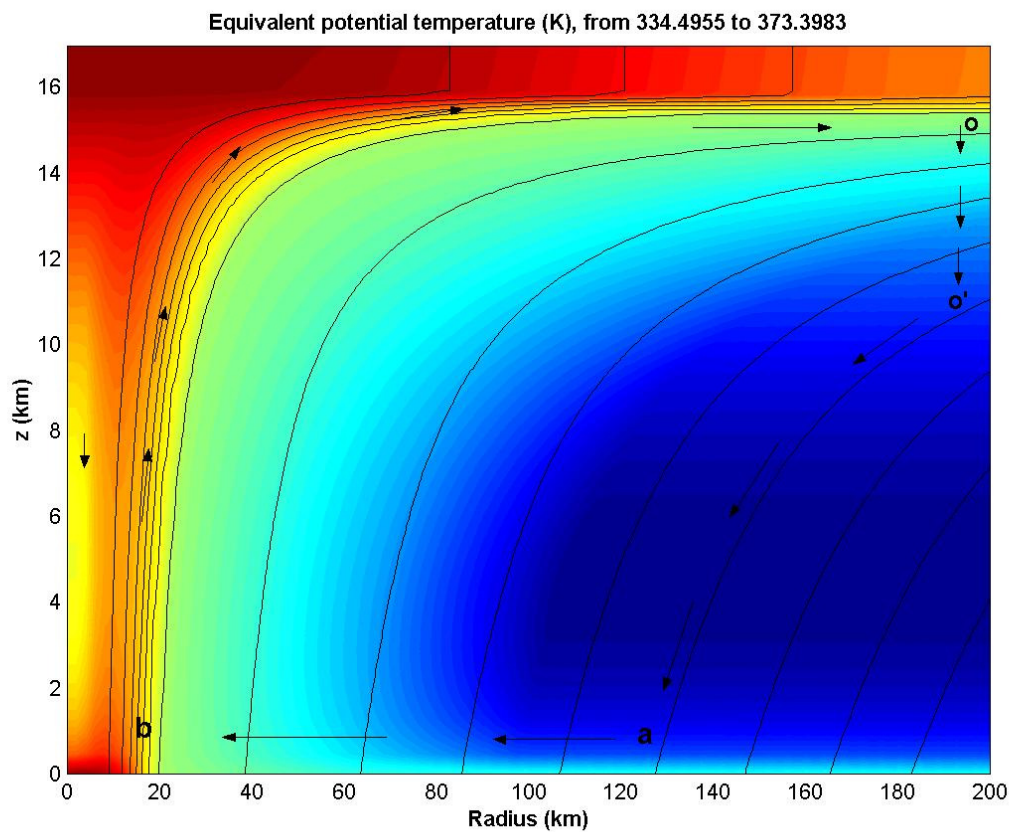


Figure 1.3.2: Vertical section of a mature tropical cyclone, showing the equivalent potential temperature field (colors, increasing in value inwards) and of specific absolute angular momentum around the cyclone axis (lines, increasing outwards). Adapted from Emanuel (2003).

After mathematical implementation of this theory, the TC potential maximum wind speed squared is given by (Bister and Emanuel, 1998):

$$V_p^2 = \frac{C_k}{C_D} \frac{T_S - T_0}{T_0} (k_0^* - k^*) \quad (1.3.1)$$

where C_k and C_D are dimensionless surface exchange coefficients for enthalpy and momentum between the sea and the air that appear in the traditional formulation of the surface turbulent fluxes, T_S is the temperature of the sea surface (hot source in the Carnot cycle), T_0 is the average temperature of the upper area of the cyclone (cold source of the Carnot cycle), k is the specific humid enthalpy of the air near the surface, and k_0^* is the value of the enthalpy for the air in contact with the sea, which is considered saturated with water vapor at the temperature of the sea. Details of the calculation may be found in Bister and Emanuel (2002), and a Fortran subroutine to calculate the potential intensity is available at <http://wind.mit.edu/~emanuel/home.html>.

1.4 Tropical cyclones and climate change

The relationship between tropical cyclone hazard and climate change has been studied extensively. The potential for regional changes in future tropical cyclone frequency, track and intensity is of great interest. It is well known that oceans will heat up, which induces to think about higher tropical cyclone risk. Nevertheless, IPCC AR4 simulations suggest a reduction in the global frequency of hurricanes in a warmer future climate scenario, with a potential increase in intensity in some locations (Emanuel et al., 2008). The models developed by Knutson et al. (2010) also suggest that the frequency of Atlantic hurricanes and tropical storms will likely be reduced in the future. Despite these coherences, there are uncertainties for quantifying and locating risky areas depending on the models and used techniques.

However, AR5 is less confident than the AR4 of increases in intense tropical cyclone activity: “Confidence remains low for long-term (centennial) changes in tropical cyclone activity, after accounting for past changes in observing capabilities. However, it is virtually certain that the frequency and intensity of the strongest tropical cyclones in the North

Atlantic has increased since the 1970s” (IPCC, 2013). A number of studies since the AR4 have attempted to project future changes in tropical cyclone tracks and genesis at inter- or intra-basin scale (Leslie et al., 2007; Vecchi and Soden, 2007b; Emanuel et al., 2008; Yokoi and Takayabu, 2009; Zhao et al., 2009; Li et al., 2010b; Murakami and Wang, 2010; Lavender and Walsh, 2011; Murakami et al., 2011a, 2013). These studies suggest that projected changes in TC activity are strongly correlated with projected changes in the spatial pattern of tropical SST (Sugi et al., 2009; Chauvin and Royer, 2010; Murakami et al., 2011b; Zhao and Held, 2012) and associated weakening of the Pacific Walker Circulation (Vecchi and Soden, 2007a), indicating that reliable projections of regional tropical cyclone activity depend critically on the reliability of the projected pattern of SST changes. Nevertheless, assessing changes in regional tropical cyclone frequency is still limited because confidence in projections critically depend on the performance of control simulations (Murakami and Sugi, 2010), and current climate models still fail to simulate observed temporal and spatial variations in tropical cyclone frequency (Walsh et al., 2012).

Although there are several studies about the relation between TC and climate change, we would like to focus on strategies to evaluate future risk, in particular, on the use of an empirical genesis potential index (GP) presented in Emanuel and Nolan (2004). They used monthly reanalysis data to relate the spatial and temporal variability of TC genesis to a limited number of environmental predictors. This GP index is defined as:

$$GP = |10^5 \eta|^{3/2} \left(\frac{H}{50}\right)^3 \left(\frac{V_{pot}}{70}\right)^3 (1 + 0.1 V_{shear})^{-2} \quad (1.4.1)$$

where η is the absolute vorticity at 850 hPa in s^{-1} , H is the relative humidity at 700 hPa in percent, V_{pot} is the potential intensity in ms^{-1} (eq. 1.3.1), and V_{shear} is the magnitude of the vertical wind shear between 850 and 200 hPa in ms^{-1} . Studies like Camargo et al. (2007) show that this index reproduces quite well the reanalysis-observed phasing of the annual cycle of GP in a given region. A direct application of this concept is the analysis of how the GP index is modified in global warming simulations such as the IPCC runs.

Another methodology pursued in Emanuel et al. (2006) is the use of both thermodynamic and kinematic statistics derived from global models or reanalysis gridded data to produce

large numbers of synthetic tropical cyclones (Appendix A), and these synthetic storms are then used to characterize the tropical cyclone climatology of the given global climate.

1.5 Objectives and outline of the thesis

After this introduction, a main question emerges: “what about medicanes in the Mediterranean area?”

On one hand, we are wondering why these kind of “tropical” cyclones occasionally develop over the Mediterranean Sea. Differences between tropical oceans and the Mediterranean Sea are obvious, but we hypothesize there shall be some similarities between the respective atmospheric environments which make their development possible. We will also want to explore the role of the large scale meteorological parameters on medicane development and properties.

On the other hand, we are concerned about how climate change will affect the medicane risk. We hypothesize that climate change will affect the intensity and distribution of medicanes as it does for tropical cyclones.

To this aim, this thesis is organized in four parts, comprising different points of view necessary to understand the problematics with medicanes. The remainder of Part I is focused on the creation of a database of events. Part II deals with the characterization of the large-scale meteorological environments associated to medicane development and maintenance, against other severe storms over the Mediterranean area (Chapter 3) and with evaluating the role of the surface fluxes on medicane properties (Chapter 4). In Part III, we assess the medicane risk under present and future climate conditions using two different methodologies: an oriented dynamical downscaling (Chapter 5) and using a high-resolution global climate model (Chapter 6). Finally, Part IV summarizes the main conclusions of this thesis and sketches an outlook of more future work.

Chapter 2

Creating a database of events¹

How often do medicanes actually occur? Are there favored locations within the Mediterranean for their development?

2.1 Introduction

Cyclone dated on January 26th, 1982, close to Libya was the first Mediterranean tropical storm detected and it was studied by Ernest and Matson (1983). From this time on, several “case studies” have been explained by different point of views. Despite some studies have collected a few medicane events to evaluate common patterns in their behaviour (e.g. Fita et al. (2007); Picornell et al. (2014)), there is a deficit regarding a systematic compilation of cases and the definition of objective selection criteria. For this reason, our first goal is to create this database of medicane events.

Cyclone climatologies characterize genesis areas, tracks, lifetimes, etc. Some of them pay also attention to their characteristics, as size and intensity, specially when their detection is done by automatic techniques. But owing to the small size and maritime characteristics

¹The content of this chapter is based on the papers (i) Tous, M. and R. Romero, *Medicanes: cataloguing criteria and exploration of meteorological environments*, Tethys 8 (2011), pp. 55-63; and (ii) Tous, M. and R. Romero, *Meteorological environments associated with medicane development*, Int. J. Climatol. 33 (2013), pp. 1-14.

of medicanes, these storms are not well captured in traditional Mediterranean cyclone climatologies. This could be possible using higher resolution analysis data and finer observational networks over the Mediterranean Sea, but nowadays these are not available yet.

MEDEX project (Mediterranean Experiment on Cyclones that produce high impact weather in the Mediterranean) was an international project which elaborated a dynamic climatology of cyclones that produce high impact weather in the Mediterranean. It was based on ERA-40 reanalysis over the period from September 1957 through August 2002, with grid outputs every 1.125° lat-lon, every 6 hours (00, 06, 12, 18 UTC). Cyclone detection is based on Picornell et al. (2001) and it is summarized in three main steps: 1) to locate all the relative minima of pressure (they will be considered as potential cyclones in each analysis); 2) to study the behavior of the pressure field along eight directions surrounding the initial minimum, demanding a pressure gradient (calculated until 850 km, in 50 km intervals) higher to 0.5 hPa/100 km (equivalent to geostrophic winds higher than 5 m s^{-1}) in at least six directions; and 3) to join too near minima (less than 4 grid points, which it is about 170 km in Mediterranean latitudes). Other details of the study can be found also in Buzzi et al. (2005), and main meteorological parameters related with these cyclones (as temperature, humidity, circulation, etc.) are available in <http://medex.aemet.uib.es>. Given the size of medicanes, with diameters about 200-300 km both in satellite images and in past event studies, it is logical to understand why this project could not include medicanes in its database. Nevertheless, this list of MEDEX events will be used to compare medicane properties with other high impact Mediterranean cyclones.

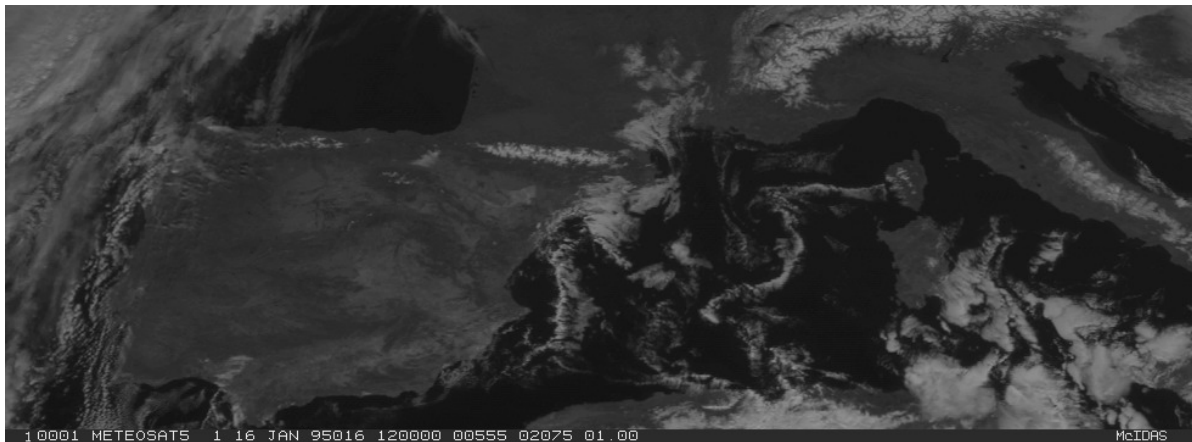
Once the use of reanalysis data has been refused due to their coarse resolution, a direct visual satellite image analysis appears as the best way to detect medicanes. The use of satellite images to track and document tropical cyclones has been a fundamental tool for the issue of advisories (e.g. at the NOAA/National Hurricane Center) and also for the study (Ernest and Matson, 1983; Reale and Atlas, 2001; Jansà, 2003) and the forecast of their Mediterranean analogues. For these reasons, the use of satellite images has been recognized as a useful way to consistently detect storms and, in this case, medicanes. In satellite images, medicanes tend to exhibit a clear circular eye surrounded by a convective eyewall and a roughly axisymmetric cloud pattern (Mayençon, 1984).

2.2 Use of Meteosat

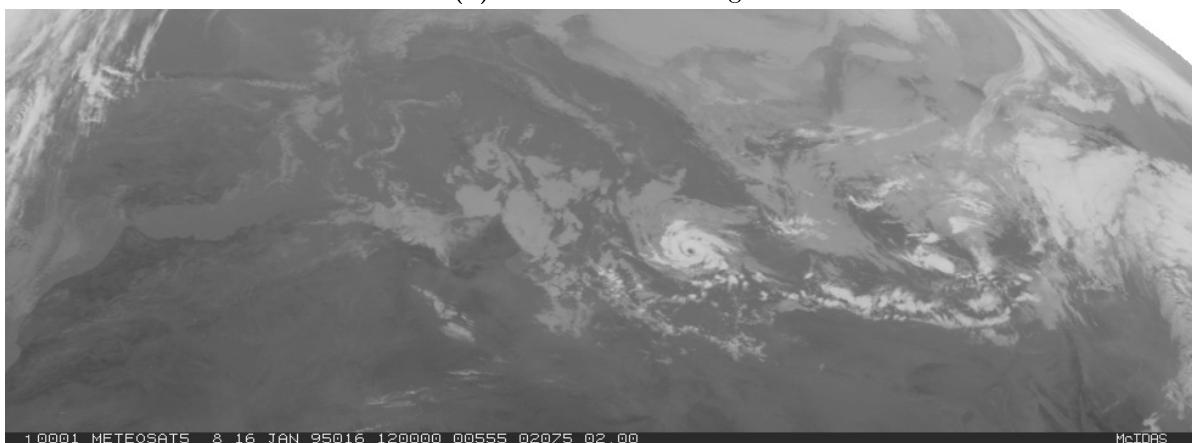
Meteosat-1 was launched in November 1977. The first generation of Meteosat (FMG) satellites (Meteosat-1 to Meteosat-7) provide continuous and reliable meteorological observation from space every 30 minutes in three spectral channels (visible, infrared and water vapor). In 2002, the first second generation satellite was launched, allowing the reception of 12 channels with a better spatial resolution and transmitting the information every 15 minutes. Nowadays, the use of Meteosat Third Generation data is expected to start in 2019, with even more resolution and number of channels (16). In this study, just images from FMG will be used. It will be considered that the calibration of the different satellites has been done by Eumetsat and, consequently, these data can be processed directly without taking care of which satellite it has come from.

Visible (VIS) satellite (Fig. 2.2.1a) images capture the solar energy reflected from the Earth-Sun system between the spectral range of 0.5 to 0.9 μm , and the brightness (and their images) will depend on their albedo, solar radiation intensity and its relative elevation angle to the ground. Spatial resolution at the ground pixel size (nadir) is 2.5 km x 2.5 km. Infrared (IR) satellite images (Fig. 2.2.1b) have an spatial resolution at nadir of 5 km x 5 km and work between the spectral range of 10.5 to 12.5 μm . The satellite measures the radiance emitted by Earth-Atmosphere bodies taking advantage of the atmospheric spectral window around 11 μm . Because of this, each body (considered as a blackbody) follows Planck's law and its temperature can be calculated. Water vapor (WV) satellite images (Fig. 2.2.1c) have the same spatial resolution than infrared ones, working between 5.7 and 7.1 μm . These images provide knowledge about the contained humidity in mid and high troposphere, but without referencing any particular level.

Although VIS images have the best resolution, their temporal limitation (daytime) and layer restrictions (high-troposphere clouds can hide medicanes) disallow us to make an useful medicane tracking. IR images are presented as the best option due to their temporal continuity and easy interpretation.



(a) Visible channel image.



(b) Negate of infrared channel image.



(c) Water vapor channel image.

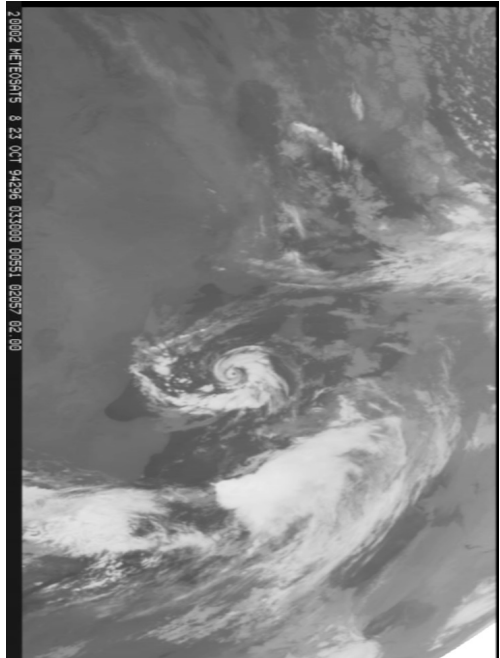
Figure 2.2.1: Meteosat image examples of January 16, 1996, at 12 UTC: a) Visible channel (western Mediterranean); b) Infrared channel (whole Mediterranean area); and c) Water Vapor channel (whole Mediterranean area).

2.3 Criteria establishment

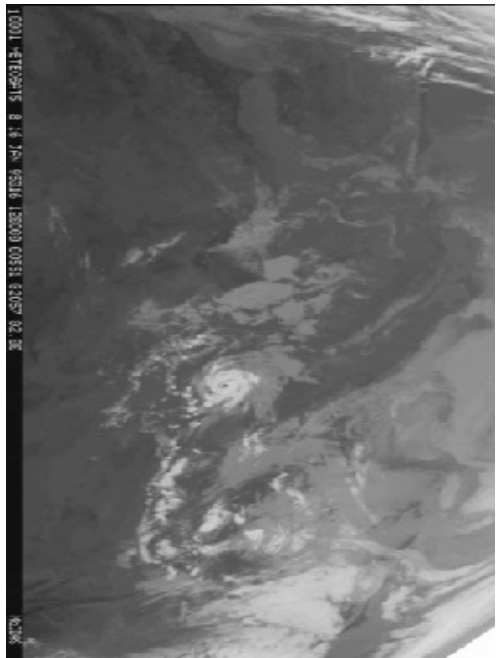
The full collection of Meteosat satellite images, from 1982 to 2003 at 30 min intervals, is used to detect medicanes in this study. The display of all these images has been done editing monthly films (where each frame is an IR image) focused over the Mediterranean Sea. Structures similar to those of tropical cyclones (with a clear circular eye surrounded by a convective eyewall and a roughly axisymmetric cloud pattern (Mayençon, 1984)) have been searched. After a first screening looking for highly symmetric structures that resemble tropical cyclones, 220 events (MED220) have been found during the period.

From these cases, after observing the development also through the same channel, some of them were revealed as baroclinic in nature. Confusion between these cases is not easy to avoid. In Fig. 2.3.1 we can observe three examples of the IR channel of Meteosat satellite referring to severe weather events. Fig. 2.3.1a corresponds to a “comma cyclone” because of its shape. It could seem as a previous stage of a medican system, not formed yet, but after observing its development it is clearly baroclinic. Fig. 2.3.1b is a medican. Its development does not follow the traditional Mediterranean cyclone evolution but it follows the pattern of a tropical cyclone. Furthermore, tropical characteristics are found on it (e.g. Pytharoulis et al., 2000). Finally, Fig. 2.3.1c follows again baroclinic development although the disturbance evolves into a symmetrical structure during its occlusion phase, probably under increasing diabatic influences around its core. Consequently, in these examples, just Fig. 2.3.1a can be considered a medican.

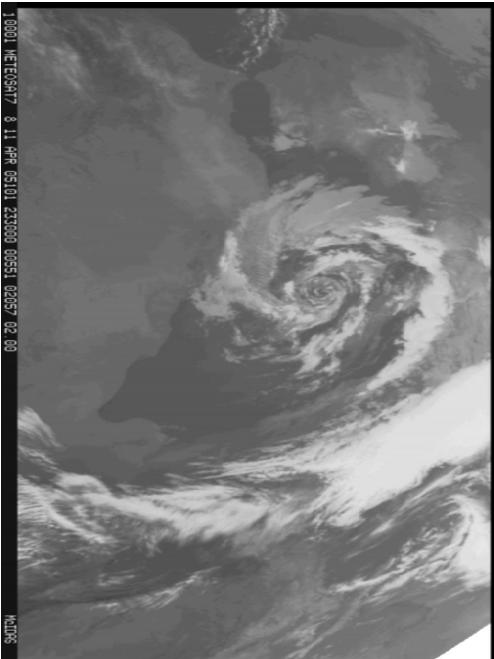
These facts lead us to conclude that it is necessary to impose stricter criteria to identify medicanes using satellite images. These criteria are based on the detailed structure, the size and the lifetime of the systems, all of them assessed in the IR channel. First of all, medicanes must have a continuous cloud cover and symmetric shape around a clearly visible cyclone eye. Secondly, medican diameter must be less than 300 km: due to the size of the Mediterranean Sea, heat fluxes from the sea to the atmosphere (that are one of the main characteristics in tropical cyclones development and, by extension, in medicanes) can not create larger cyclones. And finally, the last requirement is a lifetime of at least 6 h. This limit ensures a sufficient tracking and, for our further purposes in the thesis, enough time to evaluate some large-scale meteorological parameters associated with these cyclones using the European Center for Medium-Range Weather Forecasts (ECMWF) reanalyses ERA-40 and other climatological data.



(a) “Comma cyclone” on 23 October 1994 at 03:30 UTC.



(b) Medicane event on 16 January 1995 at 12:00 UTC.



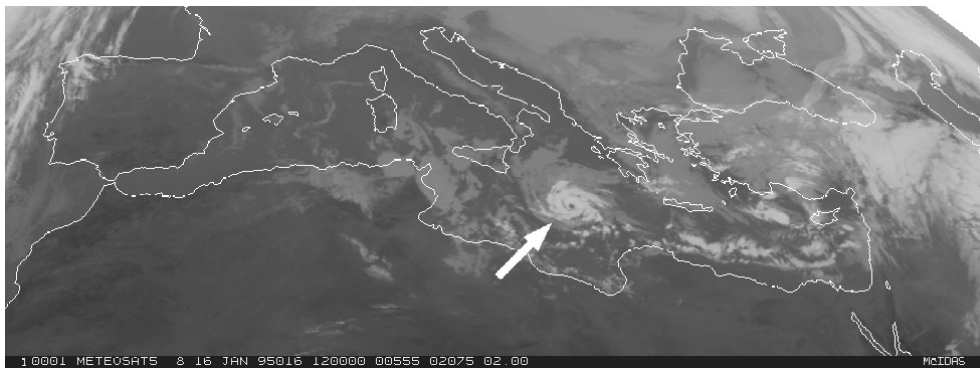
(c) Large and highly symmetric baroclinic cyclone on 11 April 2005 at 23:30 UTC.

Figure 2.3.1: Satellite images of significant cyclonic events. Figures a) and c) do not correspond to medicane events; Figure c) does.

Code	Date	Time (UTC)	Lat. (N)	Lon. (E)	Max. Diam. (km)	Lifetime (h)
M01	1983-Sep-29	12	41.1	6.8	220	90
M02	1984-Apr-07	06	36.4	19.2	230	36
M03	1984-Dec-29	06	35.4	11.6	220	60
M04	1985-Dec-14	12	35.5	17.6	290	54
M05	1991-Dec-05	12	36.2	16.7	320	30
M06	1995-Jan-15	18	37.4	19.1	200	78
M07	1996-Sep-12	12	39.4	2.8	170	12
M08	1996-Oct-06	18	37.2	3.9	240	90
M09	1996-Dec-10	00	40.3	3.7	230	48
M10	1998-Jan-26	12	36.7	17.9	250	30
M11	1999-Mar-19	06	38.5	19.6	250	30
M12	2003-May-27	00	40.1	2.8	280	42

Table 2.1: Date, approximate time of the mature phase (00, 06, 12 or 18 UTC); latitude and longitude of the mature cyclone center; and maximum diameter and lifetime of the 12 detected medicanes.

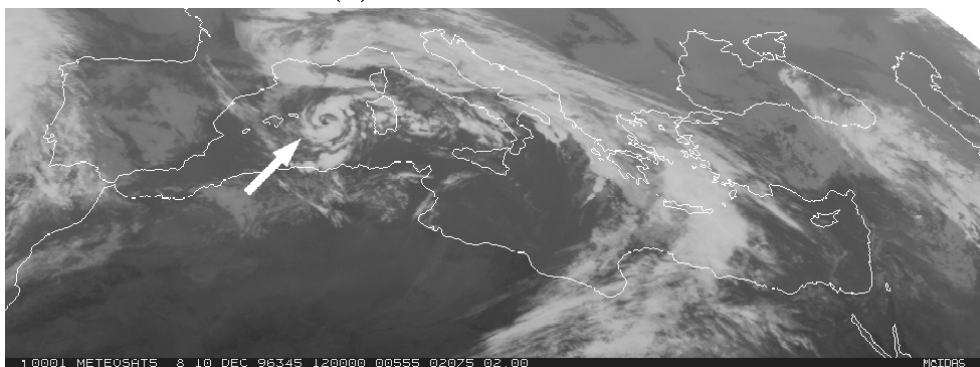
The application of these criteria has resulted in the detection of six cases. Six additional events studied by some authors (as Homar et al., 2003), which were also revealed as medicanes, are included in the list although their visual appearance in satellite images do not entirely fulfill the above criteria (e.g. the diameter can be slightly larger than 300 km, or the cloud cover or cyclone shape can not be perfectly continuous and axisymmetrical, respectively). Nevertheless, the eye of the medicane must be visible in all cases, although it may be partially covered by high clouds. At the end, 12 events have been identified as medicanes (Table 2.1, some examples in Fig. 2.3.2).



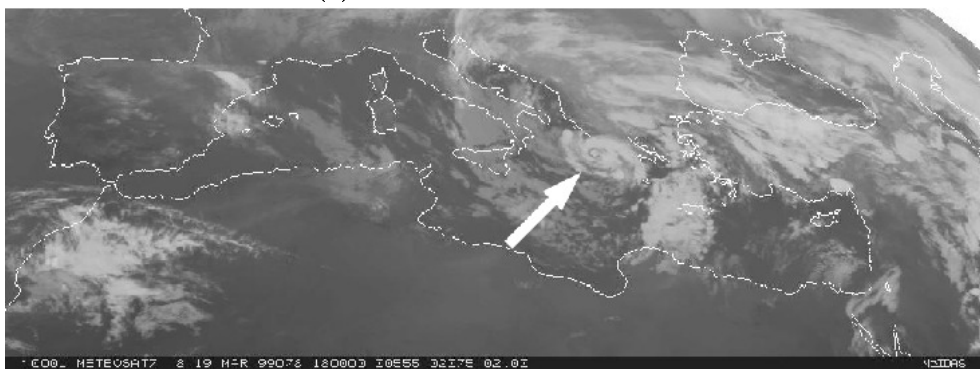
(a) 16 January 1995, 12 UTC.



(b) 9 October 1996, 21 UTC.



(c) 10 December 1996, 12 UTC.



(d) 19 March 1999, 18 UTC.

Figure 2.3.2: Examples of medicanes as seen in the IR channel of Meteosat satellite (taken from Table 2.1)

The lifetime of the detected medicanes ranges from 6 to 72 h. In situations of longer duration, the cyclone has different states of intensification. Printed date in Table 2.1 is fixed as the first time when it is possible to infer the mature phase of the medicane, that is when the cyclone eye is clearly observable.

2.4 Medicane spatial and temporal distributions

The spatial distribution of Mediterranean cyclones is not uniform. Alpert et al. (1990) and Campins et al. (2011) located two preferred regions: Cyprus and the Gulf of Genoa. Shaded areas in Fig. 2.4.1 represent the spatial density of intense cyclones (that is with a surface geostrophic circulation greater than 7 gcu, where $1\text{gcu} = 10^7 \text{ m}^2 \text{ s}^{-1}$). Although intense cyclones have virtually occurred everywhere in the Mediterranean, there are again two preferred regions of cyclogenesis: Italian maritime areas and Ionian and Aegean Seas. It should be kept in mind that part of the Atlantic Ocean is included in the domain of the MEDEX project, so some statistical results using this database can be slightly adulterated by non-Mediterranean cyclones.

The density distribution of the MED220 events at mature state is represented as dashed lines in Fig. 2.4.1. They are located preferably in the Central and Western basins: the area between the Balearic Islands and Italian peninsula contains most of these cyclones. The 12 detected “true” medicanes (black points) are situated in the Central and Western regions of the Mediterranean Sea, but in different areas than those described above: Medicanes lie over the Ionian and Balearic Sea. It must be highlighted that despite that the more intense MEDEX cyclogenetic center is located in the Gulf of Genoa, no mature medicane is located near this area. It is also striking that no case has been detected in the vicinity of Cyprus, although it is considered one of the most active areas for cyclogenesis.

With regard to the period of occurrence, medicanes are more frequent in winter like intense baroclinic Mediterranean cyclones (Campins et al., 2011) and autumn, but they have also occurred in early spring and late summer (Fig. 2.4.2). This fact indicates a notable difference with respect to tropical cyclones, which happen only in a few specific months of the year (for example, in the Atlantic basin lasts between June and November), when the SST is at its highest. On the contrary, in the Mediterranean basin, SST changes are not as abrupt as in the oceans and even in cold seasons it remains quite warm. As it

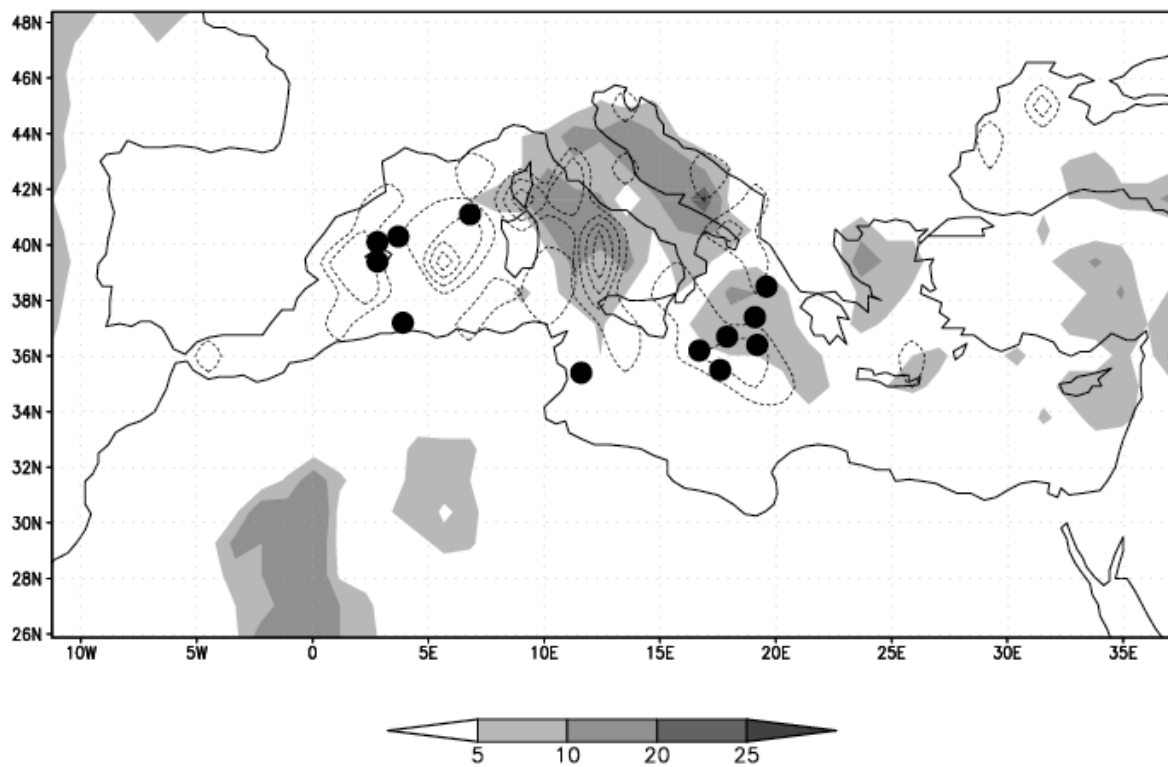


Figure 2.4.1: Spatial density distribution of intense cyclones from the MEDEX project (shaded) as number of events in a square of 1.125° lat-lon; density distribution of MED220 cyclones (dashed lines, contour interval is one event/ $(1.125^\circ)^2$ starting at value 1; and the 12 detected medicanes (black points).

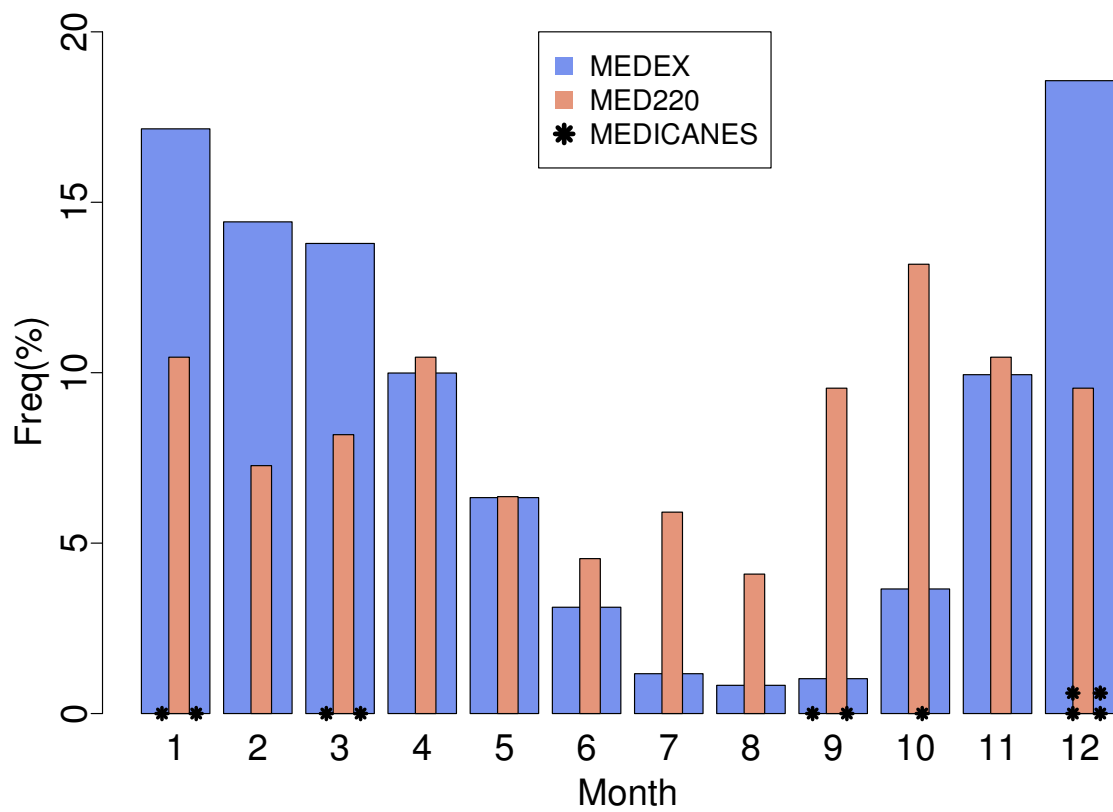


Figure 2.4.2: Monthly frequency distribution (%) of intense cyclones of the MEDEX project (blue bars), MED220 events (orange bars) and detected medicanes (stars).

was explained in Section 1.3, heat and moisture fluxes are responsible for tropical cyclone development, which means that, if there are cold enough air inclusions to promote these fluxes, a pro-medicane environment can be established.

Part II

EXPLORING THE METEOROLOGICAL ENVIRONMENTS

Chapter 3

Meteorological environments characterization¹

We hypothesize that a comparison of some large-scale meteorological pro-medicane environments against the generality of intense cyclonic situations should reveal useful discrimination variables among the set of thermodynamical descriptors.

3.1 Introduction

Several synoptic analyses performed on known cases of medicanes (e.g. (Pytharoulis et al., 2000; Homar et al., 2003; Emanuel, 2005a; Fita et al., 2007)) show how their structures are not detached from the general atmospheric circulation, but based on a large-scale baroclinic disturbance that affects the Mediterranean, and it is only in the mature phase that they are detached to create their own development and life cycle. Generally, medicanes originate in deep cyclonic conditions, with cut-off (closed circulation at high levels, extended to the surface) and cold-core (where the interior air is cooler than contiguous areas) forming in the middle and upper troposphere, from the “breaking” of Rossby waves.

¹The content of this chapter is based on the paper Tous, M. and R. Romero, *Meteorological environments associated with medicane development*, Int. J. Climatol. 33 (2013), pp. 1-14.

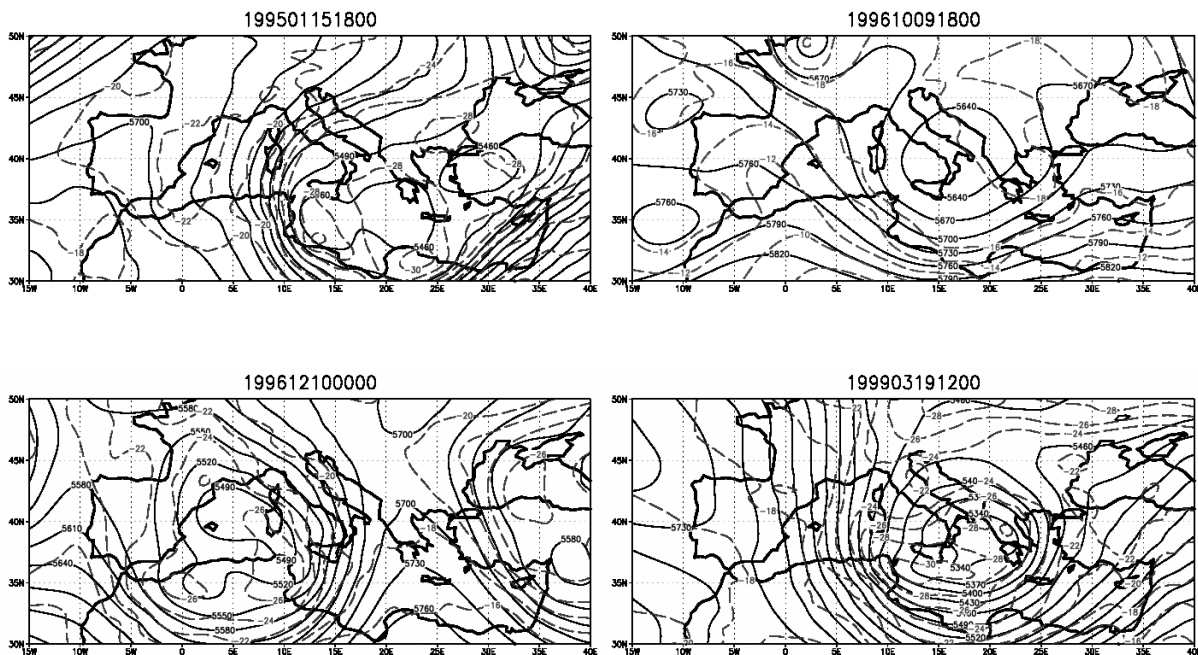


Figure 3.1.1: Geopotential height (gpm, continuous lines) and temperature ($^{\circ}\text{C}$, dashed lines) at 500 hPa for some medicane events listed in Table 2.1 (also shown in Fig. 2.3.2).

When a low is close to the Mediterranean (or is formed above), the air of the lower layers rises, generally through large vertical movements, it is cooled and its relative humidity continues rising until reaching saturation and releasing (perhaps massively) condensation latent heat. It therefore becomes a system which could lead to the evolution of a medicane. Assuming that the vertical wind shear is not great either, and the local potential intensity (representing the maximum surface wind speed that it can reach) increases, the sea-atmosphere thermodynamic imbalance is intensified. This humid air may inhibit the formation of descending convective fluxes, which are one of the factors that prevent tropical cyclogenesis. Numerical experiments carried out by Emanuel (2005a), using a non-hydrostatic model, show that these deep cut-off lows are the perfect setting for incubating warm-core cyclones on a small scale, such as medicanes (Fig. 3.1.1).

Despite these arguments, the existence of these cold and deep lows over the Mediterranean is more frequent than real cases of medicanes. For this reason, it is presumable that some very special meteorological conditions are needed for medicanes to be developed. These

conditions are not yet fully known and are difficult to determine, as only few studies are available. Therefore, this thesis proposes a set of meteorological variables that, compared against the climatologies of Mediterranean cyclones of the MEDEX project, will help to distinguish precursor and non-precursor factors of large-scale cyclones associated with medicanes.

While ordinary winter storms are baroclinic in origin (drawing their energy from the available potential energy associated with large-scale horizontal temperature gradients), medicanes operate on the thermodynamic disequilibrium between the Mediterranean Sea and the atmosphere. That is, their energy source is the massive latent heat release occurring in convectively driven cloud systems rooted in a continuously moistened boundary layer. In this respect, as well as in their visual appearance in satellite images, medicanes are much like tropical cyclones. Thus, it seems reasonable to apply the concepts and tools developed for the well known hurricanes to these Mediterranean analogues. An exercise like this has been proven very useful for understanding the mechanics of polar lows (Emanuel and Rotunno, 1989).

3.2 Selected parameters

Following the trajectory of the center of the medicanes throughout its lifespan, since we are able to identify the first traces until the trail disappears completely, some of the large-scale characteristic parameters of hurricane-prone environments will be analyzed here: the presence of cyclonic low-tropospheric vorticity (AVOR850, calculated at 850 hPa level), substantial mid-tropospheric relative humidity (RH600, calculated at 600 hPa level), high (relative to air) sea surface temperature (SST), and low values of tropospheric wind shear (VSHEAR8525, calculated between 850 and 250 hPa levels). Furthermore, also the diabatic contribution to the surface level equivalent potential temperature local tendency (DIAB1000) is strongly related to tropical cyclone development, so it is considered here too. This diabatic term is related with the sea-atmosphere sensible and latent heat fluxes. Owing to the temporal discretization of the available meteorological fields, this parameter is calculated as:

$$DIAB1000 = \left[\frac{\theta_e(t + dt) - \theta_e(t - dt)}{2 dt} - Adv \theta_e(t) \right] \quad (3.2.1)$$

where the advection term, $Adv \theta_e(t)$, is formulated through finite spatial differences at the time t , and dt indicates the time interval of the used analysis data.

On the other hand, the idealized model which compares tropical cyclones with Carnot cycles (introduced in Section 1.3) has also been used for medicanes. This theory allows to determine the potential intensity (maximum wind speed, MAXWS) of the storm from the environmental conditions (Bister and Emanuel, 1998):

$$MAXWS = \sqrt{\frac{C_k}{C_D} \frac{T_S - T_0}{T_0} (k_0^* - k^*)} \quad (3.2.2)$$

where T_S is the SST, T_0 the mean temperature at the top layer of the idealized storm, k the specific enthalpy of the air near the surface, k_0^* the enthalpy of the air in contact with the sea, assumed to be saturated with water vapor at sea temperature, and C_D and C_k are the dimensionless transfer coefficients of momentum and enthalpy.

Finally, the empirical genesis potential index (GP, now renamed as GENPDF for medicanes), which combines the previous MAXWS with AVOR850, RH600 and VSHEAR8525, has been also evaluated in order to predict medicane genesis:

$$GENPDF = |10^5 AVOR850|^{3/2} \left(\frac{HR600}{50} \right)^3 \left(\frac{MAXWS}{70} \right)^3 (1 + 0.1 VSHEAR8525)^{-2} \quad (3.2.3)$$

This index has been successfully tested against the true space-time probability of tropical cyclone genesis. Preliminary analysis for the Mediterranean (Romero and Emanuel, 2006) concluded that it is a suitable diagnostic indicator of the potential of synoptic environments for medicane development. Hence, GENPDF appears to be a good candidate in our objective of describing and identifying as best as possible the meteorological environments conducive to medicanes. In its original formulation, this index was adjusted as number of events per decade in a square of $2.5^\circ \times 2.5^\circ$ lat-lon. In the case of medicanes, this adjustment is not consistent with the rare occurrence of events, but the units are not used and only a qualitative analysis is provided here.

Parameter	Definition	Units
AVOR850	Low-tropospheric (850 hPa) vorticity	10^{-5} s^{-1}
DIAB1000	Diabatic contribution to surface level (1000 hPa) equivalent potential temperature local tendency	$^{\circ}\text{C} (12 \text{ h})^{-1}$
RH600	Mid-tropospheric (600 hPa) relative humidity	%
SST	Sea Surface Temperature	$^{\circ}\text{C}$
VSHEAR8525	Tropospheric wind vector difference between 850 and 250 hPa	m s^{-1}
MAXWS	Idealized maximum surface wind speed, or Potential Intensity	m s^{-1}
GENPDF	Empirical genesis index described by Emanuel (2005a)	-

Table 3.1: Summary of the large-scale meteorological parameters considered in this study, their definition and the used physical units.

A summary of the large-scale meteorological parameters calculated in this study is presented in (Table 3.1). All these parameters are calculated from the ERA-40 reanalyses corresponding to cyclone maturity time and have been averaged in a square of $600 \times 600 \text{ km}^2$ around the cyclone detection point. In fact, for these calculations, the satellite-observed maturity time is shifted to the closest analysis time among 00, 06, 12 or 18 UTC, and the cyclone center is also replaced according to the ERA-40 resolution ($\sim 120 \text{ km}$). Since the ERA-40 dataset ends in 2002, the medicane of May 2003 (M12) will not be considered in this analysis. GENPDF has an additional variety also: GENPDFmax, which is the maximum value of the GENPDF index found in the averaging square.

3.3 M06 parameter sequence

M06 corresponds to the event occurred between 14 and 16 January 1995, also referenced in the introduction of the thesis (Chapter 1). This medicane was originated in the Ionian Sea, moved to south-southwest direction towards Lebanon coast, when it arrived on 17th and then disappeared. As it is shown in Fig. 3.3.1, the cyclone eye was visible from 15 January at 06 h. Between days 16 and 17, continuity in cloud cover around the cyclone center (one of the conditions required to be cataloged as medicane) is not present. Accordingly, even the cyclone life continues, the medicane phase is considered finished.

High values of DIAB1000 are observed during most of the event (from 14th to 16th, Fig. 3.3.2a). First value represented in this figure is the absolute maximum. This high value of sensible and latent heat transfer from the sea is caused by the large difference of temperatures with the atmosphere, and moderate/high values of surface winds. Then, a second maximum is found at 15-06h and a third one on 16-06h. From 17th, it attains similar values to intense cyclones of MEDEX project, corresponding to the medicane dissipation, but highlighting a fourth maximum (less intense than the others) on 17-06h.

Although the maximum at 15-06h could be the direct responsible for the medicane genesis (because it occurs at the same time when the medicane eye appears), this scenario is not plausible: some time is required for the disturbance to note the effects of the heat transfer on its development. For this reason, the absolute maximum in the figure (the first value) represents better the main heat fluxes that cause the medicane genesis, although it is possible that the real maximum had occurred earlier during the cyclone life, before its

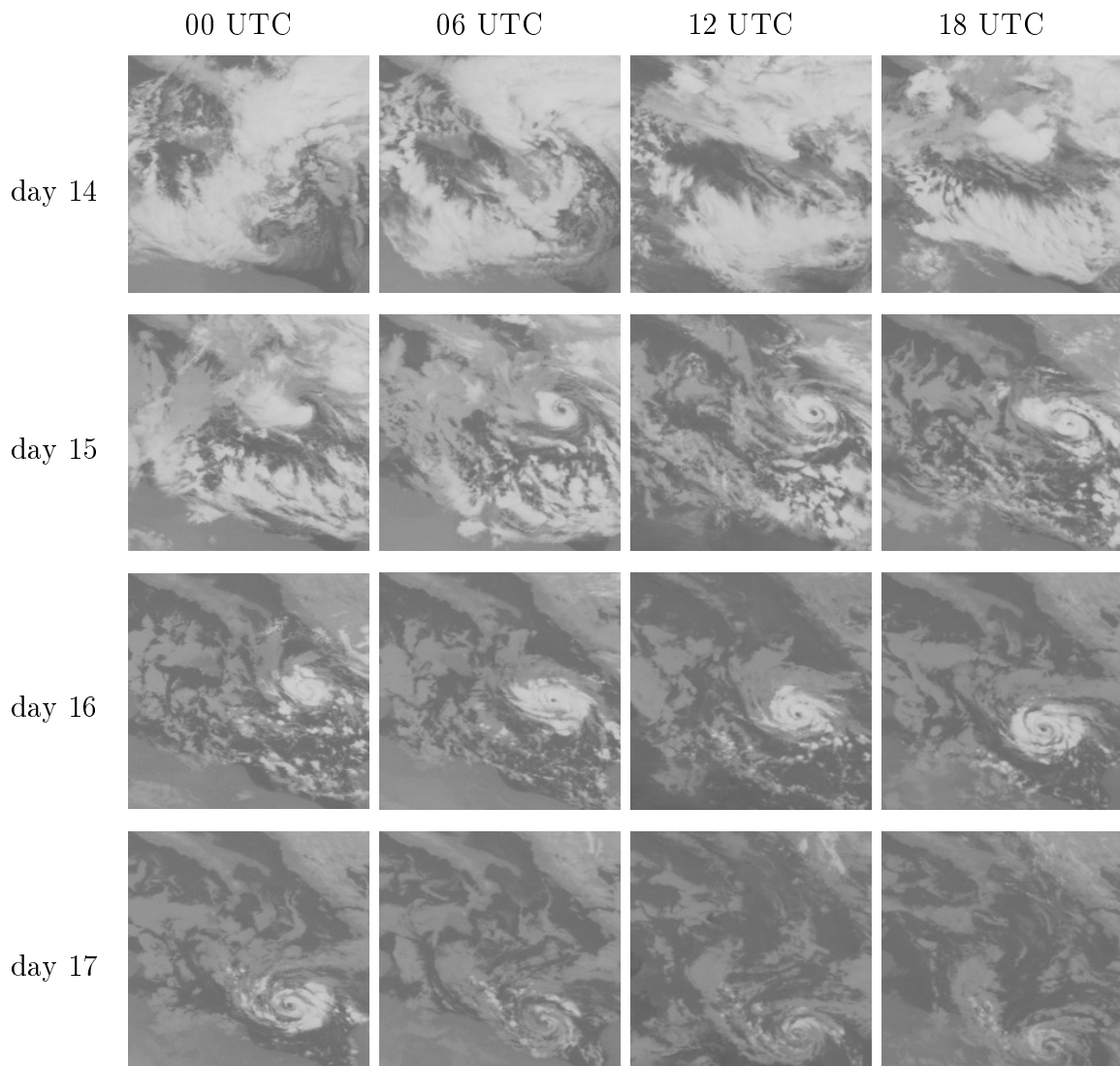
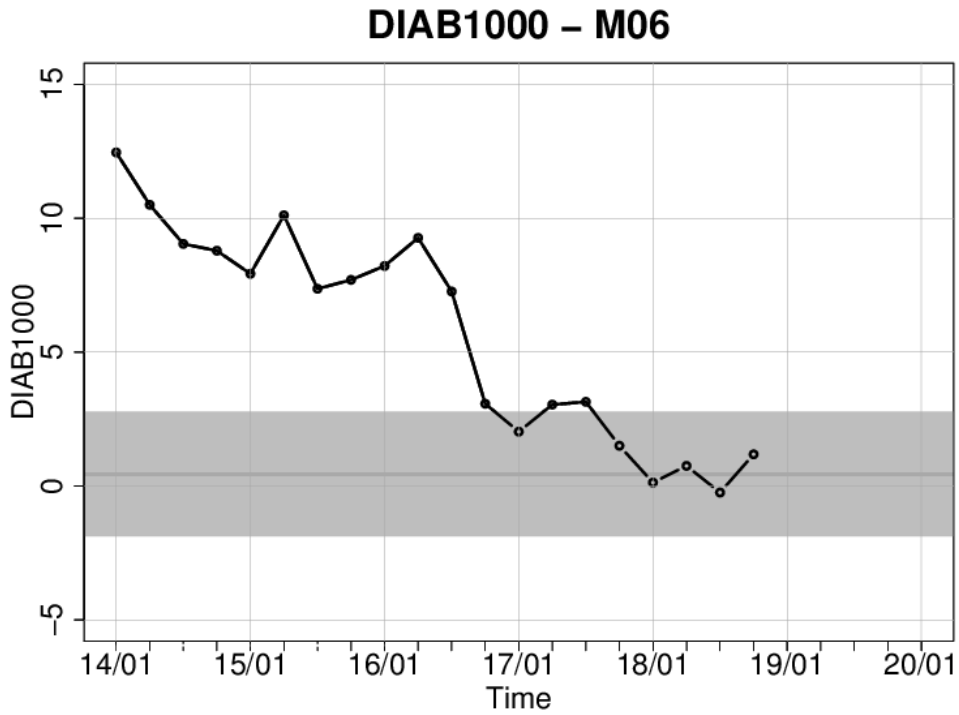


Figure 3.3.1: Evolution of the medicane dated on January 1995 to the south of Italy. Mature phase starts at 06 h on the 15th, identified by a clear visible cyclone eye.

a)



b)

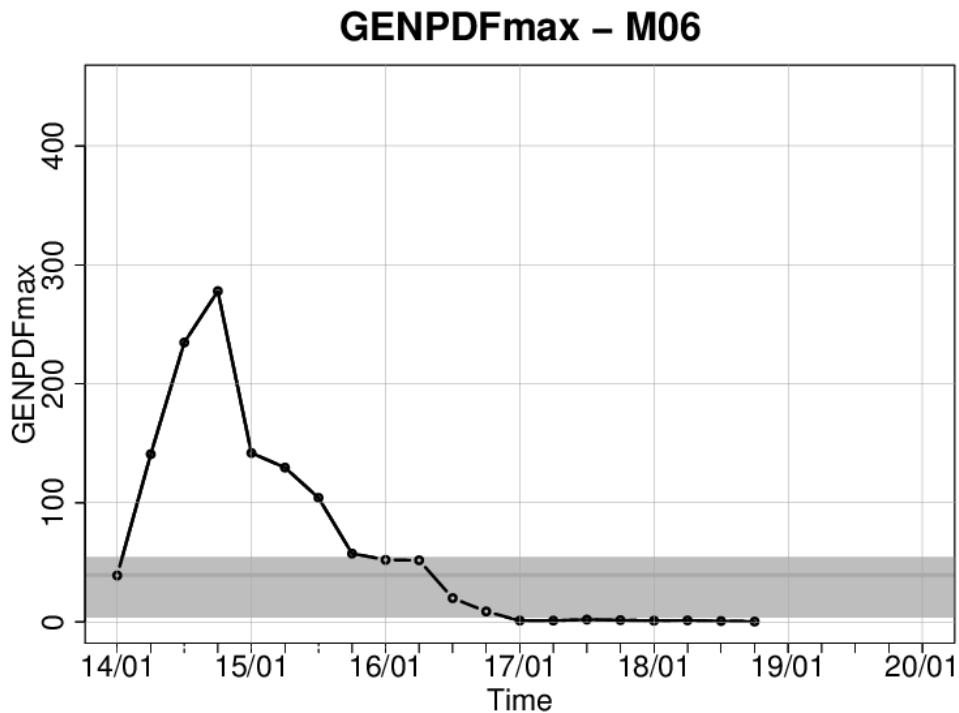


Figure 3.3.2: Evolution of DIAB1000 (top) and GENPDFmax (bottom) values along time (time step=6 h), from 14 to 18 January 1995, for the referenced medicane (sequence shown in Fig.3.3.1). The dark grey line represents the mean value of the intense MEDEX cyclone distribution and the shaded area, the interquartile.

track can be detected. Comparing with other events, the maximum would be expected one or two time steps before the detected track (that is, about 12 h before the mature phase).

Second and third maxima values correspond to heat transfers which would allow the medicane to keep its structure. As it is shown in Table 2.1 and in Fig.3.3.1, this is one of the longest medicanes detected, so these fluxes are needed in order to maintain medicane properties. The fourth maximum appears close to the Libyan coast, but the movement of the medicane over land does not allow the necessary sustainment, and the storm disappears.

With reference to GENPDF_{max} (Fig.3.3.2b) a clear maximum is appreciated on 14-18h and a slight decrease on 15th between 06 to 12h. At the beginning of the day 16th, values keep similar to intense MEDEX cyclones, dropping to zero at the end of the same day. For these reasons, four singular points are identified: main maximum (14-18h), first smooth fall (15-06/12h), constant values (16-00h) and null values (from 17-00h). The main maximum appeared about 12 hours before the presence of the medicane eye. It is a remarkable fact because this relation has been verified for all the studied medicanes, and it will be used in Chapter 5. The other singularities are related with the medicane sustainment.

3.4 Comparison against MEDEX intense cyclones

As it was mentioned earlier, the occurrence of cold upper lows over the Mediterranean is not uncommon, whereas medicanes are rare phenomena, suggesting that very special meteorological conditions are necessary to medicanes to occur. The use of the kind of dynamically oriented climatologies designed in MEDEX² has been applied to attempt a statistical discrimination between precursor and non-precursor medicane cyclonic environments. The large-scale nature of the precursor cyclones (Fig.3.1.1) allows for identifying and three-dimensionally characterizing, in currently available analyses, the

²The framework of the MEDEX project developed a very complete climatology of Mediterranean cyclones, which also involves the three-dimensional characterization of the disturbances in terms of dynamical, thermal and humidity environmental variables: vertical depth, vorticity, circulation, steering wind speed, temperature gradient and relative humidity (Campins et al., 2006).

	MEDEX		MED220		MEDICANES	
	5%	95%	5%	95%	Min.	Max.
AVOR850	10.2	18.8	9.5	16.8	9.6	17.7
DIAB1000	-5.9	6.4	-2.9	5.8	0.2	7.7
RH600	30.8	89.9	44.8	80.9	49.2	80.9
SST	7.9	19.0	13.1	24.0	15.0	23.2
VSHEAR8525	7.3	42.3	6.2	24.1	4.7	29.0
MAXWS	0.3	49.1	13.3	55.2	31.6	49.5
GENPDF	0.0	16.8	0.2	32.7	0.9	36.6
GENPDFmax	0.0	61.5	0.7	120.9	3.8	329.5

Table 3.2: Summary of compared meteorological parameters (according to units described in Table 3.1) between three lists of events: intense cyclones of MEDEX database, MED220 cases and medicane list. MEDEX and MED220 described through 5 and 95 quantile values, and MEDICANES through minimum and maximum values among the 11 cases.

environments in which medicanes develop. A summary of the results is contained in Table 3.2.

Most significant results come from DIAB1000, SST and GENPDF parameters, and for this reason, they will be discussed in more detail below (Fig. 3.4.1 and 3.4.2).

DIAB1000 ingredient is linked to sea-atmosphere sensible and latent heat fluxes, and positive values would indicate a flux of enthalpy directed from the sea to the atmosphere. Typical Mediterranean cyclones (including intense cyclones of MEDEX project) do not reach high values of this flux or a preferential direction, so its distribution is basically symmetrical and concentrated at low values. MED220 events show a tendency for positive values of the parameter. For medicane cases, none of the 11 events presents negative DIAB100 and, in some cases, values are very high evidencing the important role of the sea-atmosphere enthalpy flux on medicane development (Fig. 3.4.1a).

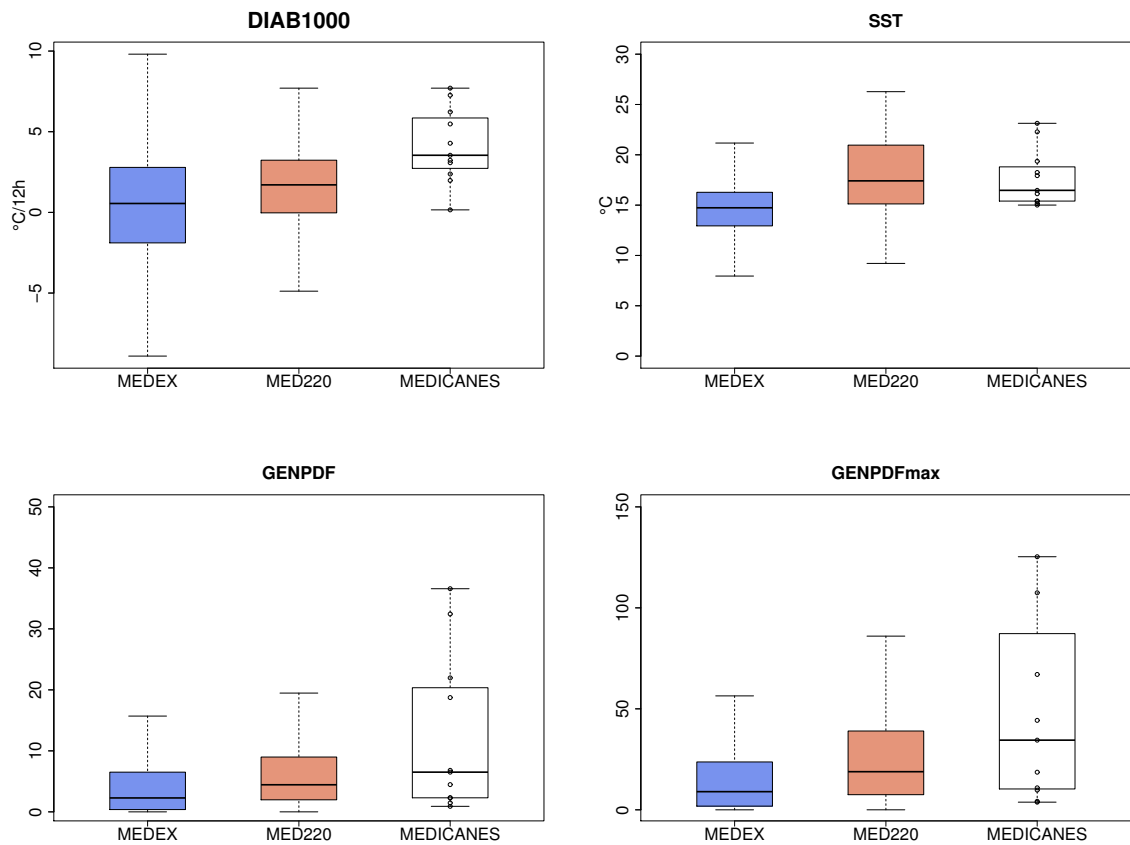


Figure 3.4.1: Boxplot diagrams of the indices DIAB1000, SST, GENPDF and GENPDFmax for intense cyclones of MEDEX database (blue), MED220 cases (orange) and medicane events (white).

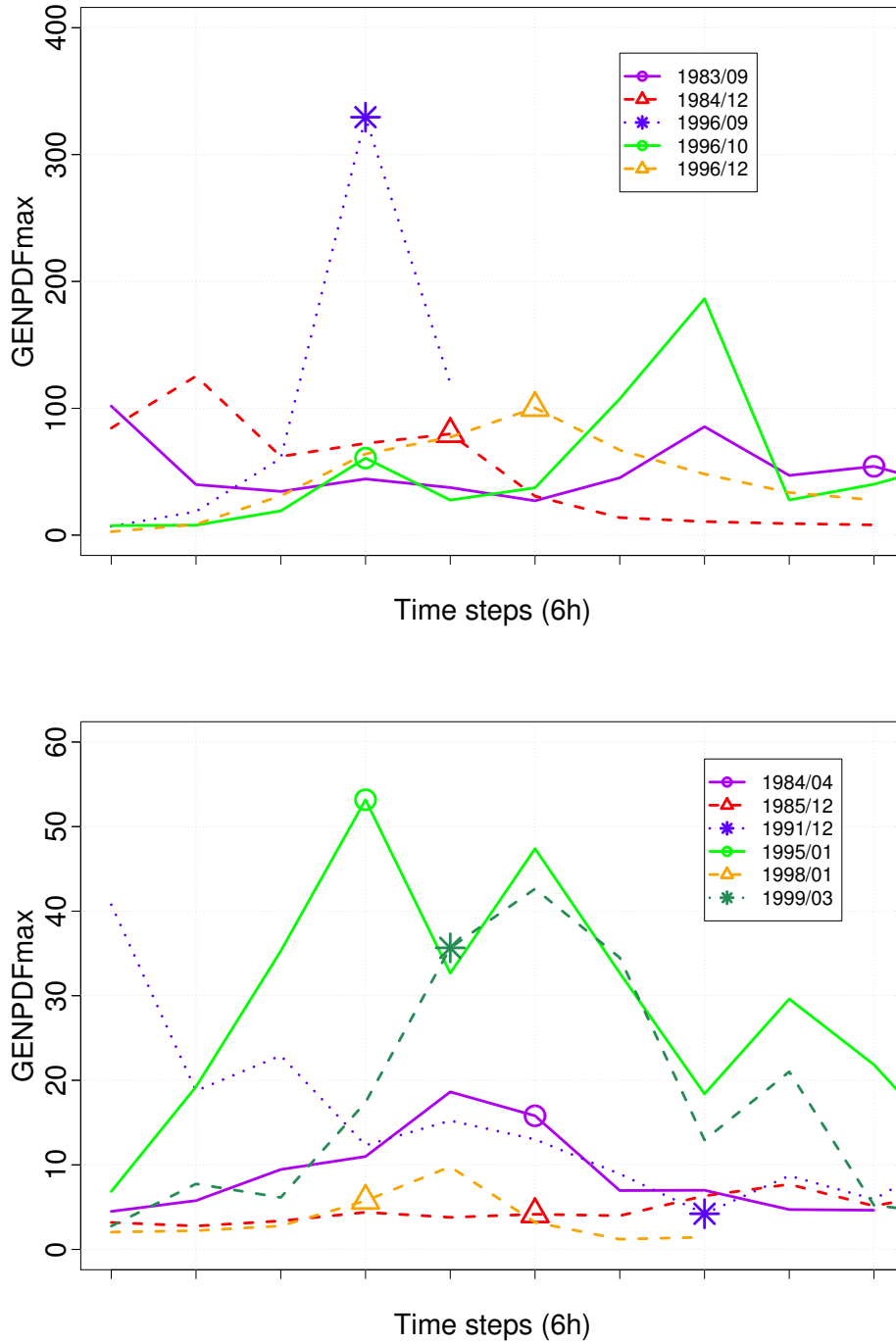


Figure 3.4.2: Evolution of GENPDFmax parameter during the lifetime of each medicane (lines), with the symbol indicating the cyclone maturity time. Two figures with different vertical scale to improve clarity.

Warm SSTs, especially if there is cold air at upper levels, promote high thermodynamic contrasts with height and convective or latent instabilities in the troposphere. While most intense cyclones have a SST around 15°C , this temperature seems to be a lower bound for the medicane events, because the SST in these cases was never colder than that value (Fig. 3.4.1b). However, SST values from Mediterranean cyclones and medicanes show a significant difference with the results of tropical cyclone studies. It is well known that the minimum SST to produce a hurricane is 26°C (Trenberth, 2005). This value is never attained for Mediterranean cyclones, since an SST exceeding 26°C is only reached in the southernmost sectors of the Mediterranean Sea, during the summer months. Clearly, the sea-atmosphere thermodynamical disequilibrium driving this kind of storms can operate at the much lower sea temperatures of the Mediterranean thanks to the prominent cold air intrusions that affect its latitude, while in the warmer tropics, free of the baroclinic influences, elevated SSTs become necessary.

Finally, the empirical index GENPDF exhibits a high spread of values in medicane events, ranging from 0.9 to 36.6, whereas most intense MEDEX cyclones have very low values of this index (Table 3.2 and Fig. 3.4.1c). This difference is even more evident when calculating GENPDFmax (Fig. 3.4.1d). In this case, values are around 50, some of them are greater than 100, even surpassing 300 (out of the figure) in the case of September 1996 (M07).

As expected, the highly symmetrical MED220 cyclones tend to occur in environments with intermediate values of GENPDF and GENPDFmax. An improved description of medicane environments is possible if, instead of analyzing a single moment, the entire lifetime of the medicane is considered (Fig. 3.4.2). This figure synthesizes the evolution of GENPDFmax parameter for our medicanes, following the cyclone-inferred cyclone center since its inception, through its mature phase until its complete dissipation. Typically, the medicane environments present an increase of GENPDFmax during the incipient phase of the system, attaining the maximum values close to the mature phase.

3.5 Conclusions

The temporal pattern of the empirical genesis index becomes useful for the identification of potential medicane situations, although it is clear that the discrimination power

of GENPDF index is only relative. First, there is a significant fraction of cyclonic environments showing high and sustained values of the index but not producing distinguishable medicanes, presumably as consequence of the relatively small size of the Mediterranean Sea and the ubiquitous baroclinic and orographic effects that disrupt to proto-cyclone. Second, high values of the index should be considered, at most, a necessary but not sufficient ingredient for medicane development, very much the same role that high amounts of convective available potential energy (CAPE) in a certain environment would play in severe convection development.

Chapter 4

Sensitivity to surface heat fluxes¹

Once assumed the importance of sea surface heat fluxes on particular medicane events (e.g. Homar et al., 2003), it would be desirable to assess whether a common pattern is found for the generality of medicanes. For this reason, this part of the study will evaluate quantitatively the effects of these fluxes on medicane properties, more specifically on their trajectories and intensification, including whether there is a necessary condition for the medicane genesis itself. Then, a collection of control simulations has been run in the first place to evaluate the ability of a mesoscale model to reproduce medicane events, an usual requirement for the subsequent planned methodology. After that, the sensitivity analysis aimed at determining what is the specific role of surface heat fluxes on medicane characteristics has been carried out, including a qualitative interpretation based on the spatial distribution over the Mediterranean of the enthalpy fluxes during the episodes.

4.1 Introduction

A set of numerical control simulations (hereafter, CTR) was run in order to determine if the model physical parameterizations, other chosen parameters (simulation period, domain, resolution, etc.) and the input initial and boundary conditions are suitable to reproduce successfully the medicane events (Table 2.1). Given that medicanes are

¹The content of this chapter is based on the paper Tous, M. and R. Romero and R. Ramis, *Surface heat fluxes influence on medicane trajectories and intensification*, Atmos. Res. 123 (2013), pp. 400-411.

deep cyclones with a low-mid tropospheric warm core, it would be expected to find a quasi-symmetric intense low-pressure center at sea level with an isolated warm-core structure aloft (in our case, evaluated at 700 hPa level) in order to consider that the model simulates the medicane correctly.

As it was mentioned earlier, synoptic-scale analyses for an illustrative example tend to confirm the hypothesis made by some authors (e.g. Pytharoulis et al., 2000; Homar et al., 2003; Emanuel, 2005a) that medicanes are not fully isolated structures of the atmospheric circulation. They require a large-scale baroclinic disturbance evolving over the Mediterranean and only during the mature or late stages of this parent cyclonic storm, a medicane might develop. They almost always develop when a deep, or cut-off, cold core cyclone is present in the upper and middle troposphere, usually formed as a result of the “breaking” of a synoptic scale Rossby wave. As Emanuel (2005a) showed through his numerical experiments using an axisymmetric, cloud-resolving nonhydrostatic model, these conditions are indeed ideal incubators for surface flux-driven, small-scale, warm-core cyclones. An illustrative example can be explored in Fig. 4.1.1.

An additional set of simulations (hereafter, NOFLX) has been performed to confirm the important role of air-sea interaction in medicane development. In these simulations, surface sensible and latent heat fluxes (SurFlux) are explicitly set to zero in the MRF boundary layer parametrization (see next section for the configuration of the model). By comparing both types of simulations, we can establish how important is the SurFlux in the development and intensification of medicanes. But not only it is possible to examine if the surface heat fluxes are an essential factor for their formation, it is also possible to assess if different patterns of behavior arise depending on how the SurFlux spatial distributions evolve in relation to the medicane trajectory, from genesis to mature state. For that purpose, as surrogates of SurFlux maps, it is determined from CTR outputs the moist enthalpy differences over the Mediterranean between the sea surface level (SST level) and a near atmospheric level (2 m):

$$\begin{aligned} SurFlux &= K_{SST}^* - K_{2m} \\ \text{where } K &= (C_{pd} + r_t C_l)T + L_v r \end{aligned} \tag{4.1.1}$$

In the expression, the star (*) indicates saturation conditions at SST. SurFlux has J kg^{-1} units, and the total water mixing ratio (r_t), in this case, can be approximated to r , the

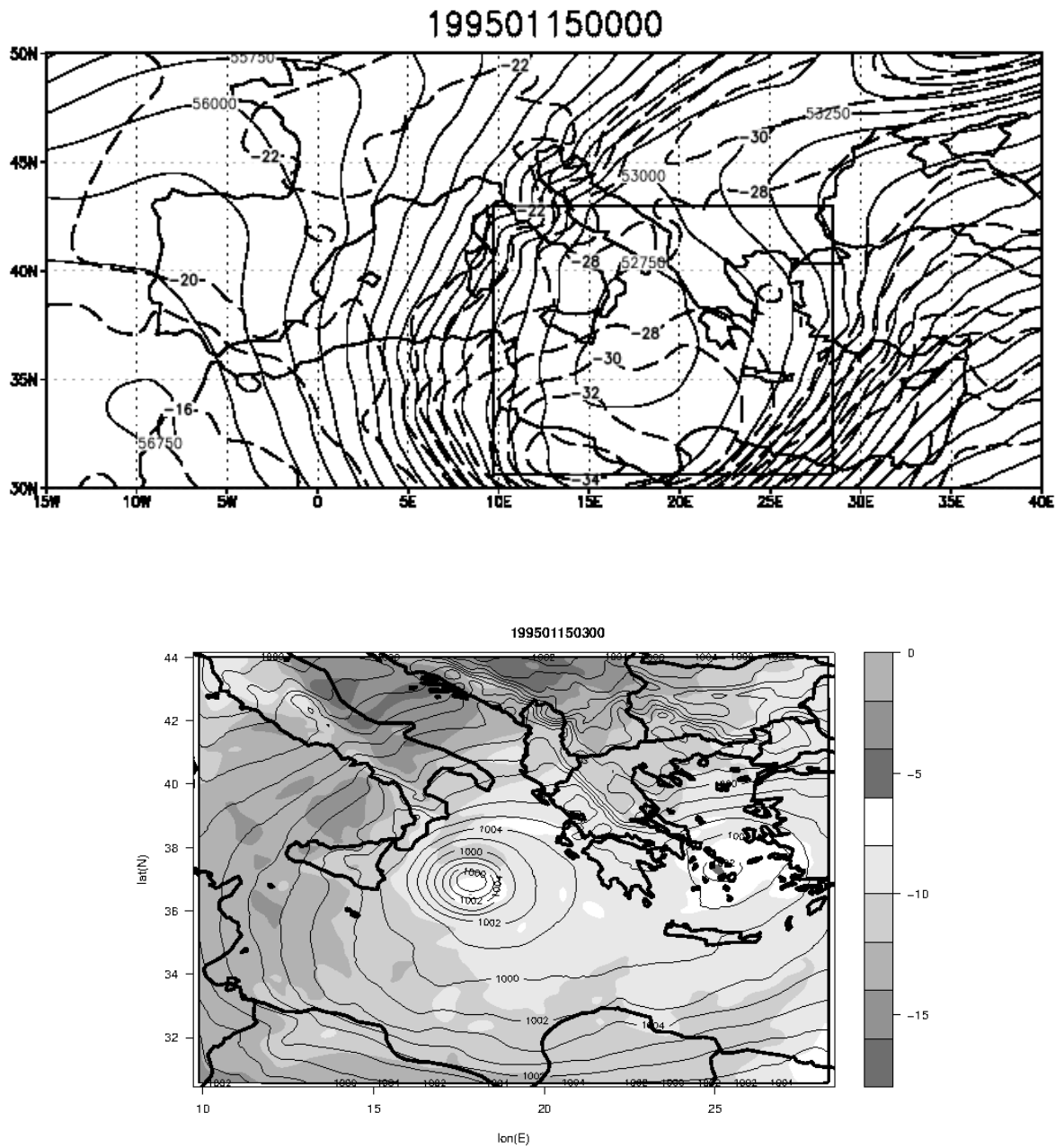


Figure 4.1.1: M06 event. Top: Geopotential height (gpm, continuous lines) and temperature ($^{\circ}\text{C}$, dashed lines) at 500 hPa on January 15th 1995 at 00 UTC. Simulation domain is represented as the square; Bottom: Simulated sea level pressure (every 2 hPa, continuous lines) and temperature at 700 hPa level ($^{\circ}\text{C}$, filled contours according to scale) by the CTR simulation on January 15th at 03 UTC.

vapor mixing ratio. It should be reminded that the moist enthalpy surface fluxes, largely regulated by the difference expressed in the equation, become a key ingredient in the air-sea interaction theory of tropical cyclones (Emanuel, 1986).

Furthermore, the distribution of tropospheric precipitable water (PRWA, in mm) close to medicane environments will be beared in mind during the analysis. This meteorological variable is closely related with SurFlux, specifically with the evaporation from the Mediterranean Sea.

4.2 Capability of the MM5 model to simulate medicane events

The model used in this study is the non-hydrostatic version of the Fifth-Generation NCAR/Penn State Mesoscale Model MM5v3 (Dudhia, 1993; Grell et al., 1995). Each simulation lasts 48 h, starting about 24 h before the mature phase of the observed medicane, and the forecast output is recorded every 3 h during all the period to be sure to include the formation phase of these storms. The simulation domain spans a grid of 196 x 196 points spaced 7.5 km in the zonal and meridional directions and in each case it is centered at the location of the observed mature phase. In the vertical, 31 terrain-following σ levels were used with enhanced resolution in the lower troposphere. The diabatic heating associated with the latent heat released in the convective cloud systems developed during the simulation is particularly relevant in this study. The Kain and Fritsch (1990) convective parameterization scheme was used here. The microphysics scheme Reisner graupel, based on a mixed-phase scheme but adding graupel and ice number concentration prediction equations, is used for the resolved-scale moist processes. For boundary-layer processes, a modified version of the Hong and Pan (1996) PBL scheme, also called MRF, was applied which uses a counter gradient term and K profile for diffusion processes.

Meteorological grid analysis data from the ECMWF were used for the initialization and boundary forcing of the simulations. The best possible horizontal resolution of these analysis was considered, which depends on the year but is about 85 km, and they are available every 6 h (at 00, 06, 12 and 18 UTC). Observations from soundings and surface

stations stored in the Global Telecommunication System (GTS) archive were also ingested to improve the fields according to the initialization scheme explained in detail in Grell et al. (1995), and in this case, the availability is every 6 h for surface data (like analysis data) and 12 h for other levels (at 00 and 12 UTC).

Although from Fig. 4.1.1a it would not be possible to anticipate a medicane development, the CTR mesoscale simulation (Fig. 4.1.1b) evidences the development of a tropical-like cyclone during the simulation period. In this case, the time shown is 03 UTC on January 15th, 1995. A symmetric intense cyclone (with a pressure gradient of 13.82 hPa in 142.5 km) and a warm core is clearly developed to the east of Sicily. The last steps of the simulation period (here every 3 h) are shown in Fig. 4.2.1. After medicane genesis during the late hours of January 14th, the low becomes intense and keeps its symmetry and warm core during the rest of the simulation. The lifetime of this long-lasting medicane was 78 h according to satellite archive, then it is logical that, at the end of the simulation, the cyclone is still quite intense.

Since there is not a clear definition of what is already a medicane just looking at the meteorological fields, it is not practical either to determine precisely the first moment the simulated cyclone can be classified as medicane. Some authors use the cyclone evolution in the phase diagrams developed by Hart (2003). These diagrams permit to classify the cyclones as symmetrical or asymmetrical, and as cold or warm core structures. In the thesis this method is not used because its parameters were adjusted for much bigger cyclones (in the order of tropical cyclones) than medicanes, and also on the basis of lower-resolution grid data. Furthermore, it is not the goal for now to catalog the transition phase from a regular cyclone to a medicane; a mere qualitative assessment of the capability of the model to simulate the medicane is enough for our purposes. Even so, after looking at the simulation of the present case, we will consider that the medicane has been fully developed at 00 UTC January 15th (Fig. 4.2.1). The simulation goes ahead on time of the true event, because satellite images show that mature phase is reached at 18 UTC the same day.

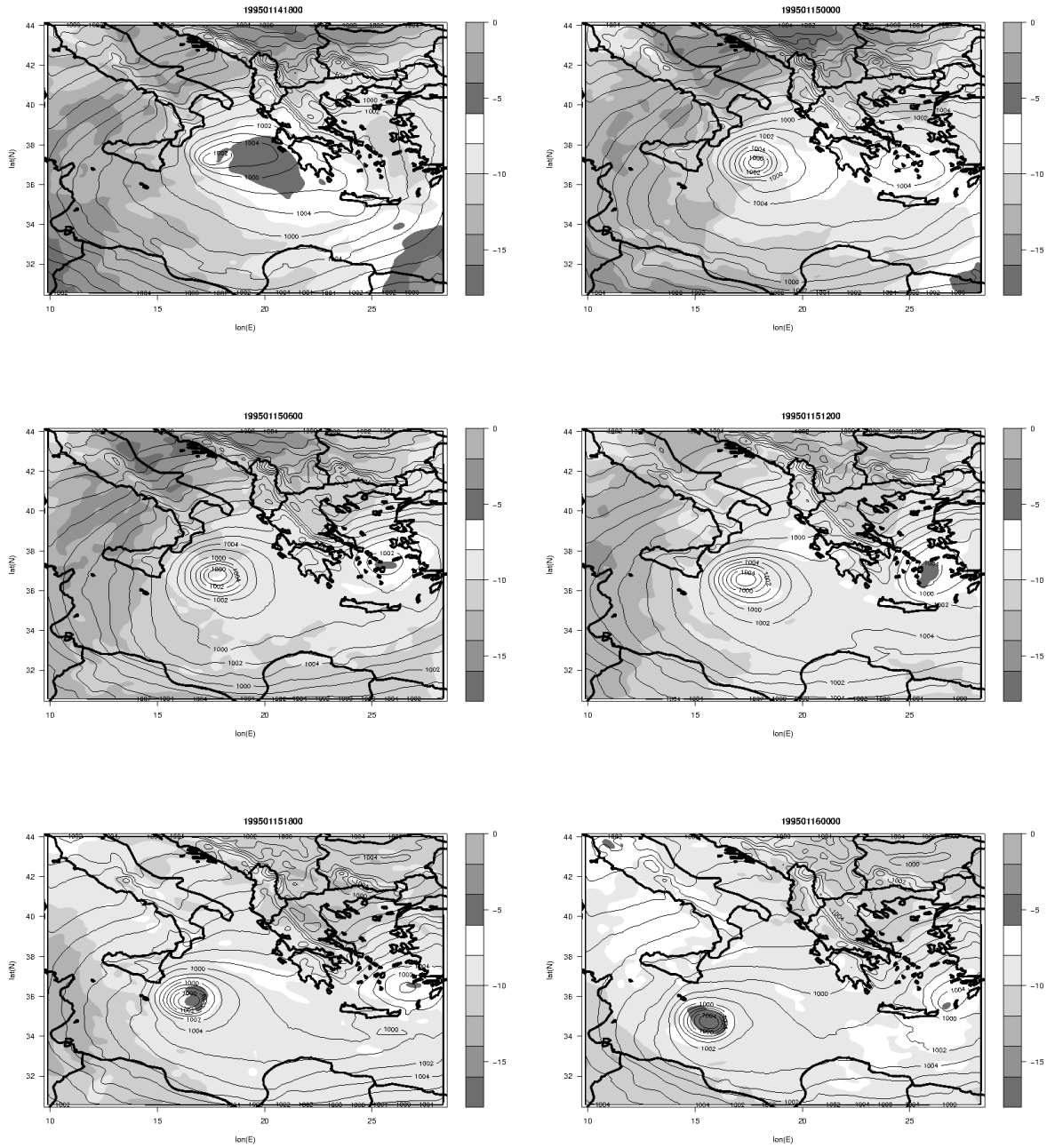


Figure 4.2.1: M06 event. Simulated sea level pressure (every 2 hPa, continuous lines) and temperature at 700 hPa level ($^{\circ}\text{C}$, filled contours according to scale) by the CTR experiment.

4.2. CAPABILITY OF THE MM5 MODEL TO SIMULATE MEDICANE EVENTS

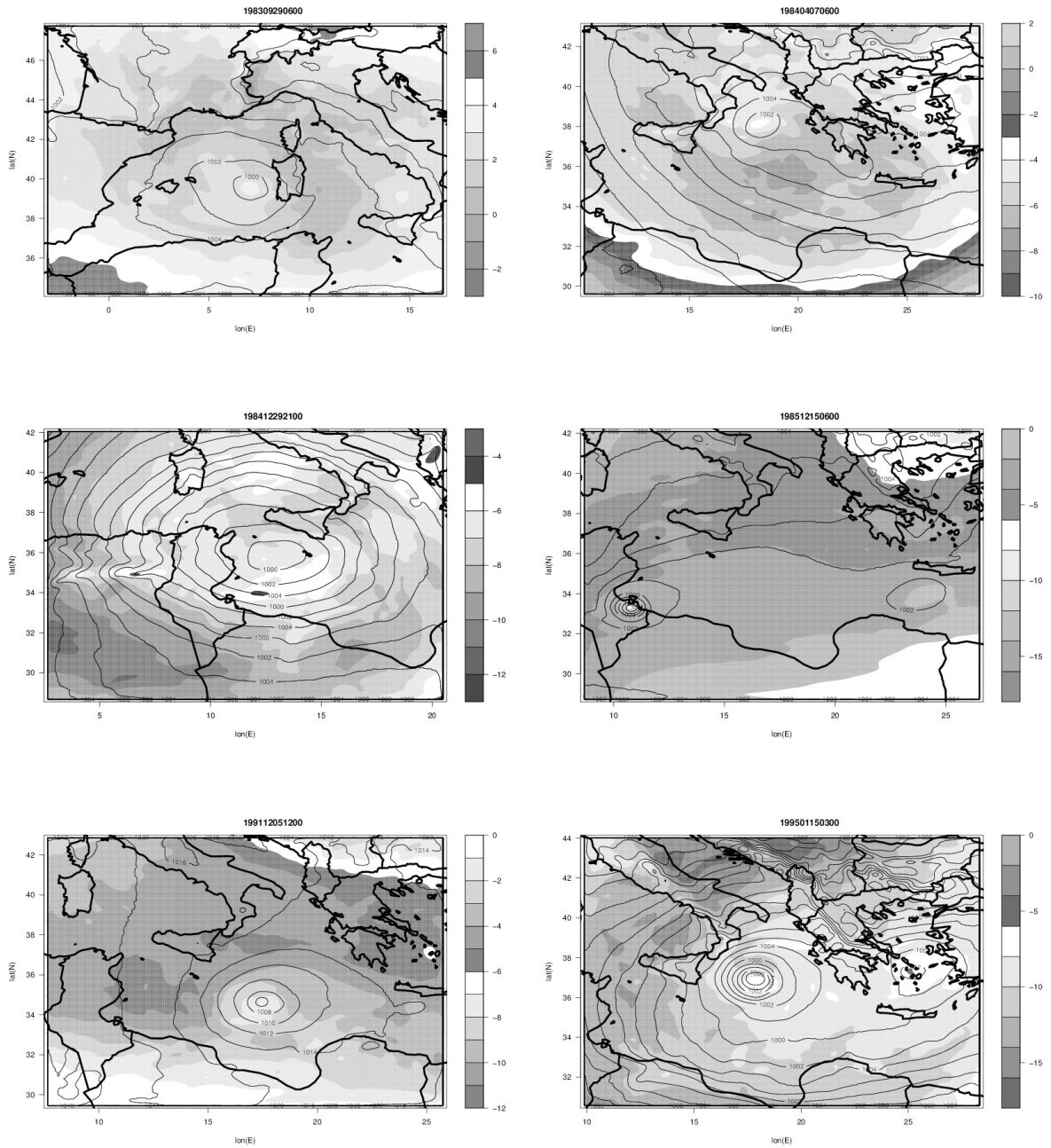


Figure 4.2.2: As in Fig. 4.2.1 but for representative times of M01-M06 CTR simulations (from left to right and from top to bottom, respectively).

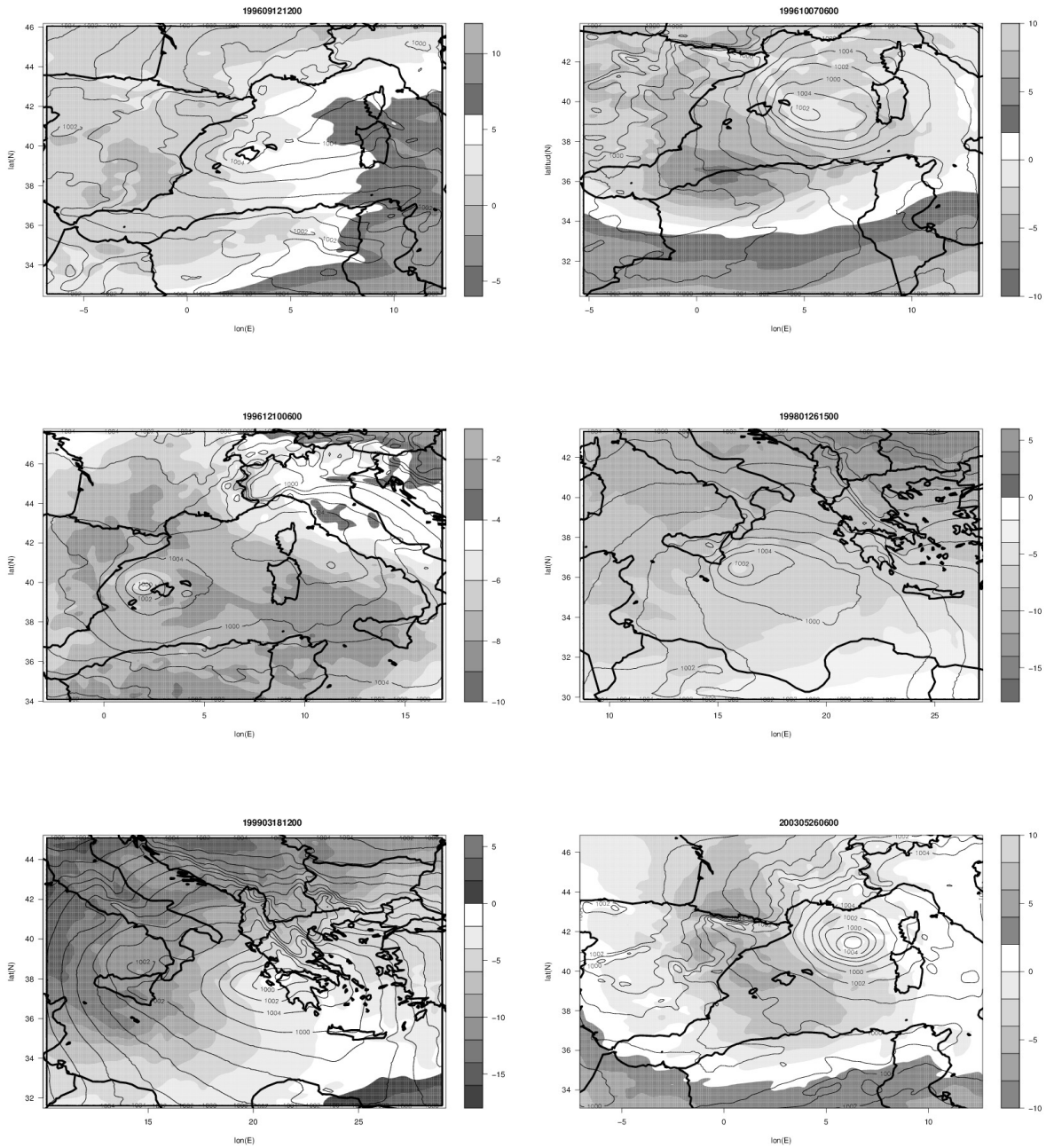


Figure 4.2.3: As in Fig. 4.2.1 but for representative times of M07-M12 CTR simulations (from left to right and from top to bottom, respectively).

4.3 Surface heat fluxes influence

Figs. 4.2.2 and 4.2.3 exemplify the ability of the model to simulate medicane-like storms. Most of the cases are well represented, especially M04, M05, M06, M09 and M12. Even though cases M01, M02, M07, M08, M10 and M11 become less intense, a small cyclone with a warm-core is still simulated, so the model configuration is considered adequate. Just M03 does not evolve into a medicane or a similar structure. M07 and M08 simulated storms have very short lifetimes (significantly less than real events), not enough to properly follow their characteristics. For these reasons, M03, M07 and M08 are discarded for the next steps.

4.3.1 Surface heat fluxes influence on medicane trajectories

In this section, NOFLX simulations are compared with CTR ones. Apart from possible temporal shifts, three main responses are examined: 1) changes in the track position (i.e. medicanes do not follow the same trajectories); 2) in medicane speed (i.e. for the same time, the translation of their centers between two or more time steps differs); and 3) in the lifetime of the cyclone.

The events have been grouped in three different cases depending on which kind of SurFlux influence they exhibit: track location influenced (TR1), speed and/or lifetime influenced (TR2) and no significantly influenced (TR0). M04, M06 and M10 are included in TR1; M02, M05, M09 and M12 as TR2; and M01 and M11 as TR0. For the sake of brevity, only one example of each category is described in detail: M06, M09 and M01, respectively (Fig. 4.3.1).

- TR1. Already at the first simulation steps, CTR and NOFLX simulation differ in trajectories for M06 (Fig. 4.3.1a). NOFLX simulation trajectory lies on the eastern side of the CTR one. This also happens in M04 but not in M10, where the relative positions of the tracks are on the other way around (i.e. westward from CTR). Going back to M06, it is possible to observe a shift between trajectories of about 160 km. This distance is kept approximately constant during most part of the evolution. Furthermore, keeping in mind that the diameter of this medicane is up to 300 km (Fig. 4.2.1), this spatial shift is considerable.

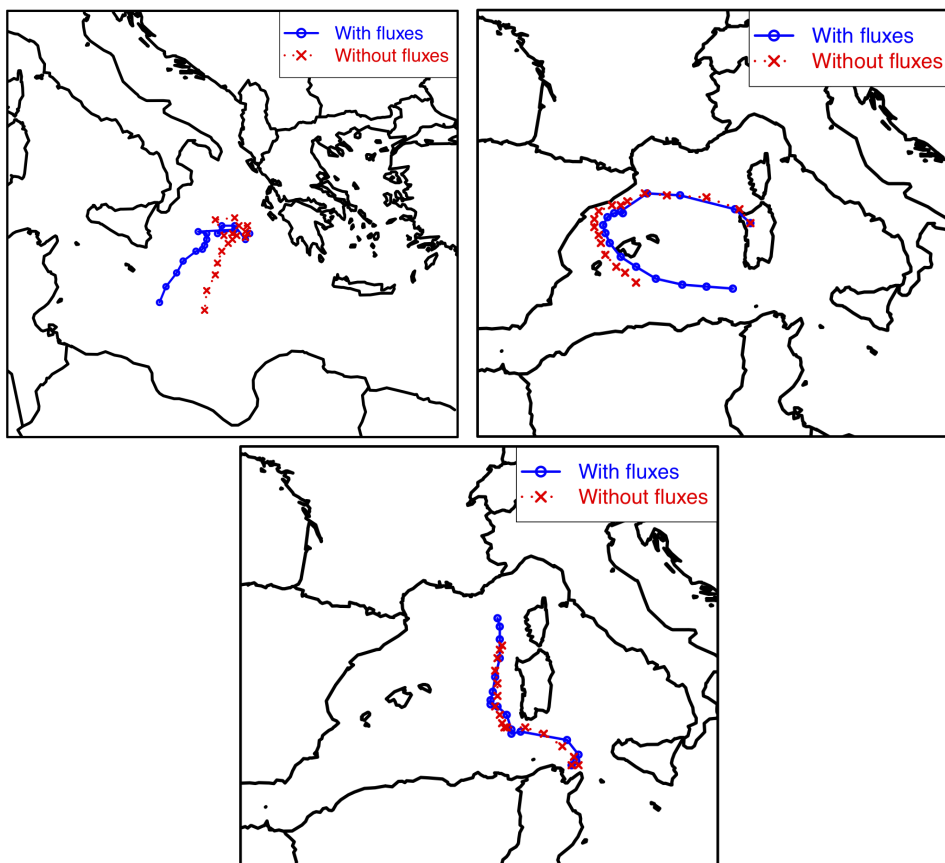


Figure 4.3.1: Examples of how the surface heat fluxes influence the cyclone trajectories for the: Top left, M06 (TR1, location influenced); top right, M09 (TR2, speed and/or lifetime influenced); and bottom, M01 (TR0, no significantly influenced).

- TR2. This group also exhibits some spatial shifts in the medicane tracks (Fig. 4.3.1b), but this difference is much lower than in TR1, while the main effects in this case come from the medicane speed and/or lifetime. Accordingly, both trajectories accumulate a difference in length of 330 km at the end of the simulation. In two cases (M02 and M05), NOFLX simulated cyclone vanishes before CTR (these lifetime differences are 9 and 6 h, respectively). Despite this, taking as reference the last common timestep, there is also a significant difference in track lengths between both simulations. These differences in the storm speed are specially notable towards the end of the track (see Fig. 4.3.1b).
- TR0. Finally, the TR0 group (Fig. 4.3.1c) exemplifies a non significant difference between CTR and NOFLX simulations, i.e. a small effect of surface heat fluxes on medicane trajectory.

4.3.2 Surface heat fluxes influence on medicane intensification

To analyze the surface heat fluxes influence on medicane intensification, the central minimum sea level pressure of the simulated cyclones is considered. Therefore, this value is tracked along the full cyclone trajectory whenever it is possible to recognize a cyclonic structure, not necessarily with pure medicane characteristics.

The results confirm the cyclogenetic action of the surface heat fluxes on this kind of storms (Fig. 4.3.2). As in the previous section, it is possible to recognize three distinct kinds of influences. The first one consists of small differences in pressure values at the beginning of the development (although CTR simulations have lower values), followed by a big drop just in CTR and a slight recovery (or filling of the disturbance) but not reaching NOFLX higher values (IN1). The second kind of influence (IN2) is a growing difference between minimum pressures during the full cyclone lifetime. This difference can be higher or lower depending on the event, but at the end of the simulations, there is noticeable disparity in cyclone intensity. Finally, the last group comprises the low influence cases (IN0). The same events used to explain the influences on trajectory (M06, M09 and M01) are also useful in this section.

- IN1. M06 CTR simulation is shown in Fig. 4.3.2a as an example of IN1, presenting much lower values than NOFLX during all the period. The high deepening rate in

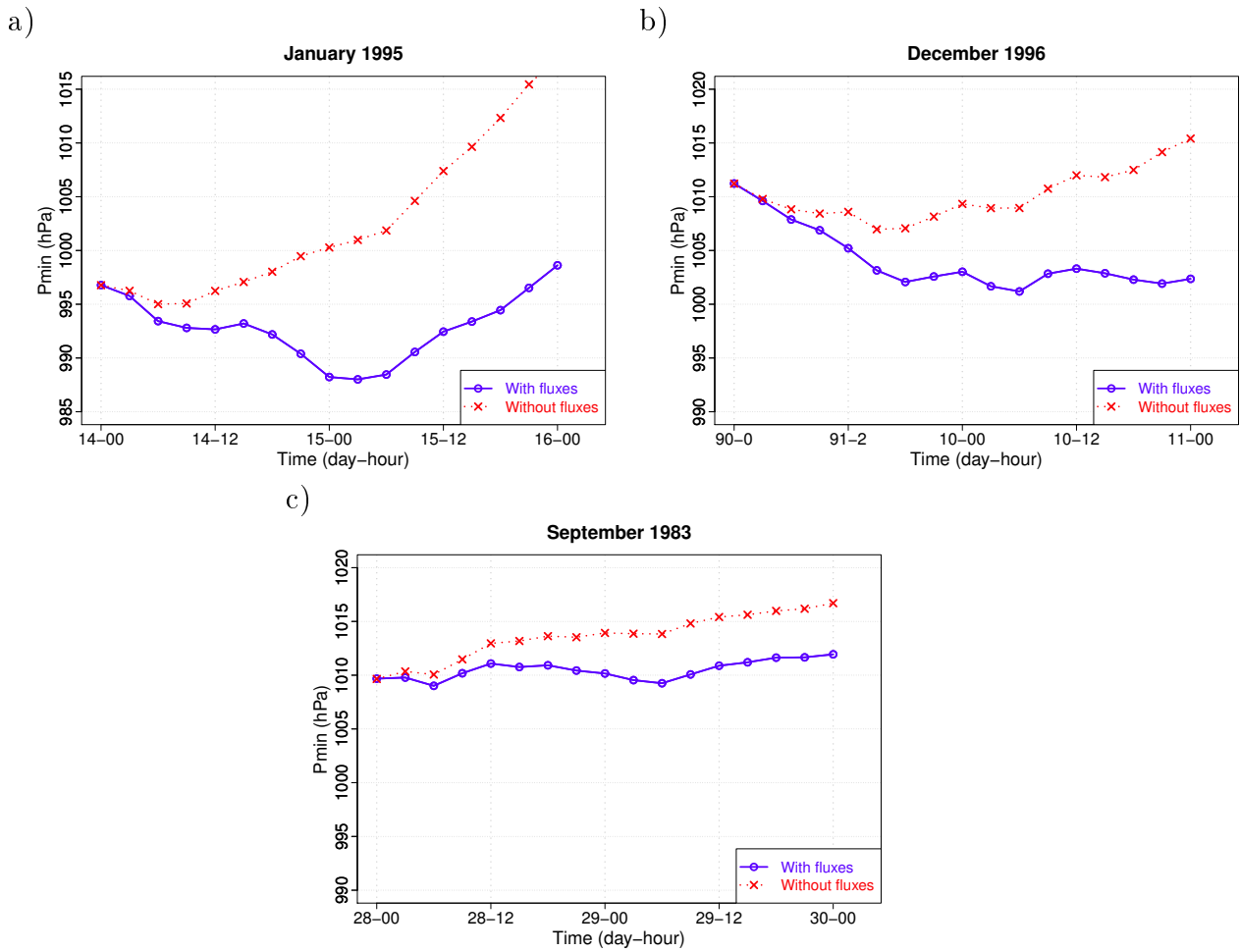


Figure 4.3.2: Examples of how the surface heat fluxes influence the cyclone intensification for the a) M06 (IN1, big drop just in CTR), b) M09 (IN2, growing difference) and c) M01 (IN0, low influence).

CTR starts on January 14th at 15 UTC, leading to a minimum central pressure of 988 hPa on January 15th, at 03 UTC. It is not until 15 UTC that the system has filled and the initial values are restored. The minimum central pressure value in NOFLX is reached at the third time step of the simulation, so it can be seen that the system is ineffective in gaining intensity during the simulation. On January 15th at 03 UTC, the central value is 1001 hPa, 13 hPa higher than in CTR.

- IN2. A case of growing difference between the cyclone pressure minima can be seen in Fig. 4.3.2b. At the moment when CTR medicane has its minimum values (that is on December 10th at 06 UTC), there is a gap of 7.2 hPa with respect to the NOFLX weaker cyclone. At the end of the simulation, this difference grows up to 13.0 hPa.
- IN0. Lastly, simulations as M01 (Fig. 4.3.2c), do not present a notable difference between simulated central pressures, just slight changes (it is logical to understand that cyclone intensification is positively related with heat fluxes although this dependence is not as crucial in this case). In CTR simulation it is possible to determine two minima: the first one, as it happened before, occurs during the first time steps, so it will be not considered because the system is still under the influence of the spin up process of the model; and the second one, occurring on September 29th at 06 UTC, is taken as representative of the medicane. In this case, the central pressure does not drop too much, and the minimum value is fixed at 1009.2 hPa. At the end of the forecast period, when the difference between the two simulations is maximum, it is of 4.8 hPa. As it has been noted, these values are weaker than in the other cases.

4.3.3 Interpretation in terms of precipitable water and SurFlux distributions

Once confirmed the different types of SurFlux influences on medicane properties, it is time to analyze the connection with the spatial patterns of the physical variables. To this end, the SurFlux potential distribution via Eq. 4.1.1 is compared with precipitable water maps in CTR and NOFLX simulations. The same events used in previous sections are also studied here (Figs. 4.3.3-4.3.5).

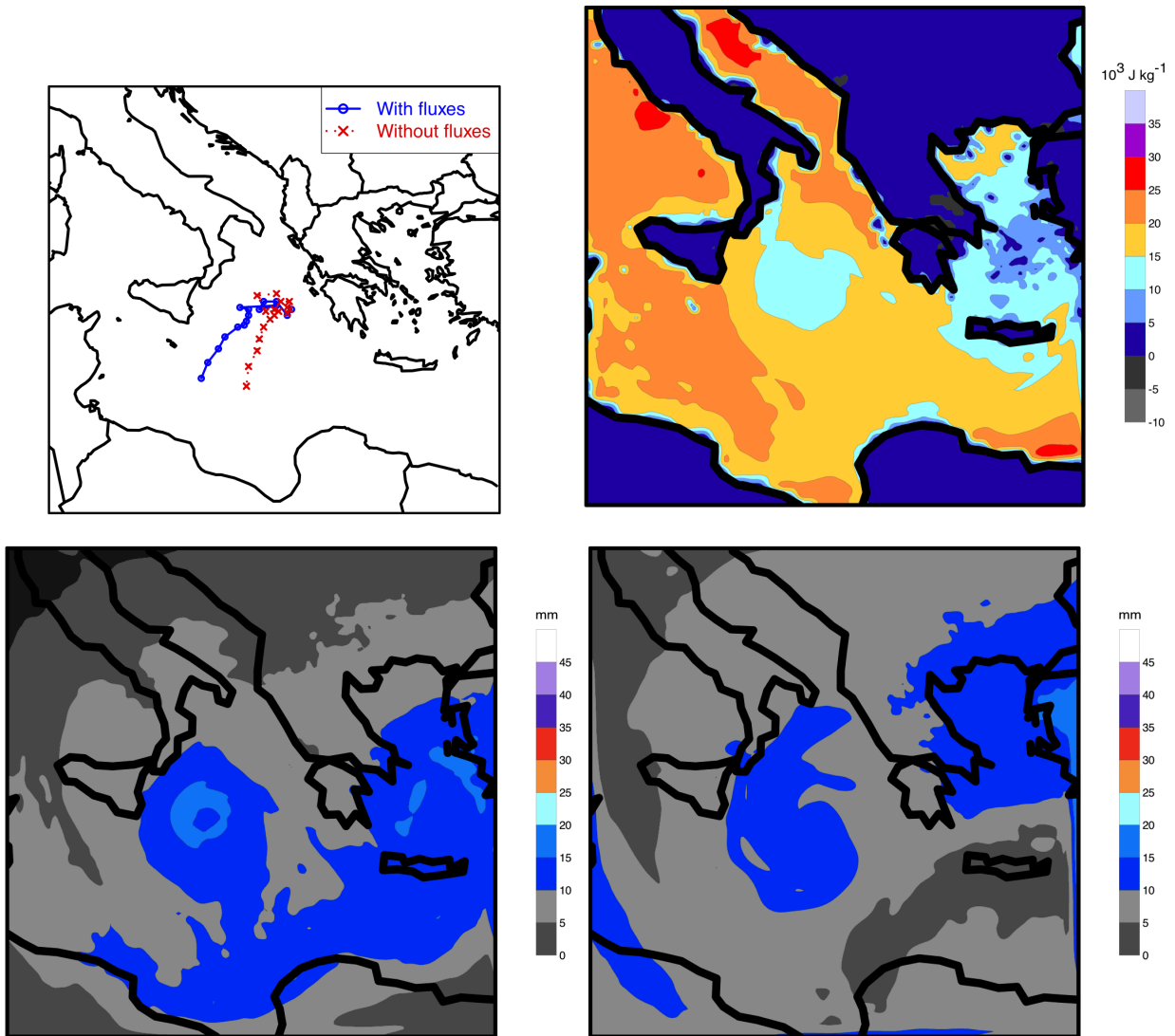


Figure 4.3.3: M06 event (on January 15th 1995 at 12 UTC), representative of TR1 and IN1 classes. Top left: trajectories with and without fluxes (blue and red, respectively). Top right: SurFlux potential (filled contours, in 10^3 J kg^{-1}). Bottom left: PRWA in CTR simulation (filled contours, in mm). Bottom right: PRWA in a NOFLX simulation (filled contours, in mm).

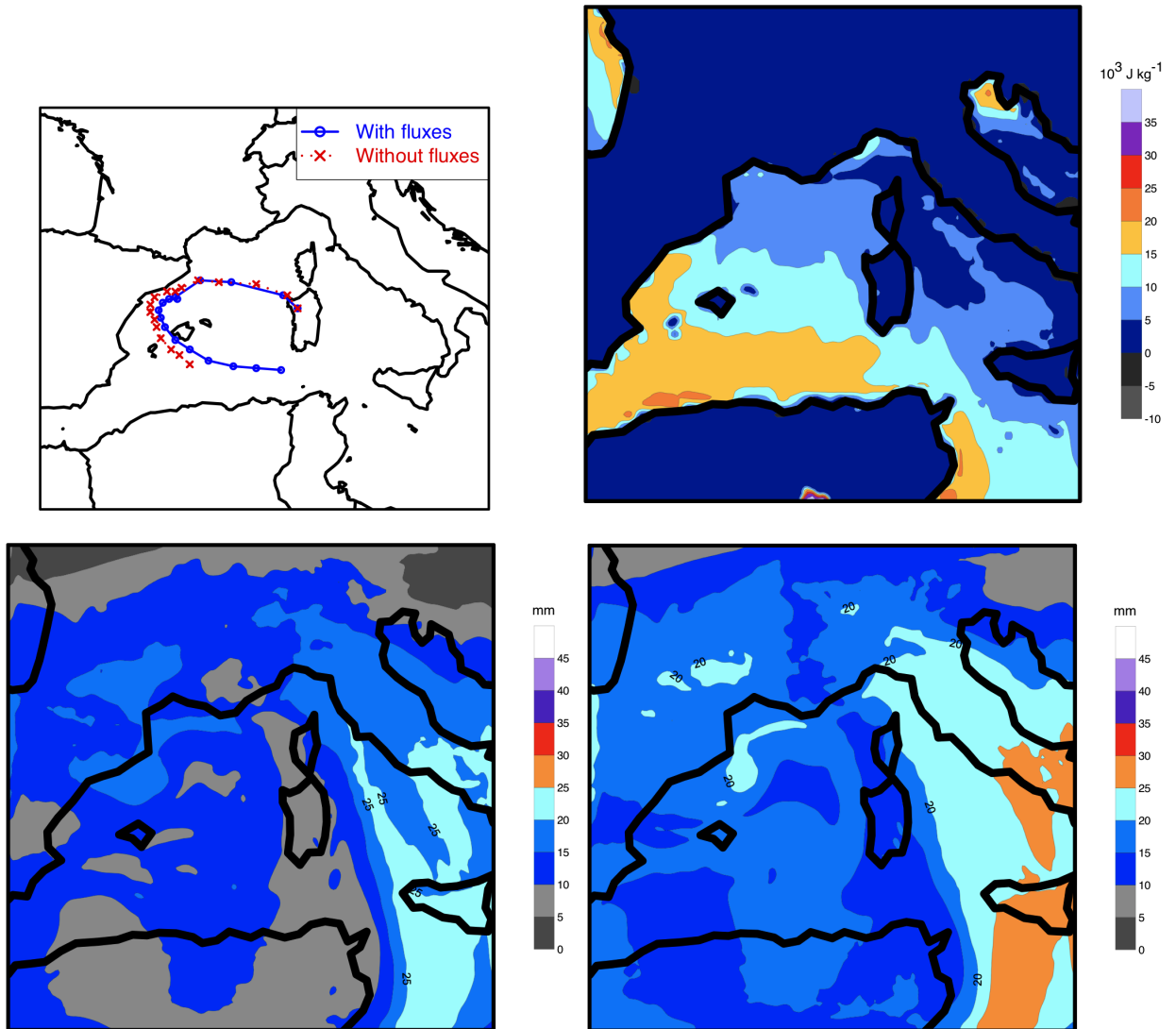


Figure 4.3.4: M09 event (on December 10th at 12 UTC), representative of TR2 and IN2 classes. Top left: trajectories with and without fluxes (blue and red, respectively). Top right: SurFlux potential (filled contours, in 10^3 J kg^{-1}). Bottom left: PRWA in CTR simulation (filled contours, in mm). Bottom right: PRWA in a NOFLX simulation (filled contours, in mm).

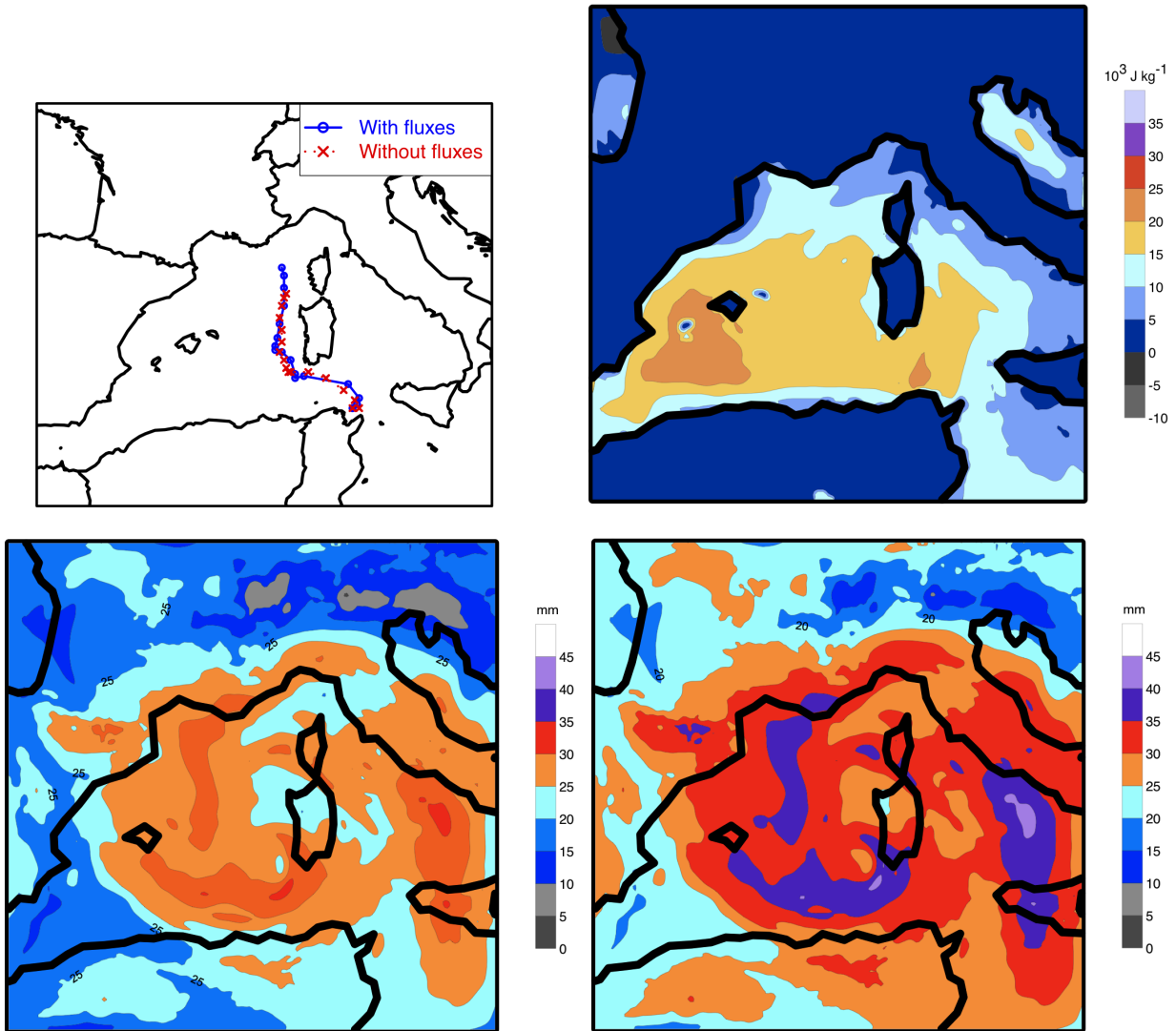


Figure 4.3.5: M01 event (on September 29th 1983 at 00 UTC), representative of TR0 and IN0 classes. Top left: trajectories with and without fluxes (blue and red, respectively). Top right: SurFlux potential (filled contours, in 10^3 J kg^{-1}). Bottom left: PRWA in CTR simulation (filled contours, in mm). Bottom right: PRWA in a NOFLX simulation (filled contours, in mm).

At the beginning of the M06 CTR simulation, low values of SurFlux occur where the parent cyclone is developing. Upper level dynamical forcing drives the cyclone to the west, where there are higher values of SurFlux, especially the latent flux contribution (not shown). Consequently, the convection increases. Faster surface winds are present, and this stimulates further the evaporation. Very high values of PRWA are concentrated in the environment around the cyclone center. The central pressure decreases and it becomes a deep small warm-core cyclone or medicane (Fig. 4.3.3). After a while, when the fluxes become lower around the cyclone position and the neighboring regions, the intensification stops, and the cyclone dynamics is determined by the large-scale circulation. In the NOFLX simulation, PRWA values are lower than in CTR one during all the simulated period, so the moist convection is less promoted and latent heat release in the troposphere is more limited. Consequently, a weaker cyclone largely influenced by the general circulation is developing in these circumstances.

In M09 case, surface potential fluxes are lower than in M06 CTR and quite uniform in distribution along the medicane path (Fig. 4.3.4). Due to this fact, the evaporation from the Mediterranean is lower and the resulting convection is not so powerful. PRWA has lower values than in the previous event, too. For these reasons, it is not possible for the cyclones to become as intense as in M06. Nevertheless, fluxes are still significant and higher values occur in the cyclone environment when it migrates southwards towards the end of the simulation, coinciding with the time period when the differences between CTR and NOFLX simulations are the largest. PRWA values are quite similar in CTR and NOFLX along the cyclone track.

In M01 CTR, higher values of SurFlux potential are found between the Iberian peninsula and the Balearic Islands, far from cyclone track (Fig. 4.3.5). After that initial period, departures in medicane properties between the two simulations remain nearly constant.

4.4 Conclusions

MM5 simulations with a horizontal resolution of 7.5 km seem to be appropriate to characterize medicane precursor situations. Most of the simulated cases show the development of an axi-symmetrical intense cyclone with a warm core. These experiments have permitted us to examine in some detail the physical mechanism involved in their

M01	M02	M03	M04
M05	M06	M07	M08
M09	M10	M11	M12

Table 4.1: Summary of sensitivity test. Influence on medicane trajectory: light, moderate and dark shaded circles indicate TR1, TR2, TR0 type results respectively (see text). Influence on medicane intensity: light, moderate and dark shaded backgrounds indicate IN1, IN2 IN0 type results respectively (see text). White boxes indicate the three medicane events that produced inadequate CTR simulations.

development and dynamical properties, as well as to make a sensitivity analysis to test and describe the air-sea interaction mechanism operating on them.

Surface heat fluxes and tropospheric precipitable water magnitudes and distributions influence medicane tracks, speed or lifetime. This influence can be on just one of these characteristics or on a combination of them, although occasionally it is almost indistinguishable, especially in those cases insufficiently matured in the simulations. The intensification of central pressure gradient in medicanes is also shown to be positively influenced by surface heat fluxes and precipitable water when the cyclone moves over areas with high sea-atmosphere moist enthalpy differences. A schematic summary of the sensitivity tests is included in Table 4.1. In general, there is a tendency for the surface heat fluxes to exert the same degree of influence (low, medium or high) on both the medicane trajectory and medicane intensity, although with some exceptions.

These results reinforce the idea of an important role of air-sea interaction for medicane development, but a crucial factor for this special type of mid-latitude warm-core cyclone seems to come from the synoptic-scale dynamical forcing.

Part III

ASSESSING MEDICANE RISK UNDER CLIMATE CHANGE

Chapter 5

Oriented dynamical downscaling¹

Oriented dynamical downscaling consists of nesting mesoscale simulations (i.e. forcing the domain boundaries with larger scale environments), in order to improve the resolution of the study area, but only in those areas and times with high probability of medicane development.

5.1 Introduction

According to Eq. 3.2.2, global warming can theoretically influence the maximum potential intensity of tropical cyclones through alterations on the surface energy flux and/or the upper-level cold exhaust (Emanuel, 1987; Lighthill et al., 1994; Henderson-Sellers et al., 1998). Observations of tropical and subtropical SST have shown an overall increase of about 0.2°C over the past 50 years. Emanuel (2005b) reports a very substantial upward trend in potential destructiveness or total power dissipation (i.e. the sum over the lifetime of the storm of the maximum wind speed cubed) in the well-sampled North Atlantic and western North Pacific, with a near doubling over that period (Webster et al., 2005). The further increase of potential intensity associated with global warming as predicted by GCMs (Emanuel, 1987) is consistent with the increase in modeled storm intensities in a warmer climate (Knutson and Toleya, 2004). In the Mediterranean, SST has increased

¹The content of this chapter is partially based on the paper Tous, M. and R. Romero, *Meteorological environments associated with medicane development*, Int. J. Climatol. 33 (2013), pp. 1-14.

around 0.6°C in the western and 1°C in the eastern basin in the last 20 years (Nykjaer, 2009). GCMs used in climate change research do not have sufficient spatial resolution yet to allow resolve explicitly depressions with the size of medicanes, but their outputs can be useful in monitoring expected changes of the large-scale environments. As it was derived in Chapter 3, high values of the empirical genesis index GENPDF are associated with medicane development. For this reason, the evaluation of the risk in this chapter is only applied in areas and time periods presenting high probability of medicane development (that is, high values of the index) instead of a general dynamical downscaling, saving computational cost.

In this case, we are going to use the MM5 mesoscale model with enough resolution to simulate medicane events even if the forcing data (in this case, GCMs) are too coarse to represent them directly, but keeping the consistence of the climatic conditions over the area, both in present and future climates. In essence, in the new technique, only medicane favorable days extracted from GCM-scenarios will be simulated in order to obtain probabilistic risk maps. The future maps will be compared against the “present” climatologies to project expected changes in medicane risk imposed by global warming.

5.2 First climatological analyses

Among the available GCM runs from the IPCC 2007 report, the resolution of the model was especially taken into account. For this reason, ECHAM5/MPI-OM (Roeckner et al. (2003), with an atmospheric resolution of 1.8° lat-lon), CSIRO-MK3.0 (Gordon et al. (2002), 1.8° lat-lon), and GFDL-CM2.1 (Delworth et al. (2006), 2° lat, 2.5° lon) are the selected models for this study. The analysis of the outputs obtained for 1981-2000 and 2081-2100 will be representative of the historical and future climates (hereafter referred to as 20C and 21C, respectively) under the “high” special report on emissions scenarios (SRES) A2 scenario (Nakicenovic, 2000). The calculated climatologies from 20C are first compared against the climatology of GENPDF derived from ERA-40 for the same period and then the changes across the century are analyzed. As mentioned previously, high values of this index would represent a higher probability of having environmental conditions favorable for medicane development. For this reason, the first analyses are focused on the exceedance over an extreme value of the index, in this case the 95 quantile calculated for the whole Mediterranean and the whole 20C period from ERA-40 database

($q_{95}ERA40=3.6$). In addition, the Mediterranean has been divided into three sectors: the Western, Central and Eastern regions, for a better summary of the results. These regions extend from Gibraltar Strait to Sicily, from this island to Greece, and east of Greece, respectively.

Figure 5.2.1 compares the four climatologies for the historical climate. All models show that high values of GENPDF are more frequent in autumn and winter than in spring and summer. The GCM models reproduce reasonably well the “observed” annual cycle of GENPDF in the three Mediterranean regions. Taking into account the high nonlinearity in its formulation (Eq. 3.2.3), the above result implies that the combination of the AVOR850, RH600, VSHEAR8525 and MAXWS ingredients is also well represented. ECHAM5 and GFDL are more similar to ERA-40 than CSIRO, which tends to underestimate the extreme values of this parameter. The lower exceedance of extreme values in Eastern Mediterranean appears to be consistent with the observed fact that medicanes tend to occur in the Western and Central regions.

Figure 5.2.2 represents the change in frequency of extreme values of GENPDF (higher than $q_{95}ERA40$) between the 20C and 21C periods for each model, in principle with greater confidence in ECHAM5 and GFDL according to the previous results. Thus, ECHAM5 reveals that the frequency of extreme values of GENPDF tends to be lower in future than in historical climate. In warm seasons, this change is not appreciable because the already low exceedance values remain low in the future, but in cold seasons, when medicanes are most frequent, the monthly frequency decays up to 5%. The GFDL model, which tends to be similar to ERA-40 in the Central and Eastern regions, shows a slight frequency increase in September in Central region and a decrease in winter in both regions. In the Western part, there is a high increase in late summer and early autumn and an equally important decrease in winter. However, it is important to remember that in this region, the 20C analysis (Fig 5.2.1) showed a frequency about 5% lower than ERA-40 results. Finally, CSIRO model shows too low frequency values in 20C and in future projection these values do not change significantly.

December was chosen for the spatial distributions illustrated in Fig. 5.2.3 because it is the month with greatest number of medicanes (Fig. 2.4.2). A first comparison between the 20C and 21C climatologies using ECHAM-5 reveals that GENPDF monthly means (like the frequency of extreme values) decrease in winter. This is in spite of the SST increases of as much as 3°C in the ECHAM-5 simulations, that might suggest an increase in GENPDF

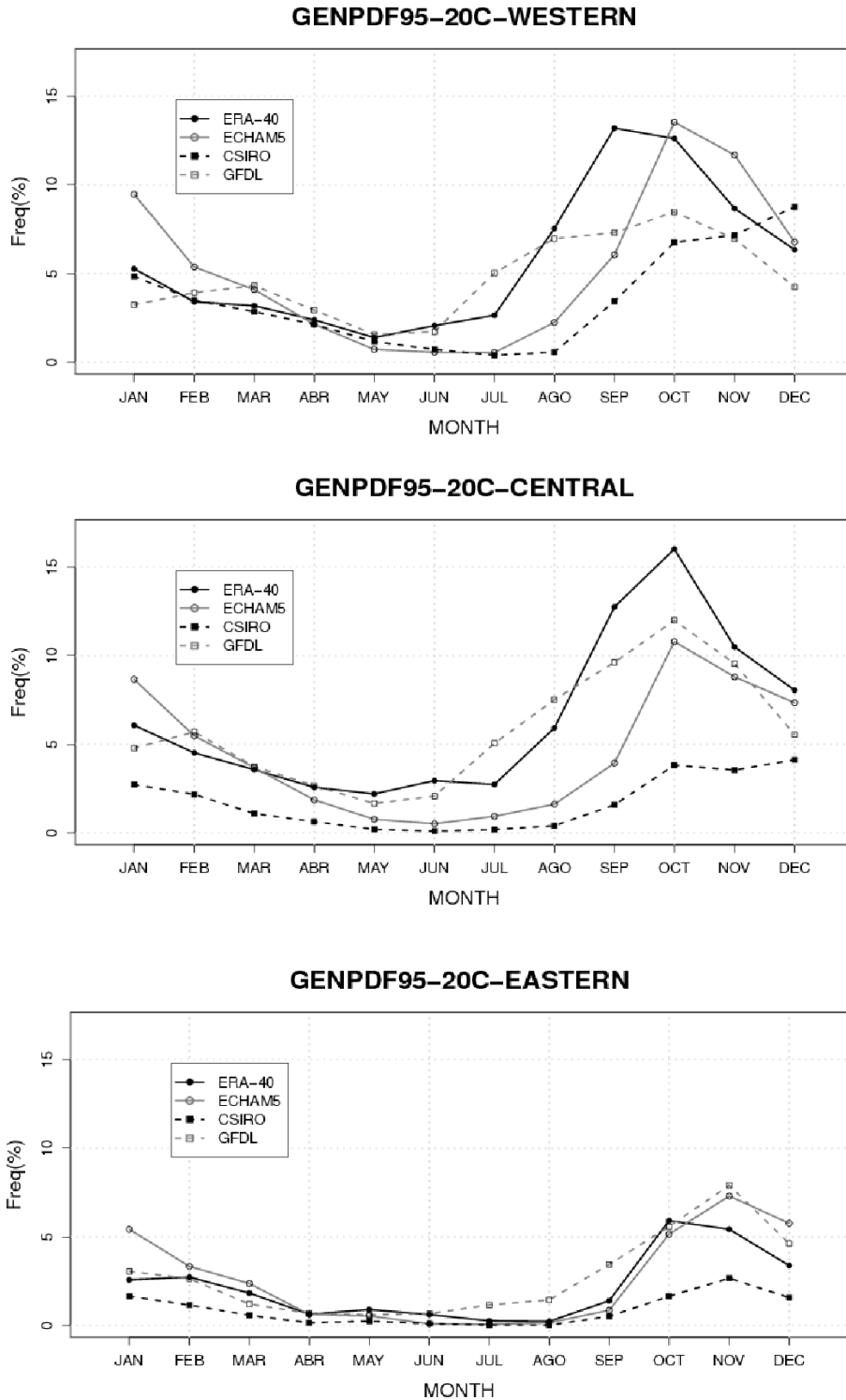


Figure 5.2.1: Monthly mean frequency of days where GENPDF is higher than q95ERA40 in 20C period according to ERA-40 (solid black line), ECHAM5 (solid grey line), CSIRO (dotted black line) and GFDL (dotted grey line) in Western (top), Central (middle) and Eastern (bottom) regions.

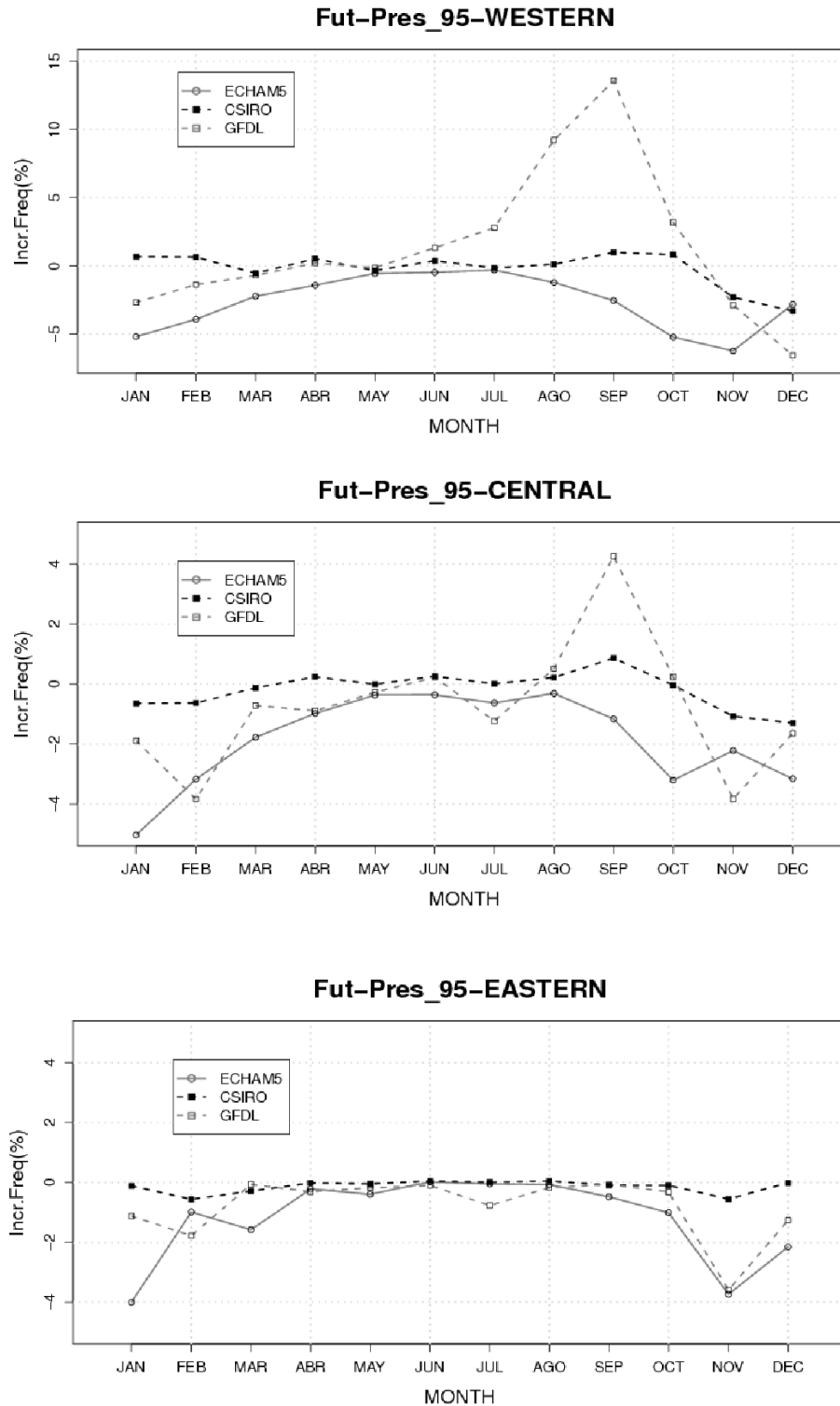


Figure 5.2.2: Changes in the monthly mean frequency of days where GENPDF is higher than q95ERA40 between the 20C and 21C periods according to ECHAM5 (solid grey line), CSIRO (dotted black line) and GFDL (dotted grey line) in Western (top), Central (middle) and Eastern (bottom) regions. Figures with different vertical scale to improve clarity.

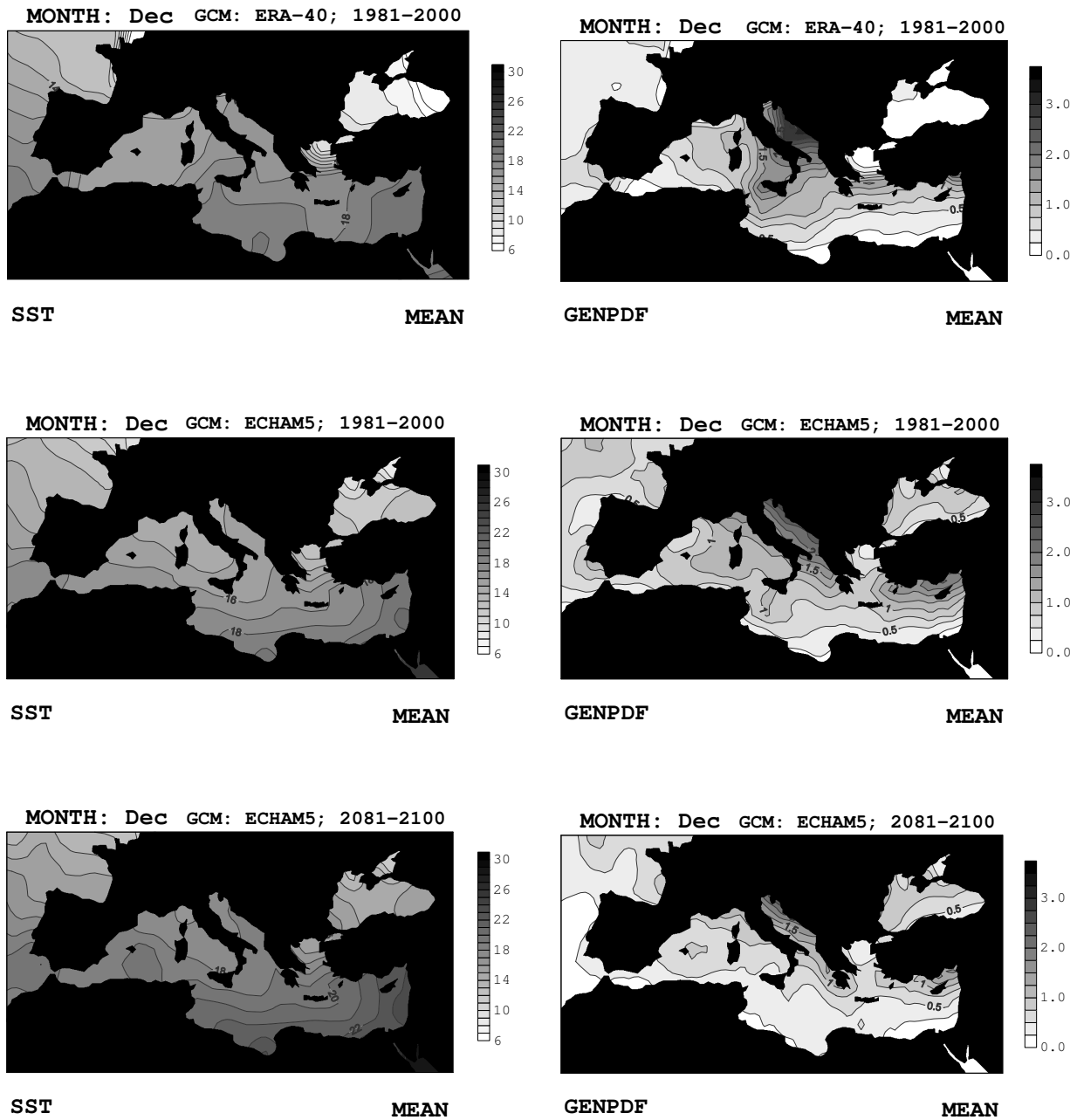


Figure 5.2.3: Spatial distribution of mean value of SST (left) and GENPDF (right) for December in the 20C using ERA-40 (top), 20C using ECHAM-5 (middle) and 21C using ECHAM-5 (bottom).

according to Eq. 3.2.3. But the complexity of the GENPDF formulation makes it evolve in the opposite way and the result is a general decrease in the probability of cold season medicane genesis. Similar deductions can be made using CSIRO and GFDL models (not shown). These results are in agreement with projected scenarios by the IPCC and other regional studies that show a lower frequency of cold low intrusions from high latitudes into the Mediterranean area (Sumner et al., 2003) and, consequently, a lower frequency of favorable meteorological conditions for medicane development. Additional statistical products and all the monthly maps can be found in <http://medicanes.uib.es>.

5.3 Capability of the MM5 model to simulate medicanes using low resolution inputs

As it was proved in Chapter 4, MM5 is able to simulate medicanes using the best possible horizontal resolution of ECMWF analyses (about 85 km) and observations from soundings and surface stations, for the initialization and boundary forcing of the runs. For our present purposes, it is necessary to test if coarser data, without observations, is enough to simulate medicanes. For this goal, ECMWF analyses data have been interpolated at lower resolution until 2.4° lat-lon grid length (about 250 km) and the medicanes listed in Table 2.1 have been tested for simulation again, expecting the same identifying attributes: quasi-symmetric intense low-pressure centers at sea level with an isolated warm-core structure aloft.

Figure 5.3.1 represents two examples of how the MM5 simulates this kind of events depending on the forcing data resolution. In all cases, medicane structures can be identified. In the first example (M06 in Fig 5.3.1), the coarsest resolution input data produces a smaller and less intense medicane, but the presence of the characteristic features is clear. Furthermore, it is able to develop a second medicane close to Crete. Even though this second medicane is not listed in our database, an accurate look at satellite images permits to identify a cyclonic center at that position (Fig. 5.3.2). In fact, this second cyclone center was not considered a medicane because its lifetime was too short (less than 6 h) and, in satellite images, its structure was not completely isolated. Moving again on Fig. 5.3.1, it is also remarkable the high intensity of the M09 simulated cyclone at both extreme resolutions. Therefore, we can conclude that MM5 simulations

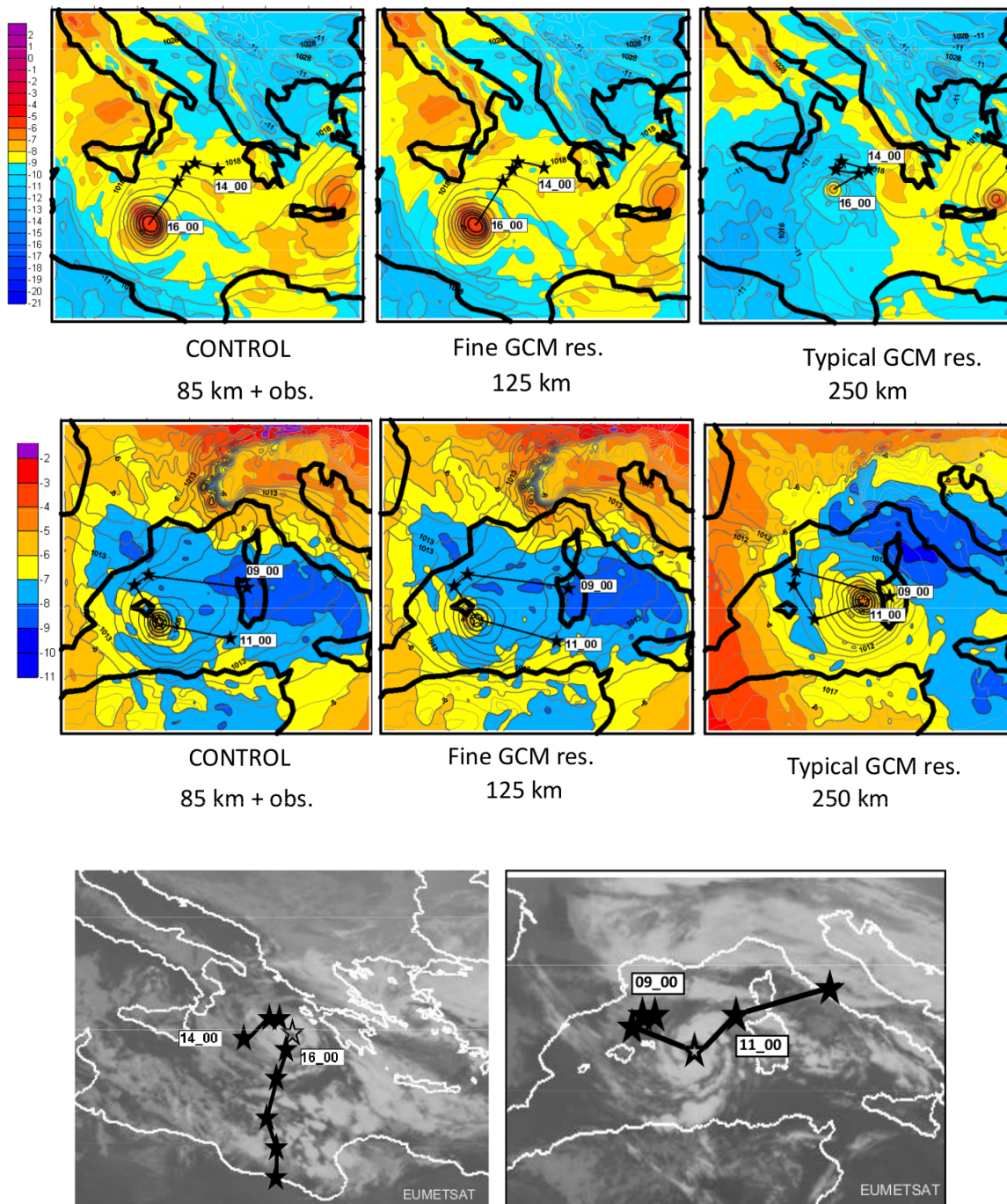


Figure 5.3.1: M06 (top) and M09 (middle) simulated medicanes at the time of maximum intensity using different resolution inputs: best resolution plus observations (left), resolution similar to a fine GCM (1.2° lat-lon; middle) and typical GCM resolution (2.4° lat-lon; right). Contoured lines represent the MSLP and colored contours, temperature at 700 hPa. On the bottom, satellite images of these events (M06 left, M09 right).

5.3. CAPABILITY OF THE MM5 MODEL TO SIMULATE MEDICANES USING LOW RESOLUTION INPUTS

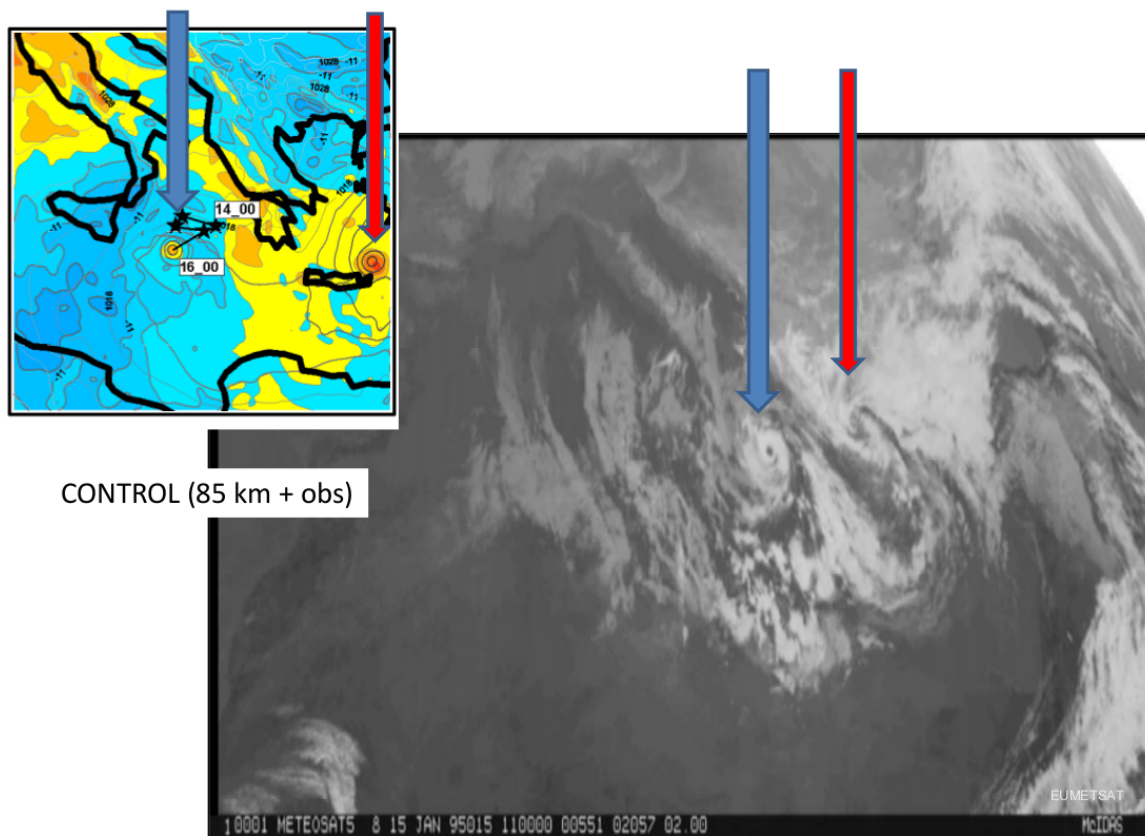


Figure 5.3.2: Comparison between a simulated event in MM5 model (using ECMWF analyses and observations as input data) and satellite data, regarding the M06 event.

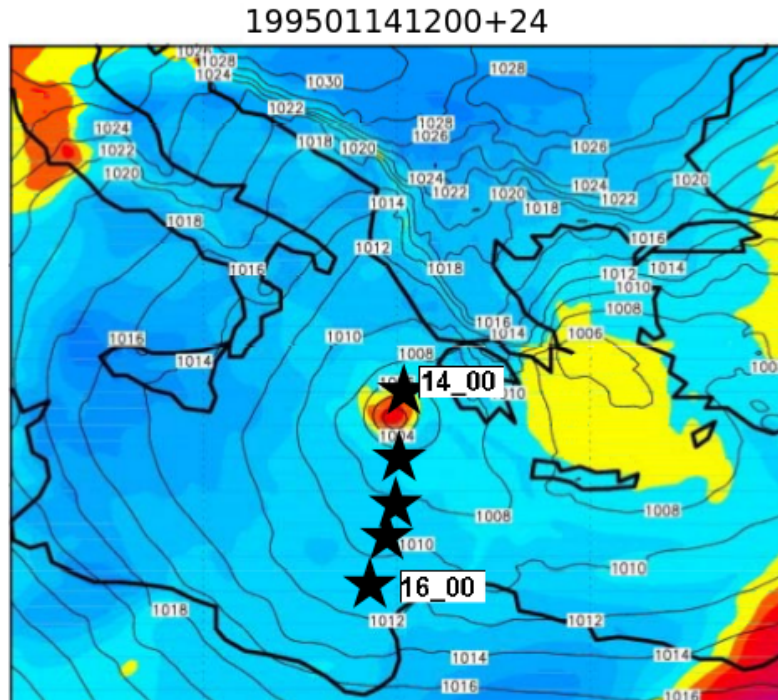


Figure 5.3.3: Simulated M06 medicane at the time of its maximum intensity using the deterministic forecast mode of the IFS TL1299L90Cy36r2 (ECMWF) as input data for the MM5 model.

at 7.5 km (and with the same configuration used in Chapter 4) forced with large-scale fields of different horizontal resolutions, including typical resolutions of GCMs, are able to develop medicane-like structures.

In addition, experiments with the deterministic forecast mode of the Integrated Forecast System (IFS) from the ECMWF (TL1299L90Cy36r2) as input data were also carried out. This data has a horizontal resolution of about 16 km, and thus provides an idea of the MM5 response using very high resolution input data. Best results are obtained for M06 (Fig. 5.3.3). An isolated small warm-core minimum pressure center is simulated in early stages of the run. Its track is similar to that derived from satellite images (Fig. 5.3.1). Although the symmetry and the isolated warm-core structure are clear, the simulated cyclones are smaller in size and weaker in intensity than in the previous simulations.

5.4 Guiding the downscaling

The use of the q95ERA40 threshold (Section 5.2) to screen medicane from non-medicane days would produce a very large amount of days to be simulated, rather inconsistent with the observed frequency of only 0.5 medicanes per year according to the database built in Chapter 2. If the medicane definition criteria are relaxed and some other similar cyclonic structures are also included, the observed frequency would be increased. Independently, an study performed by Cavicchia et al. (2014a) establishes the mean frequency of medicanes to 1.6 events per year. Accordingly, the GENPDF threshold has been arbitrarily increased to quantile 99 (q99ERA40) of ERA-40 total distribution, which corresponds to a value of 12. As it will be shown in the results, this threshold is more consistent. The frequency of medicane-prone days is still too high compared with the real medicane climatology but, as it was discussed previously, high values of GENPDF only mean an increased probability of medicane development, not its effective occurrence.

The selection of the medicane-favourable situations from GCM have been done following a few steps: firstly, a list locating (in time and space) values higher than q99ERA40 is created. Secondly, we keep only those events where these high values are extended (at least) over 40 continuous grid points. They will represent pro-medicane environments of large-enough entity. Finally, the time and position of the highest GENPDF value for each event will be selected as the central time and position of the MM5 simulation. As it was concluded in Chapter 3, the highest values of GENPDF are usually found within 12 hours of medicane maximum development. By centering the 48 h simulation at that time, a possible medicane can be fully developed during the simulation. Fig. 5.4.1 is an example of how the selection area and simulation domain are adequate for capturing the event. This selection is done using the four GCMs in both historical (20C3M) and future (SRESA2) scenarios. Note that MIROC 3.2 (Hasumi and Emori, 2004) is also included in the list of GCMs.

Following these criteria, the total number of simulations carried out is shown in Table 5.1. As it was expected, the highest number of simulations (i.e. largest probability of medicane development) is found during the cold season, specially in October. In summer, just a few possible events are detected. The monthly distribution is consistent with the results obtained in previous chapters.

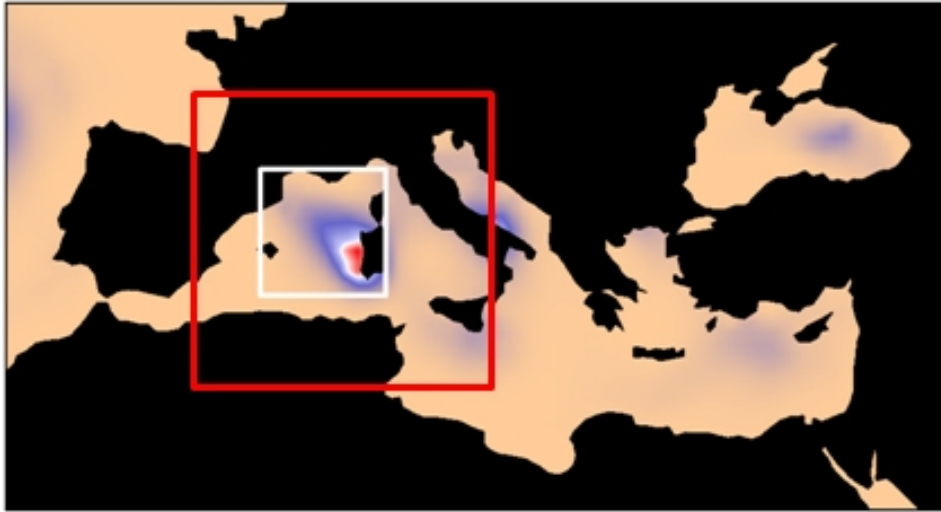


Figure 5.4.1: Example of the distribution of GENPDF values during a medicane event (color scale is orientative). The white square is centered at the position of the mature medicane event according to satellite images. The red square is the area where the simulation will be run, centered on the maximum value.

Our objective selection procedure has been tested using the ERA-40 data for the medicanes listed in Table 2.1. Just 1 out of 11 events has not been detected (the M02 case). Three examples of well detected and simulated medicanes are shown in Fig. 5.4.2. In the first example, the medicane is not intense, but a symmetric low pressure center with an isolated warm core is distinguished. In the other two examples, the simulated medicanes are more clear.

Finally, all the simulations listed in Table 5.1 have been manually checked for the presence of medicanes: axi-symmetrical and isolated intense low pressure centers with a warm core. Figure 5.4.3 reveals how the number of effective situations is reduced. Continuous lines in this figure represent the number of events simulated (Table 5.1) and the bars, the number of medicanes found in each month. In the latter case, events are also divided depending on which basin they belong to: Western (longitude up to 10 E), Central (between 10-20 E) and Eastern (higher than 20 E). Western and Central basins are the zones where most of the medicanes are simulated. However, these numbers are too high compared with other studies (Cavicchia et al., 2014a,b; Tous and Romero, 2013). It could be that our detection procedure is not well-tuned or that the model simulates false alarm events. For this reason, a mitigation of the false alarm ratio is introduced using ERA-40 results.

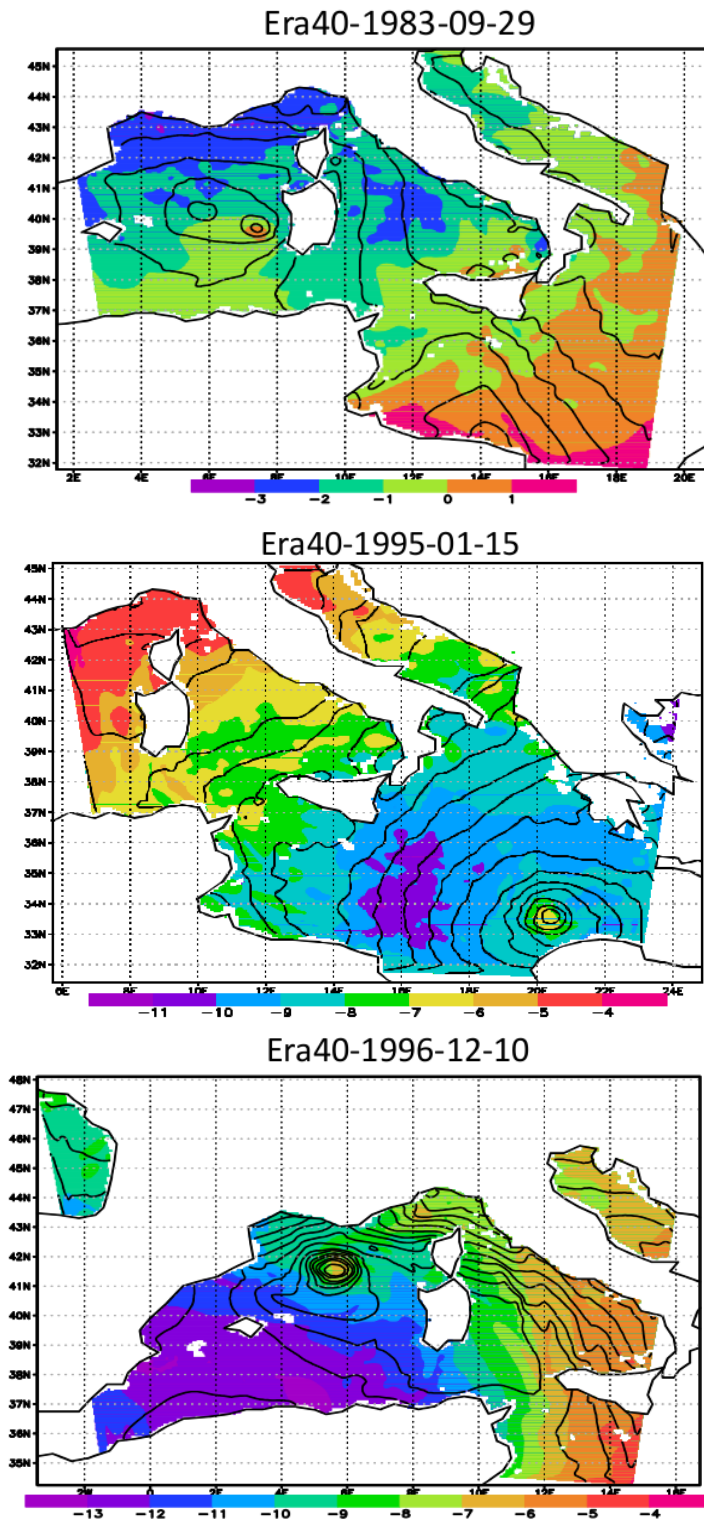


Figure 5.4.2: Examples of real medicane environments detected and simulated by following the objective algorithm described in the text (top M01, middle M06 and bottom M09). MSLP in contour lines and temperature at 700 hPa in colors ($^{\circ}\text{C}$).

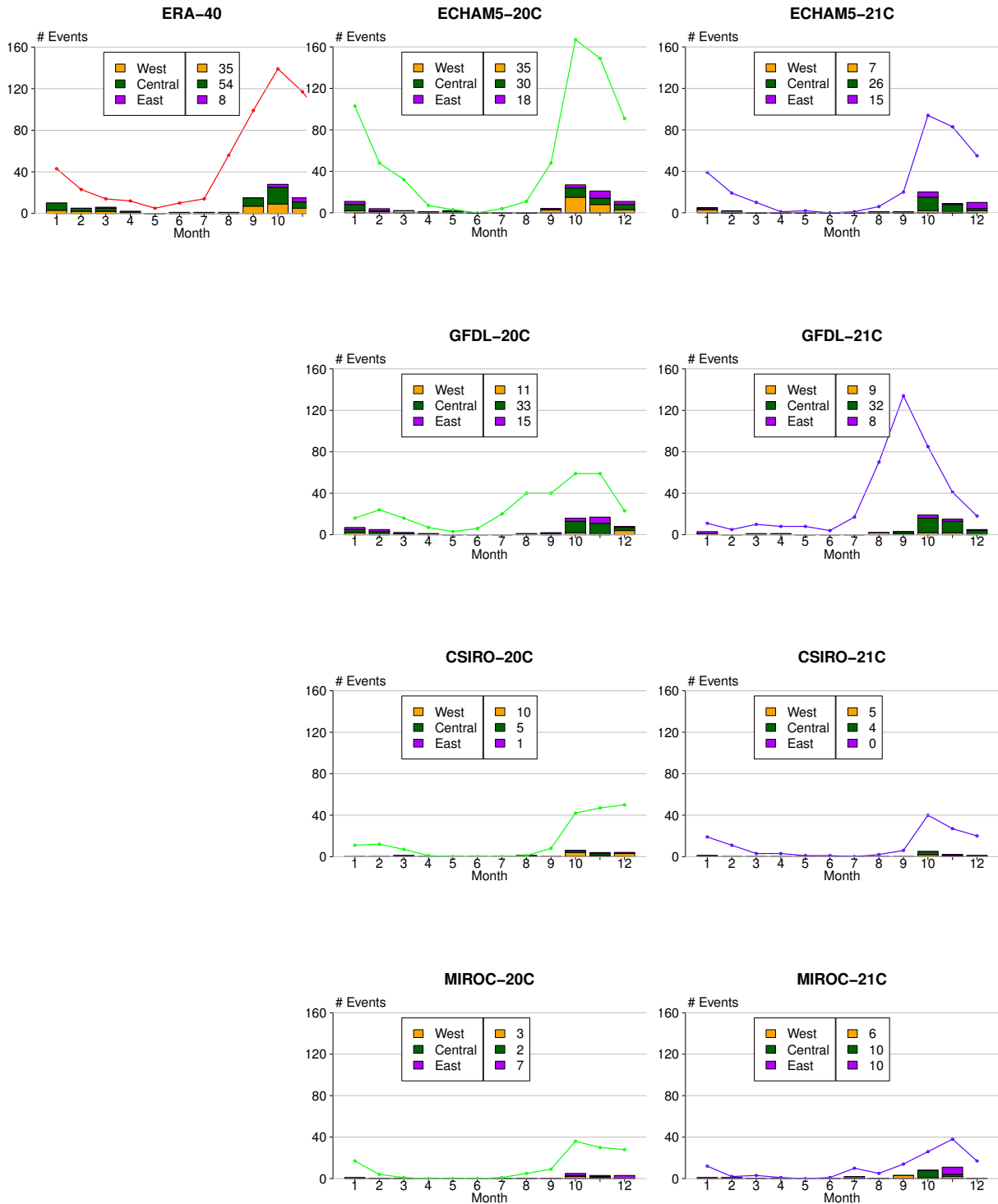


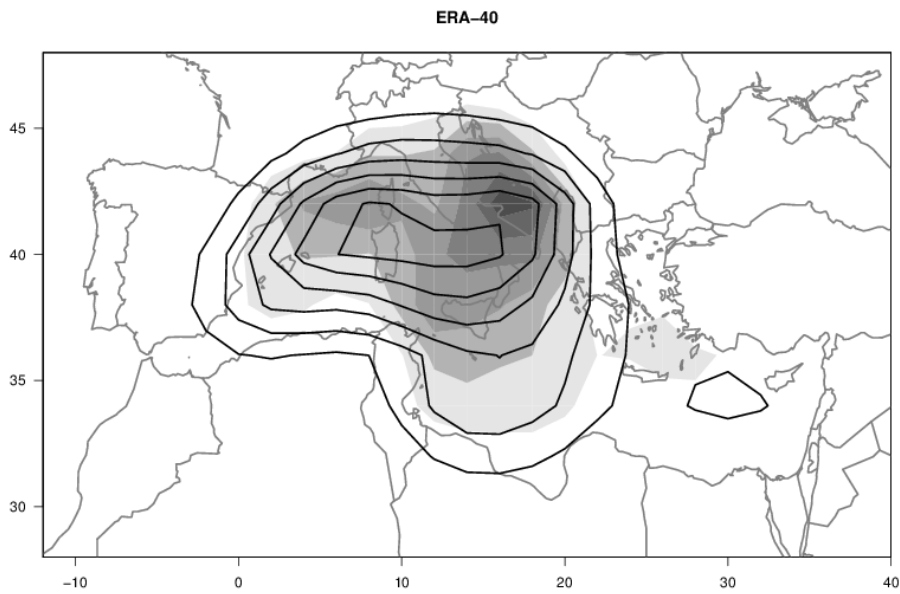
Figure 5.4.3: For each model and scenario, continuous line represents the number of simulated events in each month. Bars are the number of medicanes found in the performed simulations for the Western (orange), Central (green) and Eastern (purple) basins. The total number of medicanes for each basin is labeled.

	1	2	3	4	5	6	7	8	9	10	11	12	TOTAL
ERA-40	43	23	14	12	5	10	14	56	99	139	117	86	618
ECHAM5 - 20C	103	48	32	7	3	0	4	11	48	167	149	91	663
ECHAM5 - 21C	39	19	10	1	2	0	1	6	20	94	83	55	330
GFDL - 20C	16	24	16	7	3	6	20	40	40	59	59	23	313
GFDL - 21C	11	5	10	8	8	4	17	90	134	85	41	19	411
CSIRO - 20C	12	12	7	1	0	0	0	1	8	41	48	50	180
CSIRO - 21C	19	11	3	3	1	1	0	2	6	41	27	20	134
MIROC - 20C	17	4	1	0	0	0	1	5	9	36	30	28	131
MIROC - 21C	12	2	3	1	0	1	10	5	14	26	38	17	129

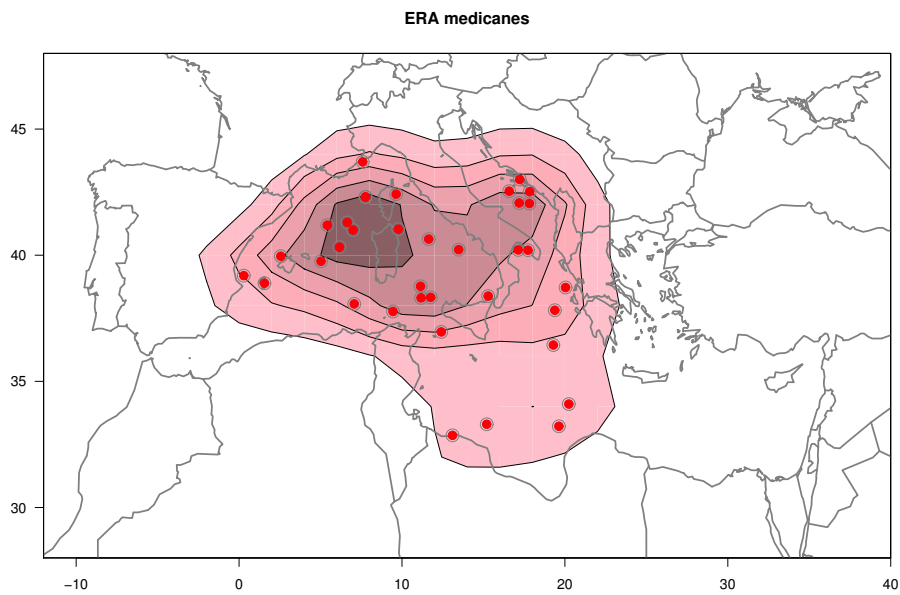
Table 5.1: Number of medicane favourable situations that are simulated, per month, depending on the model and scenario.

Specifically, since ERA-40 results can be validated using satellite images, this information becomes very useful for our purposes. In this case, we are more permissive than in Chapter 2 regarding the medicane criteria: we do not take into consideration the lifetime, and the presence of a small disturbance or cyclone with some sort of eye and continuous cloud cover around the center will be enough to pass the filter because these features will be assumed to prove medicane genesis. By this way, 36 events are found in satellite images (15 events in the Western, 19 in the Central and 2 in the Eastern basins), which represent a 37.1% of the simulated events and an “observed” frequency of 1.8 medicanes per year, similar to the 1.6 value established by Cavicchia et al. (2014a) or 2 medicanes/year assumed by Romero and Emanuel (2013).

The distribution of simulated and observed medicane events for the ERA-40 data set is illustrated in Fig. 5.4.4. In addition to the aforementioned reduction, the area with observed maximum risk is displaced westwards, more specifically, from the Adriatic Sea to the Gulf of Lion-Genoa. All the satellite events are situated in the Western and Central Mediterranean, and any simulated medicane close to Cyprus has not been confirmed in



(a) In shaded, density (events per century in a square of $2^\circ \times 2^\circ$ lat-lon) of performed simulations every 20, starting at 20. In contours, density of resulting medicanes every 2, starting at 2.



(b) Dots represent the position of confirmed medicanes in satellite images, and shaded, their spatial distribution (events per century in a square of $2^\circ \times 2^\circ$ lat-lon).

Figure 5.4.4: Spatial distribution of medicane risk based on the ERA-40 data.

satellite images. Therefore, a correction factor of 0.371 will be uniformly applied to the statistical results of all models and scenarios to produce our final results.

5.5 Results for the present and future climate

After applying the correction factor, Fig. 5.5.1 shows medicane risk maps for ECHAM5, GFDL, CSIRO and MIROC models using historical (20C) and future (21C) climate conditions. ECHAM5, GFDL and CSIRO present a future reduction of events in the amount of 42%, 17% and 43%, respectively. These values are consistent with the results presented by Cavicchia et al. (2014a), who concluded a decrease of about 20-60% depending on the emission scenario after applying dynamical downscaling to a global climate model, and with Romero and Emanuel (2013), who indicate reductions ranging from 10% to 40% depending on the GCM used.

ECHAM5 exhibits the the most similar results (both in total values and spatial distributions) with ERA-40 (compare Fig 5.5.1 with Fig. 5.4.4). For this reason, it is the model that will provide, “a priori”, most credible results. In this case, a frequency of 1.5 medicanes per year is obtained using historical conditions. These events mostly occur in the Western basin, although the maximum density is not as concentrated and it is situated slightly more to the south than in ERA-40. In the future, the amount of medicanes is reduced and its distribution moved to the East, with the maximum found near South Italy. The density of medicanes seems to increase somewhat close to the Turkish coast.

GFDL frequency of medicanes in the present climate is about 1 event per year, situating the probability maximum between the Italian and Greek coasts (5 events per century in an area of 2°x2° lat-lon, as in ERA-40). This model locates most of the events in the Central area of the Mediterranean. The western incidence seems clearly underestimated, thus shifting eastwards the general pattern. Another significant maximum is located close to Cyprus. In the future, although the number of events in both models is similar, the reduction in the frequency of medicanes is lower than in ECHAM5 (and CSIRO). The shape of the distribution does not change significantly comparing with the historical one, except for the East notorious maximum, which disappears.

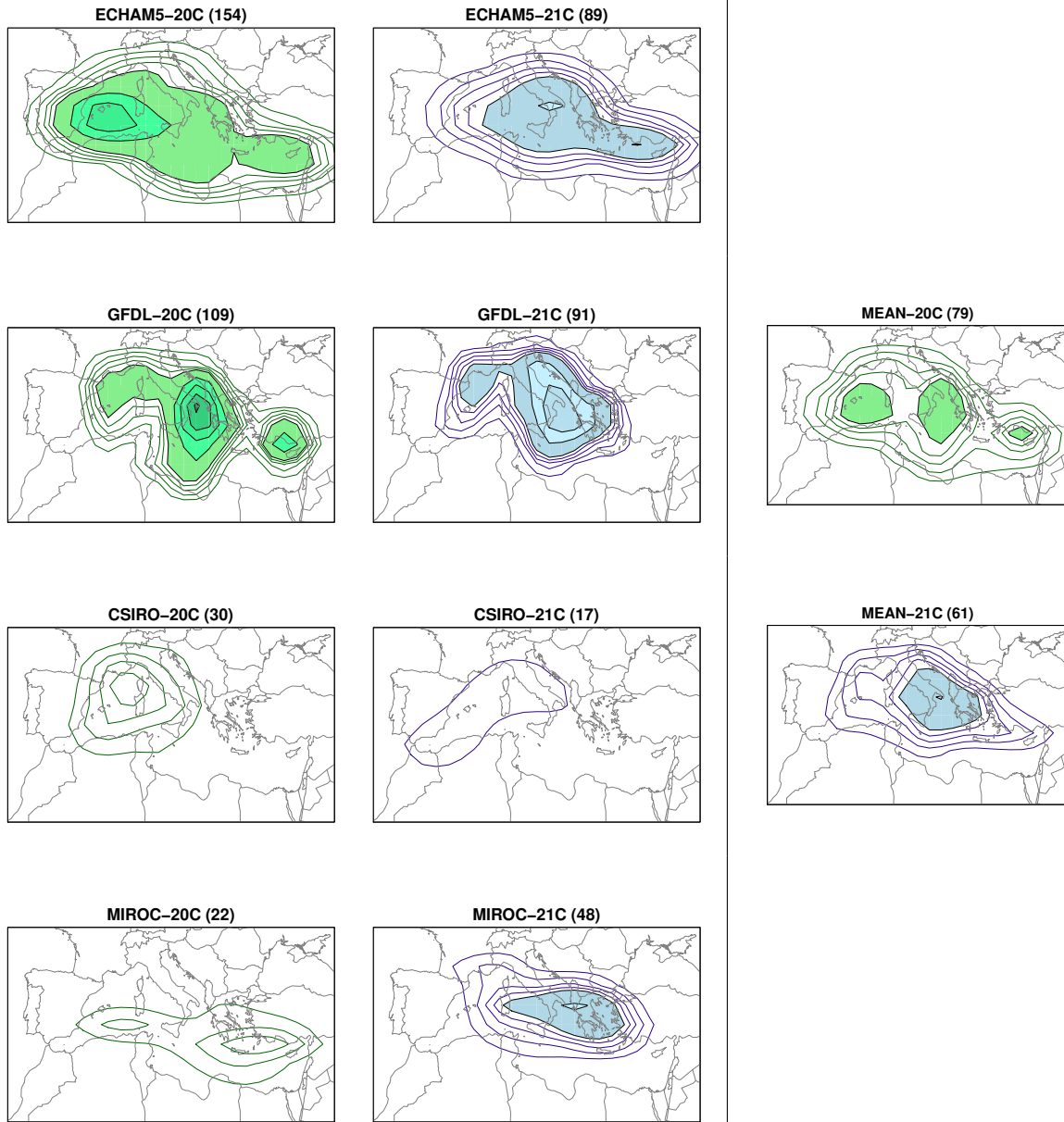


Figure 5.5.1: Left: Medicane risk density map for ECHAM5, GFDL, CSIRO and MIROC models using present (20C) and future (21C) climate conditions, in units of number of events per century in a square $2^\circ \times 2^\circ$ lat-lon. Line contours correspond to values every 0.2, starting at 0.2, and colored areas every 1. Right: GCM-Mean risk map values. Green and blue colors for present and future climate conditions, respectively.

CSIRO displays very low frequency values (0.3 events per year), but it situates the maximum density (close to 1 event per century/ $2^{\circ}\times 2^{\circ}$) to the west of Corsica, as in the ERA-40 distribution. Central events are not well represented in this model. In the future, the reduction in the number of events occurs with a similar ratio than in ECHAM5. The spatial distribution of events changes but it keeps the maximum incidence in the western and north-central areas.

Finally, MIROC model presents a very different behavior. First, the frequency of medicanes in this model is the lowest (about 1 event every 5 years) in the historical scenario, locating the maximum density of events in the Eastern basin, between Greek and Turkish coasts. The northern parts of the Central and Western basins are severely underrepresented, specially comparing with ERA-40 data. In the future scenario, MIROC is the only evaluated model in this study whose frequency of medicane events is increased (+117%). The maximum density is moved to the east of Greece.

5.6 Conclusions

The capability of the MM5 model for medicane analysis, using a resolution of 7.5 km and low resolution inputs has been proved. This fact allowed us to use a collection of GCMs to evaluate the present and future medicane risk, both from the frequency and spatial distribution points of view. The dynamical downscaling was applied just in areas with a high potential risk to develop medicanes, identified in terms of high values of the GENPDF index. These pro-medicane environments are mostly located in the center and west of the Mediterranean and during the cold seasons (autumn and winter).

After detecting medicane-like features in some of these simulations, ERA-40 results have been checked using satellite images in order to evaluate the false alarm ratio (62.9%), with reference to an “observed” frequency of 1.8 cases per year, similar to that estimated by other authors. This ratio is used to adjust the GCMs-derived statistics, resulting in diverse frequency values for the historical climate scenario, from 0.2 to 1.5 events per year. Preferential areas are not clear and depend on the model: ECHAM5, GFDL and CSIRO situate most of medicanes in Western and Central Mediterranean areas but MIROC does it in the Eastern basin. In general, all models tend to overestimate medicanes in the Eastern Mediterranean.

In future scenarios, the frequency of pro-medicane environments is similar to the historical values in most models (except for ECHAM5, which shows an important reduction of -50%) but not the frequency of simulated storms. Three of the models used in this study (ECHAM5, GFDL and CSIRO) show a decrease in simulated medicane frequencies (20-40%), and only one (MIROC) exhibits an increase (more than double the frequency of the historical period). In general, medicane risk will increase specially towards the south-east of Italy, where most models present the major density of medicanes in future scenario (ensemble mean values, Fig 5.5.1). The similar frequency between present and future in pro-medicane areas but a different rate of simulated medicanes, reinforces the idea that the empirical index used in this thesis identifies just necessary but not sufficient conditions for the medicane development. Recall also that GENPDF parameter was designed for tropical regions. It would be advisable to study a reformulation of this index taking into account the Mediterranean specificities.

Chapter 6

High-resolution global climate model¹

In this study, a cyclone track algorithm is directly applied on global climate model data generated at high resolution (HRGCM): about 25 km in the horizontal over the Mediterranean region.

6.1 Data and methodology

6.1.1 The HadGEM3 climate model

The model used in this study is an N512 atmosphere-only configuration of the HadGEM3-GA3 Met Office Unified Model. The simulations were performed as part of the UPSCALE project (UK on PRACE - weather resolving Simulations of Climate for global Environmental risk), a collaborative project between the National Centre for Atmospheric Science-Climate (NCAS) at the University of Reading, and the UK Met Office Hadley Centre (Mizielinski et al., 2014). The N512 HadGEM3-GA3.0 model has a horizontal resolution of approximately 25 km and has 85 levels in the vertical. An ensemble of five historical and three future atmosphere-only simulations were performed. Historical

¹The content of this chapter is based on the paper Tous, M., G. Zappa, R. Romero, L. Shaffrey and P.-L. Vidale, *Projected changes in medicanes in the HadGEM3 N512 high-resolution global climate model*, Clim. Dyn. (Conditionally accepted). 2015.

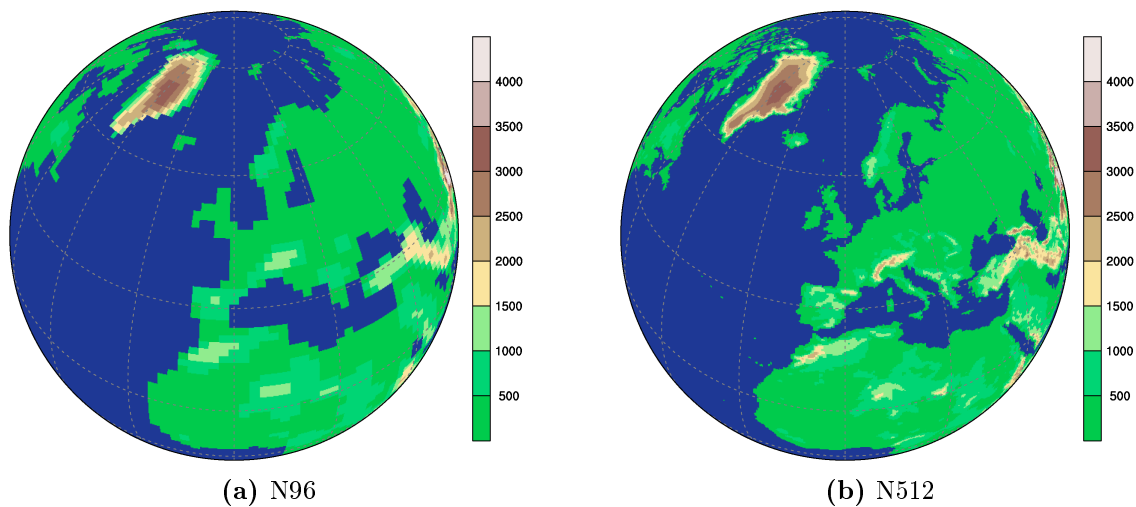


Figure 6.1.1: Illustration of grid resolutions N96 and N512 (approx. 150 and 25 km at mid-latitudes, respectively) showing the topography (height above sea level, in m) and coastline (ocean area for fractional land cover of less than 50%). (UPSCALE project website: <http://proj.badc.rl.ac.uk/upscale>).

simulations were forced with daily observed OSTIA SSTs (Donlon et al., 2012). SSTs for the future simulations were determined by adding to the OSTIA SSTs the change in SSTs from the RCP8.5 HadGEM2-ES coupled climate simulations performed for IPCC AR5. This study uses 26 years of output from one member of the historical ensemble and from one member of the future ensemble. Concentrations of carbon dioxide, methane, nitrous oxide, CFCs and HFCs were set to constant values (i.e. the mean values for 1980-2010 for the historical simulations and mean values of 2080-2110 for the future simulations). Model output is available at 6 h intervals.

To study the impact of resolution on the fidelity of climate model simulations, a series of other experiments were performed in the UPSCALE project at the lower resolutions of N96 (150km) and N216 (60km). As shown in Fig. 6.1.1, the importance of increasing the resolution in the global model becomes evident, especially around the topographically-complex Mediterranean basin. In this study, only the N512 simulations are considered but the other simulations have been investigated in other studies (e.g. Demory et al., 2014).

Previous studies have determined that intense baroclinic Mediterranean cyclones are most frequent in winter (Campins et al., 2011). Medicanes are also more frequent in winter and autumn than in the warm seasons (Tous and Romero, 2013). Subsequently, the cyclone season studied here has been defined from June to May. Thus, we use data from June 1985 to May 2011 for the historical period, and from June 2085 to May 2111 for the future period.

6.1.2 Cyclone tracking algorithm

The cyclone tracking is based on the objective feature-algorithm of Hodges (1994; 1995; 1999). The tracking algorithm has been used in previous studies analyzing the dynamics of tropical and extratropical cyclones, including polar lows (Hoskins and Hodges, 2002; Strachan and Demory, 2013; Zappa et al., 2014), the ability of climate models to represent storm tracks (Greeves et al., 2007; Catto et al., 2010; Zappa et al., 2013) and characterising their future response to climate change (Bengtsson et al., 2006; Catto et al., 2011; Roberts et al., 2015).

The algorithm locates vorticity centers at 850 hPa calculated from instantaneous wind fields. The vorticity fields used in this study have been filtered by a T40-T100 spectral filter in order to differentiate small-scale medicanes from large-scale Rossby waves. This filtering was also used to investigate the representation of polar lows in ECMWF operational reanalyses and the ERA-Interim reanalysis (Zappa et al., 2014). This filtering seems appropriate given the results of Picornell et al. (2001), where most of the cyclones found in the western Mediterranean have a radius between 150 and 350 km, with mean radius of 236 km. Moreover, the radius of medicanes have not been observed to be greater than this mean value.

Cyclone centers are identified as relative maxima in these vorticity fields exceeding an intensity of $2 \cdot 10^{-5} \text{s}^{-1}$. The tracks of the cyclones are determined by minimizing a cost function in the track smoothness (Hodges, 1999). Further conditions include: i) restricting the search region to the Mediterranean Sea plus the nearest sector of the Atlantic ocean (lat: 25N-50N; lon: 20W-50E); ii) including only cyclones with a minimum lifetime of 12 hours and iii) cyclones require a minimum in mean sea level pressure (MSLP) closely located (≤ 200 km) to the relative maximum of vorticity. The location of the MSLP

minimum is where the detected cyclone center is positioned. Only the part of the track with minimum MSLP is retained. For the medicane risk assessment in present and future climate conditions (Sections 6.3 and 6.4), some additional specific criteria will be used in the cyclone identification and tracking algorithm.

6.2 Climatology of mesocyclones in the Mediterranean

Mediterranean mesocyclone climatology from the N512 HadGEM3 historical simulation is qualitatively evaluated using the MEDEX cyclone climatology. The MEDEX climatology is based on ERA-40 reanalysis (September 1957 to August 2002, at 6h intervals) and describes the climatology of surface cyclones and their three-dimensional structure. The methodology is detailed in Picornell et al. (2001) (hereafter, P2001) and the main results are contained in Campins et al. (2011) (hereafter, C2011). In the P2001 and C2011 climatologies, the method used can be summarized in three main steps: first, surface cyclones are detected from MSLP fields; next, the vertical extension of a surface cyclone is explored by means of the geopotential height at different isobaric levels; and finally, each cyclone center is tracked in time. In C2011, 81762 cyclonic centers were detected (i.e. an average of 1817 centers per year). These centers tend to be preferentially located near Cyprus and the gulf of Genoa (see Fig. 2 in C2011).

Figure 6.2.1 shows the annual mean spatial distribution of mesocyclone feature density in the N512 HadGEM3 historical simulation. The main centre of cyclonic activity is found in the gulf of Genoa, with an average frequency of 40-50 cyclone centers per year, which is comparable to the 37.4 cyclones per year found in C2011. There is another maximum situated south of the Pyrenees, which is similar to P2001. Finally, the other notable maximum found over Cyprus in C2011 is not apparent in the HadGEM3 model. One explanation for this omission is that cyclones in this area are usually shallow and thus may not be reflected as vorticity maxima at 850 hPa. Nevertheless, a small maximum of cyclonic activity appears over the Turkish Southern coast, which is located further south than the Aegean Sea maximum in C2011. In summary, the spatial distribution of mesocyclones is qualitatively similar to that seen in the MEDEX climatology.

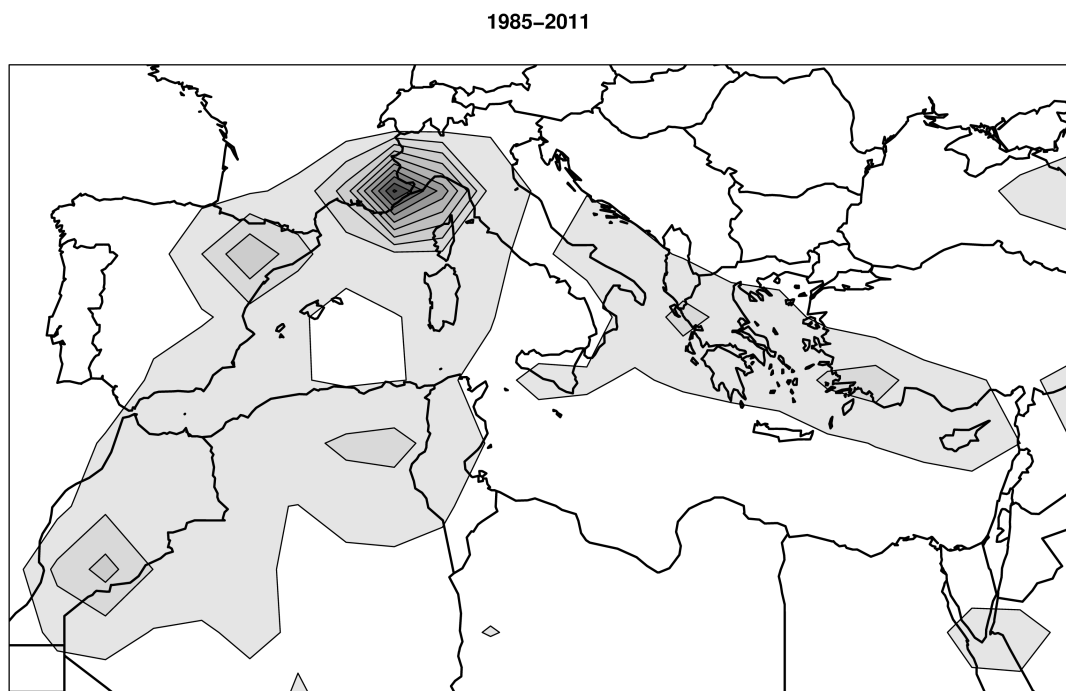


Figure 6.2.1: Density of cyclone centres per year in the N512 HadGEM3 historical simulation. Contours at every 5 minimum pressure centers per year, calculated in $2.25^\circ \times 2.25^\circ$ lat-lon boxes.

6.3 Medicane assessment: present climate

Medicanes are identified from the full set of mesocyclone tracks by applying further criteria on the lifetime, thermal structure and humidity associated to the tracks. In particular, the lifetime of the track is required to be 12 hours or longer, corresponding to at least 2 timesteps of the N512 HadGEM3 output. To capture the warm core of medicanes, the area averaged temperature within a 50 km radius centred on the MSLP minimum is required to be 1.5K warmer than the mean temperature in a larger 200 km radius area average. The choice of the 1.5K threshold follows the observation of 1.5-3.5 K warm core anomalies at mid-tropospheric levels seen in several simulated medicane events (Tous et al., 2013). Furthermore, as medicanes are associated with very moist or saturated environments, the area averaged relative humidity within 100 km radius from the MSLP minimum is requested to be greater than 70% at both 600 hPa and 850 hPa. Both the warm core and relative humidity conditions need to be satisfied for at least one time step. We find that 65 cyclone tracks satisfy the above criteria for medicane identification in the 26 years of the historical climate simulation. A visual inspection of these cases qualitatively confirms that the identified tracks show medicane-like features, and two of them are examined here in more detail in Figs. 6.3.1 and 6.3.2.

A number of medicanes have been visually inspected to assess the extent to which HadGEM3 can capture the observed structure. The first considered event (labeled MED1) forms in the Balearic Islands region between the end of October and the beginning of November. The MSLP spatial map (see Fig. 6.3.1) shows that the medicane is characterized by an isolated pressure minimum, with a high degree of rotational symmetry and a warm core. In particular, the 850 hPa temperature at the cyclone centre is found more than 3 degrees warmer than that of the surrounding environment. The near surface wind speeds in the vicinity of the low pressure reach 24.6 m s^{-1} (which is close to force 10 in the Beaufort scale). The temporal evolution of the MSLP minimum (Fig. 6.3.2) shows a remarkably large and sudden MSLP drop (21.7 hPa in 6 hours) which is also associated with a 30% increase of the maximum surface windspeed in the vicinity of the track (i.e. within a radius of 300 km from the MSLP minimum). This is a manifestation of the rapid growth rate expected in this kind of storm, although we do not have evidence of such large values in the few documented medicanes.

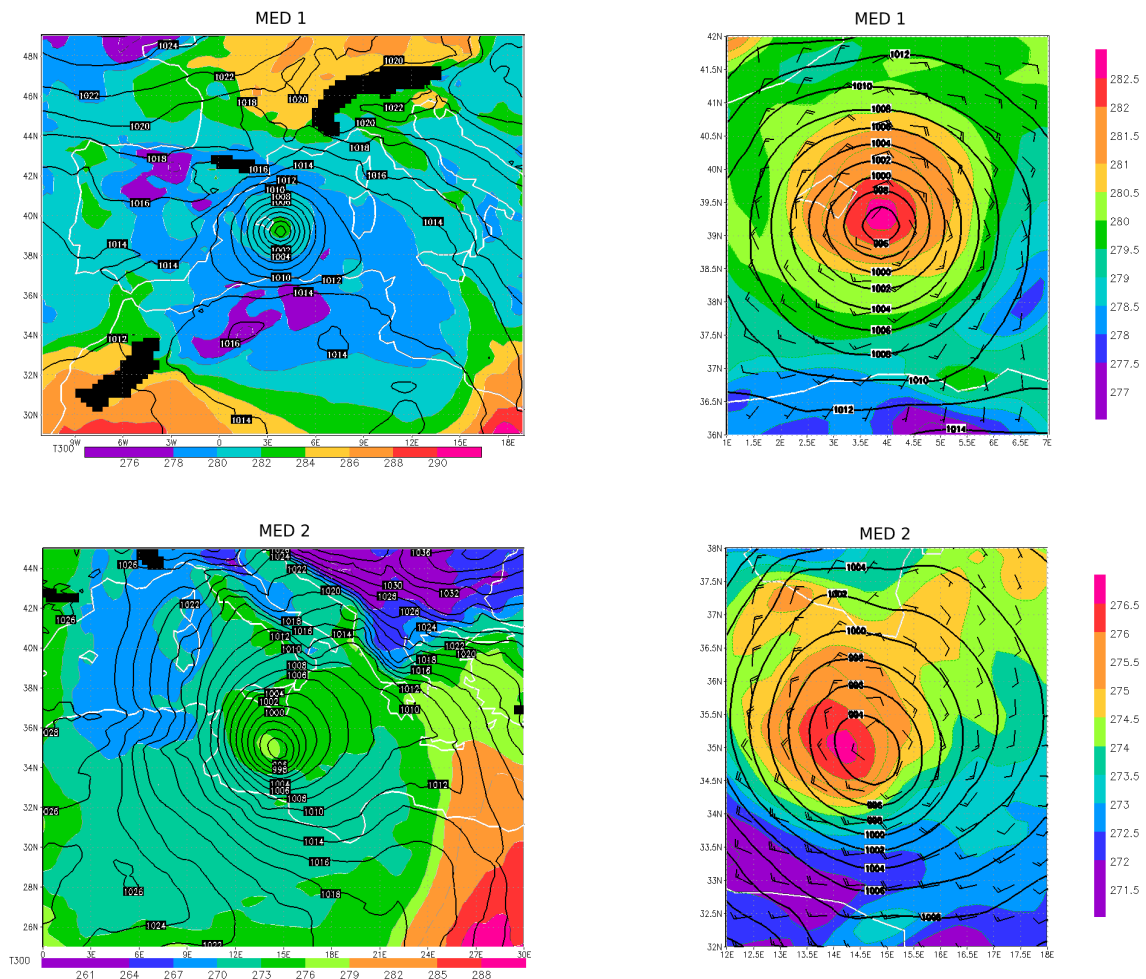


Figure 6.3.1: Spatial structure of two medicanes (top: MED1, bottom: MED2) identified in the N512 HadGEM3 historical simulation. The figures on the left (shaded contours represent temperature at 850 hPa level in K, and continuous contours, mslp in hPa) provide a description of the medicane positions in the Mediterranean basin, and those on the right (adding also winds at 10m) provide a more detailed analysis of their structure.

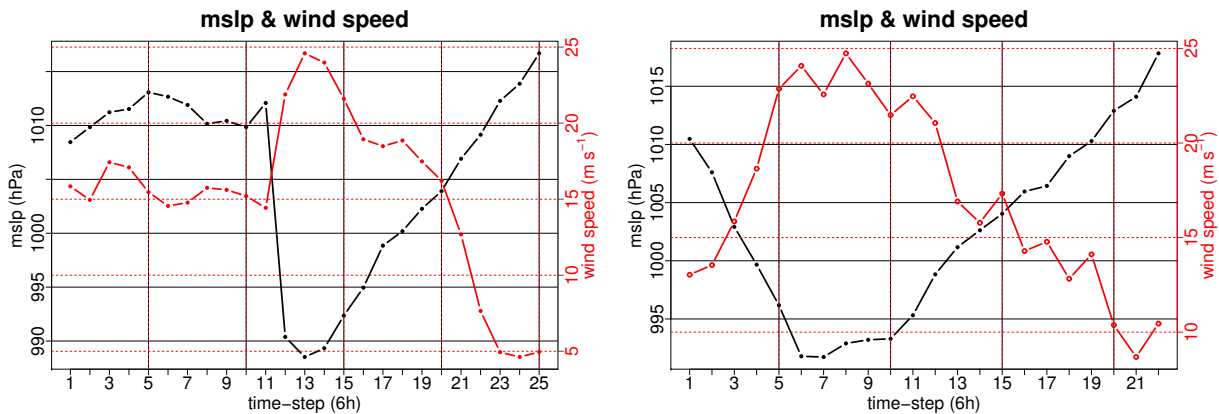


Figure 6.3.2: Lifecycle of the minimum Mslp (black dots, hPa) and maximum surface wind speed (white dots m s^{-1}) for two identified medicanes in the present day climate (left: MED1; right: MED2).

The second event (MED2) occurs to the south of Sicily in the month of February. Although it does not look as isolated from its parent cyclonic disturbance as MED1, it evolves independently from the general circulation. Symmetry and warm core attributes are also clear in MED2. MSLP minimum drops 18.7 hPa in 5 timesteps (30 hours) and the associated winds reach 24.7 m s^{-1} , which are a clear indication of the severity of the event. Growth rates of this magnitude are typically found in simulations of case studies, like in Tous et al. (2013).

Previous studies (as Cavicchia et al., 2014a; Romero and Emanuel, 2013) have determined a frequency of 1.5-2 medicane events per year, although not all of them exhibit a clearly visible tropical cyclone like structure in the infrared channel in the satellite images (Tous and Romero, 2013). Therefore, 65 medicanes in 26 years is only slightly higher than the expected frequency of occurrence of medicanes. This seems reasonable considering that we are examining a domain which marginally extends over the Atlantic ocean and it is slightly larger than in previous studies (Fig. 6.4.2).

Observational studies have found that medicanes tend to primarily form during the cold seasons (winter and autumn) because this is when cold air intrusions, in comparison with a warm Mediterranean, tend to occur. These temperature contrasts are associated with large surface heat fluxes out of the seas which help to sustain medicane development (Tous

et al., 2013). Fig.6.3.3 shows the monthly frequency distribution of the 65 identified medicanes (represented by light gray bars) in the N512 HadGEM3 historical simulation. Consistent with observations, medicanes are primarily identified in the cold season. No events are detected by the identification and tracking algorithm in the summer months, and only a few are identified in late spring. Note that the strong seasonality in medicanes formation is not found in the total set of cyclone tracks (dark bars in Fig.6.3.3) which are almost constant in number throughout the annual cycle.

The spatial distribution of the identified medicanes in the N512 HadGEM3 historical simulation (Fig.6.3.3) shows that a larger number of medicanes is detected south of the Gulf of Lion-Genoa and south of Sicily. This result is qualitatively consistent with the spatial distribution of observed medicanes found in previous studies (Cavicchia et al., 2014a; Tous and Romero, 2013). In the N512 HadGEM3 historical simulation, medicanes-like cyclones are also identified in the Black Sea. Although medicanes are even less frequent in this area, some cases have been occasionally reported. For example, Efimov et al. (2008) describes the formation of a tropical-like cyclone in the Black Sea region in September 2005. Medicanes identified in the Gulf of Biscay are also included among the objective tracks even though they are not conventional medicanes because they are not formed over the Mediterranean sea. Track points over North Africa are also of interest, showing that medicanes precursor low pressure centres can be initiated over the continent.

In summary, the identification and tracking algorithm applied to the 6 hourly N512 HadGEM3 historical simulation identified a set of Mediterranean mesoscale cyclones which share a number of similarities with the observed medicanes. In particular, the identified cyclones tend to have a similar frequency of occurrence, seasonality, spatial distribution and mesoscale structure relative to observed medicanes. Due to the insufficient resolution of the atmospheric reanalyses, it is not possible to quantitatively evaluate the biases of the model in the representation of medicanes by directly applying the identification and tracking algorithm to the reanalysis output. However, this qualitative assessment of the basic properties of medicanes gives us confidence that the 25 km resolution N512 HadGEM3 historical simulation is capable of generating medicanes-like cyclones. In the next section, we will use this methodology to assess the impact of climate change on medicanes frequency and intensity.

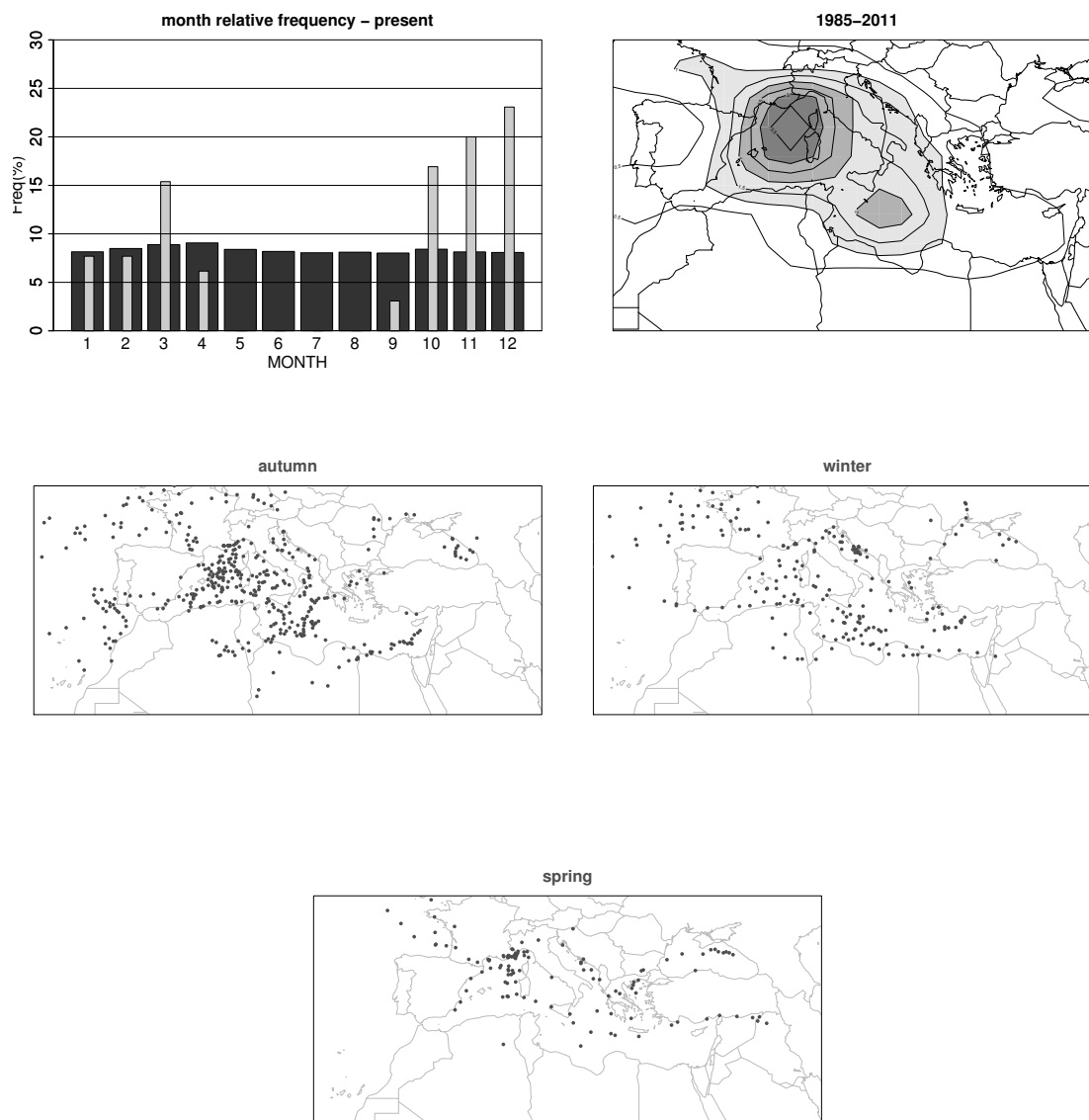


Figure 6.3.3: Monthly distribution and geographical density of the minimum pressure centers associated to medicanes for the N512 HadGEM3 historical simulation. In the histogram, dark bars represent all the minimum pressure centers and light bars those associated to medicanes. In the geographical total distribution, contours every 0.5 events per box of $2.5^\circ \times 2.5^\circ$, starting at 0.5.

	Minumum pressure centers	Number of cyclones	Medicane cyclone centers	Number of medicanes
1985-2011	147441	45013	826	65
2085-2111	145275	44291	716	44

Table 6.1: Total number of events counted by the objective tracking algorithm. “Minimum pressure centers”: Number of mslp minima accompanying the detected vorticity centers; “Number of cyclones”: Number of different cyclone tracks in which the mslp minima are grouped; “Medicane cyclone centers” and “Number of medicanes”: the subset of the events presenting a medicane phase.

6.4 Medicane assessment: future climate

The projected response of medicanes to climate change in the N512 HadGEM3 model is investigated by comparing the present day with the future climate simulations. The total number of cyclone tracks and medicanes identified by the tracking algorithm are summarised in Table 6.1. The total number of cyclone tracks is similar in the present and future scenarios, but the number of those satisfying the objective medicane criteria is reduced from 65 to 44 events, both in 26 years.

To assess the significance of the reduction in the number of identified medicanes, we model the frequency of medicanes as a Poisson distributed process. This is motivated by the low count number per year and the expectation that medicanes are dynamically independent, i.e. the formation of a medicane does not affect the probability of another medicane occurring at a later time. Using this approach, we find that the reduction in the number of medicanes is significant at the 6% level according to a two-tailed test on the Poisson mean. This reduction in the total number of medicanes (-30%) is consistent with previous studies. For example, Cavicchia et al. (2014b) found a reduction of about 20-60% depending on the emission scenario, by applying dynamical downscaling to a global climate model while Romero and Emanuel (2013) estimated a reduction of 10-40% depending on the GCM used. The projected changes in medicane frequency for individual seasons are presented in Fig. 6.4.1. The largest reductions occur in autumn (September-November) and spring (March-May), while small changes are found in winter (December-February). Although

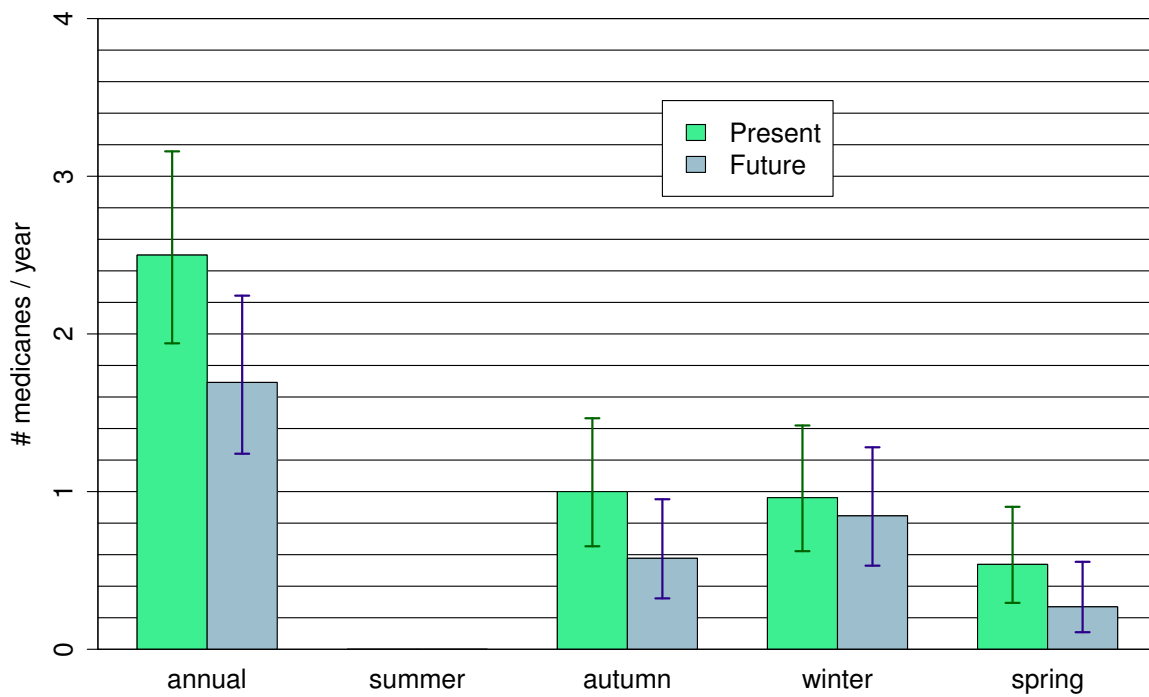


Figure 6.4.1: Annual and seasonal distribution of medicane events for the N512 HadGEM3 historical (green bars) and future climate (blue bars) simulations, showing Poisson distribution confidence intervals. Summer intervals are omitted because no medicanes are detected.

	mslp (hPa)			vorticity (10^{-5} s^{-1})			wind speed (m s^{-1})		
	1Q	mean	3Q	1Q	mean	3Q	1Q	mean	3Q
Present	985.1	992.7	1001.0	7.8	9.6	11.3	18.1	20.4	23.3
Future	993.4	998.0	1004.0	7.6	9.9	12.2	19.2	21.3	23.6
p-value (pres; fut)	0.01			0.61			0.16		

Table 6.2: Statistical results for the three most intense timesteps during the medicane phase: minimum mslp (hPa), maximum vorticity (10^{-5} s^{-1}) and maximum wind speed (m s^{-1}).

the significance of the changes in individual seasons is low (the p-values are 0.12 in autumn and 0.18 in spring), it suggests the active medicane season will tend to become more limited in winter, which is consistent with findings of Cavicchia et al. (2014a).

By inspecting the maximum near surface wind speed associated with medicanes, which is the parameter we adopt to characterize cyclone dynamical intensity, we find a slight tendency toward an intensification of medicanes under future climate conditions. For each medicane, the wind speed intensity is evaluated by considering the mean of the three maximum values of surface wind speed associated with the track. Using this approach, the mean wind speed intensity of medicanes is found to be 20.4 m s^{-1} in the present climate and 21.3 m s^{-1} in the future scenarios (see Table 6.2). The significance of the difference according to the Welch test is low (p-value 0.16), but it is consistent with findings from previous studies (Cavicchia et al., 2014b; Romero and Emanuel, 2013). Furthermore, the lifetime of the medicane tracks tends to increase in the future scenario from an average of 16 to 20 timesteps (see Table 6.3), and the number of time steps associated with intense surface wind speeds ($\text{Bft} \geq 8$) also increases from 5.4 to 7.2 time steps (significant at the 10% level according to the Welch test).

Figure 6.4.2 shows the spatial distribution of all the tracks associated with medicane events under the present and future climate simulations. Each dot represents a track point and its color the maximum surface windspeed associated with the track at that point. To analyse the medicane risk due to high wind speed, the contours represent the density distribution of the track points associated with strong wind speeds ($\text{Bft} > 8$). Although

	Cyclone lifetime steps (x 6h)			Cyclone lifetime steps (Bft \geq 8) (x 6h)		
	1Q	mean	3Q	1Q	mean	3Q
Present	11.0	16.2	21.0	2.0	5.4	8.0
Future	10.0	20.0	23.2	3.8	7.2	9.2
p-value (pres; fut)	0.13			0.08		

Table 6.3: Lifetimes steps (every 6 hours) for cyclones presenting a medicane phase, and the duration of their strong wind speeds (Bft \geq 8).

the total number of medicanes is projected to decrease in the future climate, the frequency of medicanes associated with intense wind speed becomes more frequent in the corridor between the Gulf of Genoa and south of Sicily. For example, in the Gulf of Genoa, the maximum density of medicanes in the historical simulation is about 34 cyclone centers per century per grid box of 2°x2°, while in the future this maximum density increases to about 51 cyclone centers per century. The other maximum located to the south of Sicily increases from 10 to 28 cyclones/(century,area). This suggests a possible future enhanced medicane risk in these areas.

6.5 Conclusions

A new medicane risk assessment taking into account the effects of climate change has been obtained in this chapter using a 25 km high resolution version of the Met Office HadGEM3 global climate model performed as part of the UPSCALE project. The high horizontal resolution allows medicane-like features to be represented. An objective tracking algorithm was applied to the model output, so that future changes in medicane frequency and intensity have been investigated.

The N512 HadGEM3 historical simulation has an adequate representation of general Mediterranean mesocyclones. The number of identified mesocyclones is similar to that found in two previous regional climatologies from the MEDEX project. The mesocyclone

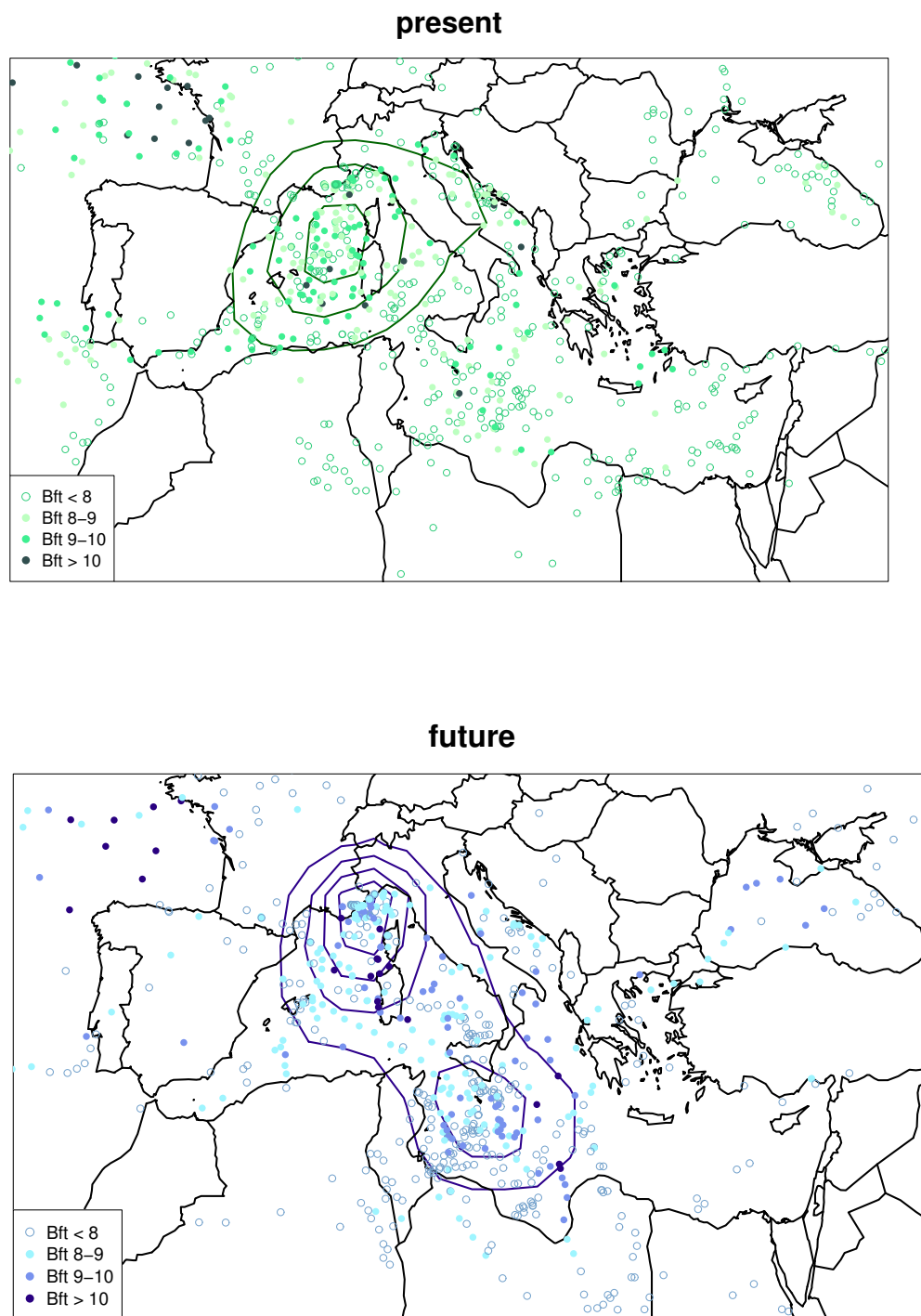


Figure 6.4.2: Spatial distribution of medicanes in the N512 HadGEM3 historical and future climate simulations as function of maximum surface wind speed (Beaufort scale). Contours every 10 intense medicane cyclone centers (with $\text{Bft} \geq 8$) per century in an area of $2^\circ \times 2^\circ$. Note some degree of overlap between different medicane positions (dots).

spatial distribution is also qualitatively consistent with these climatologies, although some discrepancies in the Eastern Mediterranean basin are identified. However, this is not an active area for medicanes.

The climatology of medicanes identified in the present day climate simulations reveals that the N512 HadGEM3 model is able to represent very intense cyclones with a warm core (the main features of medicanes). The temporal frequency and spatial distributions are also consistent with previous climatologies derived using different methods and data. Rapid intensification and strong surface wind speeds are evident for selected examples.

Future changes in the intensity and frequency of medicanes were assessed by applying the tracking method to a future N512 HadGEM3 simulation forced by the RCP8.5 emission scenario. The N512 HadGEM3 model projects that the number of medicanes will decrease in number (about -30%) but increase in lifetime and, possibly, wind speed under future climate conditions. Overall, this may lead areas such as the Gulf of Genoa and south of Sicily to be more at risk of the high windspeed generated by medicanes under future climate conditions. The general trend towards fewer medicanes but an enhanced risk of extreme winds is a common result in the existing literature on medicanes and climate change. This tendency would be a consequence of the projected increase of anticyclonic conditions over the Mediterranean region (e.g. Lionello et al. 2008). Although less frequent, mid-tropospheric cold air intrusions over the Mediterranean region would result in more effective environments for medicane intensification owing to the significantly warmer Mediterranean waters.

Part IV

CONCLUSIONS AND FURTHER WORK

Chapter 7

Conclusions

In this Thesis, we have focused on medicanes under two points of view: dynamically oriented climatologies of the meteorological environments associated to medicane development and maintenance, and quantitative assessments of medicane risk under present and future climate conditions.

The lack of meteorological observations over the Mediterranean Sea has motivated the need to build a database of medicane events using alternative methods. The list of medicanes presented in this Thesis, derived basically using satellite images and restricted criteria, provides a necessary base to grow learning about these rare but violent windstorms. In this way, 12 events have been subjectively detected during the period from 1982-2003, with all of them centered in the Central and Western Mediterranean regions and being more frequent in winter and autumn.

Due to the few number of events per year, the analysis of processes related with medicanes is difficult. Nevertheless, we have taken advantage from tropical cyclone studies to guide our medicane understanding. Reported similarities between tropical cyclones and medicanes suggest an analysis for the Mediterranean of the large-scale meteorological ingredients that are known to be associated with tropical cyclones. To better identify the very special conditions that medicanes require for their development, these large-scale meteorological parameters have been compared against the bulk of intense Mediterranean cyclones, typically baroclinic storms: the diabatic contribution to surface level equivalent potential temperature tendency, the sea surface temperature and an empirical index of

genesis of tropical cyclones have shown a modest performance. **High positive values of this diabatic contribution and a sea surface temperature greater than 15°C seem to be necessary for medicane development.** Although it has not been possible to establish a lower bound for the empirical index and it can not be used with the same interpretation than for tropical cyclones, the occurrence of medicane storms is related with high values of the index. This index has been proved useful to discriminate medicane genesis-prone environments in historical and future climate conditions.

Despite medicanes small size, mesoscale model runs at moderate horizontal resolutions (7.5 km) made with MM5 are able to simulate the formation of a subsynoptic cyclone and the general trajectory of the disturbance. For most of the cases a warm-core axi-symmetrical structure becomes evident in the simulations. The timing and precise details of the storm trajectories are shown to be more problematic when compared against the satellite images available for the events. On the other hand, a sensitivity analysis examining the role of the sea surface heat fluxes has been conducted: latent and sensible heat fluxes from the Mediterranean have been switched off during the simulations to explore the effects of these factors on the medicane trajectories and deepening rate. Results have shown **different roles of the surface heat fluxes on medicane properties** (intensification and track) depending on their magnitude and spatial distribution over the Mediterranean Sea. In this sense, three distinct patterns have been identified using the database of 12 events.

A substantial part of the Thesis deals with the problem of medicanes under climate change. Most global climate models do not have enough spatial resolution to adequately represent small features such as medicanes, and applying objective techniques to detect or track medicanes in these datasets is therefore not appropriate. For this reason, two novel and independent methods have been used: an oriented dynamical downscaling of a collection of GCMs, and the use of high-resolution global climate model data. The first method provides an ensemble of results based on GCMs also used for IPCC reports, and the horizontal resolution of the MM5 model (7.5 km) seems enough to resolve details of medicane structure. However, the concatenation of several filters in the decision of which environments are simulated, increases the risk of underresolving some medicane situations. On the contrary, the second method is a direct technique where a cyclone detection algorithm applied sequentially (with proper filtering of the input fields and selection criteria) allows the medicanes to show up naturally in a weather-resolving global climate model. Although this method operates at 25 km resolution, which is enough for

medicane representation (at least for the largest storms), the use of a single model impedes the evaluation of the uncertainties in medicane risk at the end of the century. In both methodologies, an initial test comparing results with historical climatologies have been provided.

The oriented dynamical downscaling consists in evaluating the medicane risk by analyzing only the areas and periods with high probability of genesis, improving the resolution in the selected area and forcing the boundaries with larger scale data. Results vary depending on the GCM used, but it seems that, for the historical period, the annual cycle (most events during the cold season: winter and autumn) and the preferred areas of development (Western and Central basins) are similar to other climatologies, like the database of observed events presented in this Thesis (Chapter 2) and other studies like Cavicchia et al. (2014a). In general, all models tend to overestimate medicanes in the Eastern Mediterranean. The second strategy to study medicane risk tendencies consists of applying a cyclone tracking algorithm to high resolution global model data provided by a N512 HadGEM3 simulation of the RCP 8.5 scenario. After a validation of the general Mediterranean cyclone climatology and of the ability of the model to represent very intense cyclones with a warm core (main features of medicanes), we showed that the temporal frequency and spatial distribution are also consistent with previous climatologies using different methods and data. Therefore, both methods have been proved useful to evaluate the future medicane risk.

With regard to the first method, most GCMs predict that the number of pro-medicane environments will keep similar in the future comparing with the historical data (with the cold season and western-central basins still as the most important). However, we project **a decrease in medicane frequencies (20-40%), and the south-east of Italy is presented as the area with the highest probability of medicane development.**

According to the second method, future medicanes also occur preferentially in the cold season. They tend to **decrease in number (-30%) but increase in intensity. The spatial distribution of medicanes becomes more concentrated in two areas: the Gulf of Lion-Genoa and the south of Sicily**, where the local frequency of events will increase by a factor of 1.6 and 2.1, respectively.

These general results are consistent between the two methods. **Both tend to decrease the number of medicanes in future scenarios but some of these scenarios**

show an increase in local frequencies due to the concentration of the risk area. Areas close to Italy have the highest probability of medicane occurrence (specially the south or south-east maritime areas), although the Gulf of Lion also presents high risk of events.

Chapter 8

Further work

A low number of medicanes has been reported historically. This led us to create our own database of events based on available satellite images and applying strict criteria. Despite this, the detection has been done subjectively, so there is not complete confidence in having captured all the medicanes or very similar storms. For this reason, once the criteria to discriminate medicanes from other cyclonic structures in satellite images will be completely defined, an automatic algorithm could be implemented and the database could be increased and be more robust. Phase space diagrams, like the one developed by Hart, can be a good choice to achieve such discrimination of cyclone type based on their thermodynamical attributes. This method evaluates if the cyclone is symmetric and has a warm core, two of the main characteristics of tropical cyclones (and medicanes). Actually, this procedure is accepted and used for tropical cyclones from some years ago. But because of the differences in size between tropical cyclones and medicanes, the scale and thresholds for the calculated relevant parameters should be readjusted for Mediterranean structures. Few authors like Miglietta et al. (2011); Cavicchia et al. (2014a); Picornell et al. (2014) and Picornell et al. (2014) have used this technique for medicanes, but in the first place there is not consensual criteria on which isobaric levels should be evaluated: Hart (2003), for tropical cyclones, and Miglietta et al. (2011) and Cavicchia et al. (2014a), for medicanes, consider the levels 900, 600 and 300 hPa, while Picornell et al. (2014), for medicanes, use 925, 700 and 400 hPa, arguing that medicanes are not usually as deep. Another unclarified point is the threshold of the so-called B parameter used to assess the symmetry of the cyclone: Hart (2003); Miglietta et al. (2011) and Cavicchia et al. (2014a) use $B < 10$ m/s,

and Picornell et al. (2014), $B < 7$ m/s. All medicane studies agree on reducing the radius of the calculations from 500 km (used in Hart, 2003) to 100 km, but the results are also sensitive to this parameter. For these reasons, if the database of events was larger, these parameters could be adjusted with more precision, allowing to implement more accurate differentiations of cyclones.

MM5 medicane simulations at 7.5 km horizontal resolution contain detailed information about the structure and evolution of these cyclones. Their analysis can provide useful information about similarities and differences with tropical cyclones, as well as more accurate thresholds of the environmental parameters linked to medicane development and maintenance. Furthermore, based on the model results, it would be possible to devise algorithms to calculate properties like the intensity of the wind speed given the environment of each cyclone. By this way, the estimation of how climate change would affect the risk of medicane events could be complemented. On the other hand, it has been shown many differences on Mediterranean cyclone climatologies depending on the GCM used to force the mesoscale simulations. Each global model has its pros and cons, but it is obvious they do not represent medicane distributions in the same manner. A quantitative evaluation of the reliability of GCMs to represent historical medicane occurrence could be useful in order to assign different weights to future climatic projected results. Therefore, GCMs yielding spatial and temporal medicane distributions closest to historical data would have more significance in for the future projections.

N512 HadGEM model is a high-resolution GCM with enough spatial resolution to represent medicane-like structures directly. In this Thesis, we have used one of its ensemble members to evaluate medicane risk in a future climate scenario. An extension of these results would be possible by analyzing the other members of the ensemble (4 more for the historical and 2 more for future climate conditions). As a result, uncertainties in future projected results could be calculated, improving the estimation of medicane risk tendencies at the end of the century.

Results from the first part of the Thesis (Chapter 3) have not been clear enough to permit the isolation of precise thresholds of the large-scale environmental parameters associated with medicanes (including the empirical index of genesis). In addition, a similar frequency between present and future of pro-medicane areas but a different rate of successful medicanes obtained by the oriented dynamical downscaling (Chapter 5) suggest that the empirical index as formulated here is not accurate enough to represent medicane genesis

probability. This index should be readjusted according to the medicane phenomenology and, also, using more appropriate pressure levels in its formulations (for example, using 850 and 400 hPa to express the wind shear of the environment).

The main goal of this Thesis has been to enhance the understanding of medicane development and contribute to improve medicane forecasts and climatic projections, thus helping to mitigate their present and future damaging effects. The methodologies used here can be also applied to other severe weather phenomena like heat waves, heavy rain and droughts. In this sense, the use of the new generation of GCMs available from CMIP5 and other future programs will become essential. This type of studies will serve to evaluate future impacts on nature, goods and humans exerted by extreme events and help to sustain better decisions and more effective plans of response.

Appendix

Synthetic generation of medicanes

Romero and Emanuel (2013) analyzed the medicane risk in a changing climate by applying a statistical- deterministic approach that entails the generation of thousands of synthetic storms, in order to provide a robust assessment of current and future risk functions. This method is based on the work described in Emanuel et al. (2006); Emanuel (2006) and extended in Emanuel et al. (2008), as a technique for deriving hurricane climatologies from global data provided by reanalysis or climate models.

As it is described in Emanuel's works, this approach uses thermodynamic and kinematic statistics derived from global gridded fields to produce a large number of synthetic tropical cyclones (this number is fixed by the researcher and for tropical cyclones is on the order of 10^3 - 10^4), and the storms statistics are then used to characterize the tropical cyclone climatology of the given global climate.

In first implementations, long-term records of tropical cyclones were used to build a space-time probability density of storm genesis. In the last version, this genesis estimate is replaced by a random distribution of weak warm-core vortices in space and time. These vortices play the role of a storm "seed" and its possible development, depending on environmental conditions, is evaluated in order to check if it can intensify up to tropical cyclone intensity or not. These random seeds are distributed uniformly everywhere and at all times, with associated environments consistent with the climatological statistics derived from reanalysis or GCM data: monthly means, variances and covariances of the relevant meteorological fields. Then, seeds are tracked according to the beta-and-advection model, that is, following a weighted mean environmental flow of the troposphere, plus a correction for the so-called "beta effect" owing to the Earth's curvature. Finally, the "Coupled Hurricane Intensity Prediction System" (CHIPS model) is run over each storm track producing the intensification (or not) of the storm, and

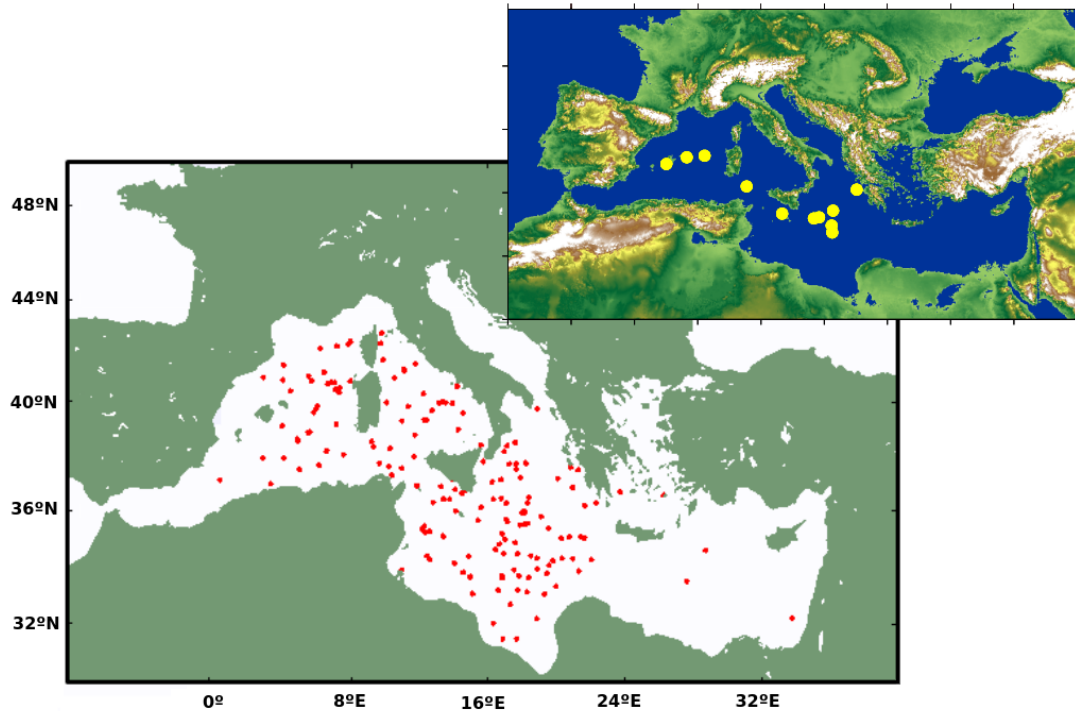


Figure A1: Top right: in yellow, the location of medicanes listed in Chapter 2. Left: in red, genesis position of synthetic tropical-like cyclones developed in CHIPS model.

providing also a radial distribution of winds. Only those events reaching a wind speed higher than a specific threshold are considered tropical cyclones (in this case, the threshold is fixed at 21 m/s) and the genesis is fixed at the time when the cyclone reaches 15 m/s. In this way, the distribution of hurricane winds at any point can be generated. By adjusting the number of seeds needed to get as many events as desired, spatial and temporal details of the frequency of tropical cyclones can be estimated.

Initially, this technique was tested by applying the last version directly to the Mediterranean basin after modifying internal parameterizations of the CHIPS model. For that test, we focused on December because it is the month when most medicanes are listed in our database (Chapter 2). We used ERA-40 data to calculate the statistical environmental parameters. Figure A1 represents a comparison of spatial distribution of tropical-like cyclone genesis over the Mediterranean Sea (forcing a total set of 200 events) with the location of observed medicanes according to satellite images. This distribution looks consistent with the historical climatology, with the maximum density to the south

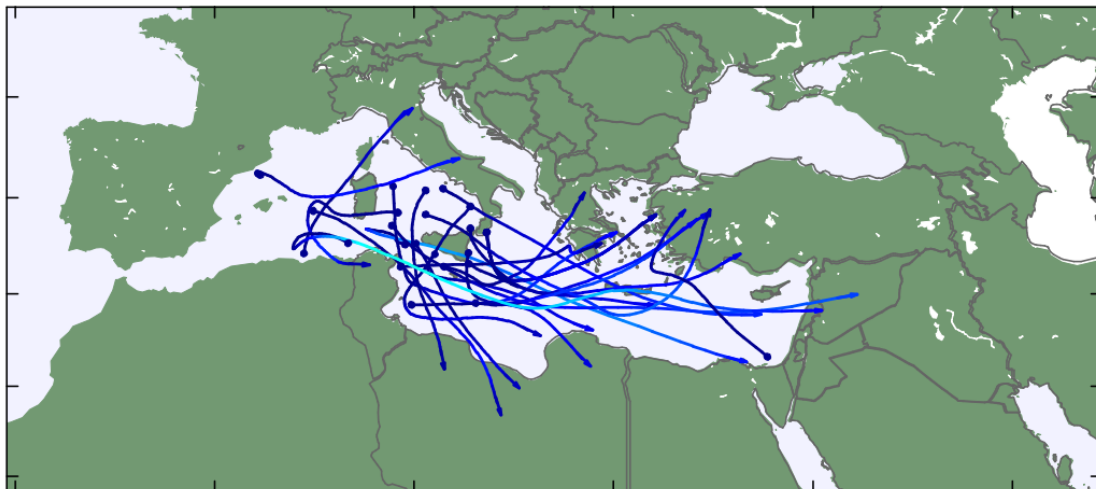


Figure A2: Tracking of 25 random synthetic events. Light blue represents higher wind speeds.

of Italy and also around Corsica and Sardinia. However, a more accurate analysis shows important deficiencies. First of all, as it is shown in Fig. A2, tracks are too long to be realistic, and the dominant displacement eastwards is not as clear in real medicane events. Also, the medicane risk in the western basin is underestimated. Furthermore, Fig. A3 represents the frequency distribution of the radius of maximum wind speed. According to this distribution, wind speed maxima are located in radius between 120 and 140 km. Since in satellite images medicanes have radius up to 150 km, synthetic events seem too large in size compared with observations.

Consequently, the original technique can not be applied directly to the Mediterranean and some changes are necessary. Among other problems, the generation of virtual environments based on “slow” climate statistics is not adequate: the use of monthly means is adequate for tropical environments, but time scales for the Mediterranean are faster owing to the mid-latitude dynamics. In addition, the characteristic modes of interrelation and organization of the thermodynamic and kinematic fields in space and time are more complex and they should be taken into account.

For these reasons, Romero and Emanuel (2013) introduced a new variant in the method. The joint spatial and temporal variability (and covariability) at synoptic scale of key ingredients for the environmental control of medicanes (potential intensity, mid-tropospheric temperature and humidity, and winds in the lower and

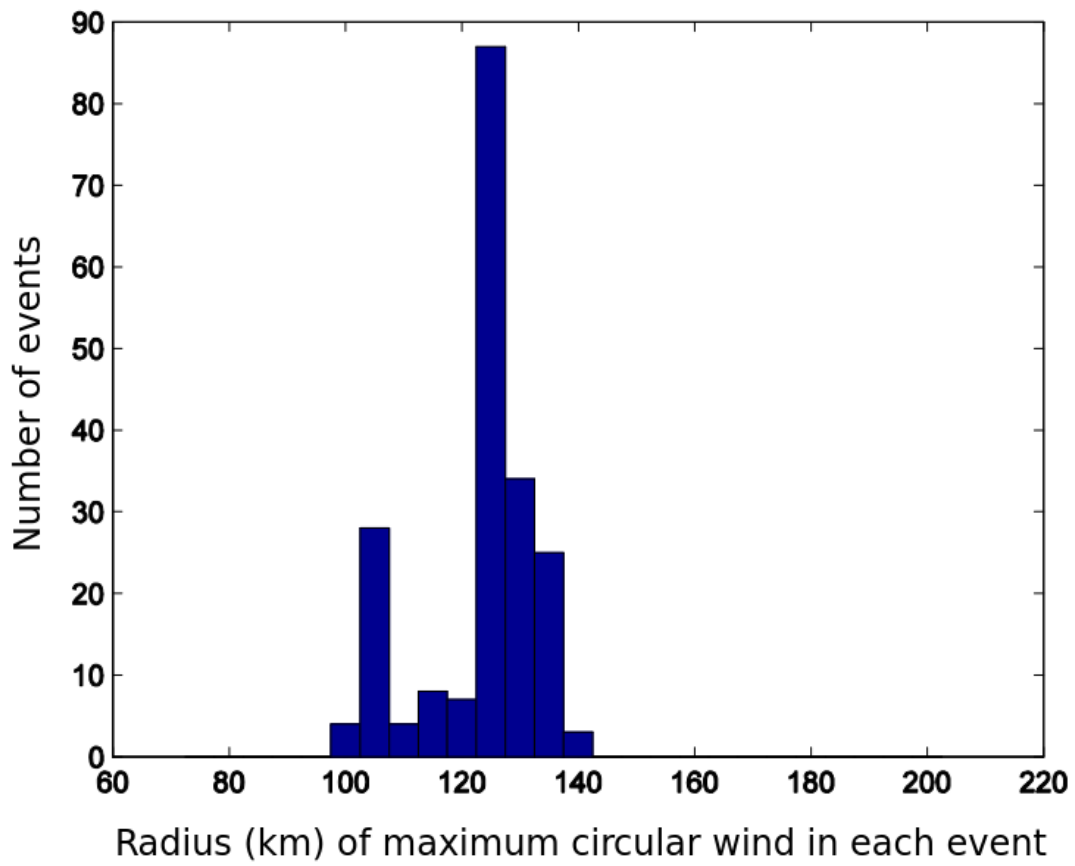


Figure A3: Number of events as function of the radius (km) of maximum circular wind.

upper troposphere) is converted via principal component analysis (PCA) into a new space represented by the resulting independent principal components (PCs). This decomposition is done for each month separately, and it is implemented in two sequential steps using daily gridded fields of these parameters. Analogues of observed synoptic states are generated by perturbing the corresponding set of PCs, and back in physical space, synthetic environments are effectively produced and finally simulated with the CHIPS model.

Nomenclature

Institutions

ECMWF	European Center for Medium-Range Weather Forecasts
FU Berlin	Free University of Berlin
NCAR	National Center for Atmospheric Research
NCAS	National Centre for Atmospheric Science-Climate
NCEP	National Centers for Environmental Prediction
NOAA	National Oceanic and Atmospheric Administration

Models

CHIPS	Coupled Hurricane Intensity Prediction System
CSIRO	Commonwealth Scientific and Industrial Research Organization (Australia)
ECHAM5	5th version of the European Centre Hamburg Model (Germany)
ERA-40	ECMWF Re-Analysis
GCM	Global Climate Model
GFDL	Geophysical Fluid Dynamics Laboratory (from NOAA, USA)
HRGCM	High Resolution Global Climate Model
MIROC	Model for Interdisciplinary Research on Climate (Japan)
RCM	Regional Climate Model
SRES	Special Report for Emission Scenarios
MM5	Fifth-Generation Penn State/NCAR Mesoscale Model

Parameters

θ_e	Equivalent potential temperature
AVOR850	Absolute vorticity calculated at 850 hPa level
CAPE	Convective available potential energy
C_D	Surface exchange coefficient for momentum
CISK	Conditional Inestability of the Second Kind
C_k	Surface exchange coefficient for enthalpy
DIAB1000	Diabatic contribution to surface level (1000 hPa) equivalent potential temperature tendency
GENPDF	Genesis potential index for Mediterranean cyclones, equivalent to GP
GENPDFmax	Maximum value of the GENPDF index in an averaging square
GP	Genesis Potential index for tropical cyclones (described by Emanuel, 2005a)
η	Absolute vorticity
H	Relative humidity
k	Specific humid enthalpy of overlaying air
k_0^*	Specific humid enthalpy at surface, supposed saturated and at the same temperature as the ocean
MAXWS	Idealized maximum surface wind speed for Mediterranean cyclones, equivalent to PI
MSLP	Mean sea level pressure
PI	Potential Intensity of a tropical cyclone, or theoretical maximum wind speed
PRWA	Precipitable water
RH600	Relative humidity calculated at 600 hPa level
SST	Sea Surface Temperature
SurFlux	Surface sensible and latent heat Fluxes
T_0	Averaged temperature of the upper area of the cyclone
T_S	Temperature of the sea surface (\equiv SST)
V_{pot}	Potential Intensity (\equiv PI)
V_{shear}	Vertical wind shear

VSHEAR8525 Tropospheric wind shear between 850 and 250 hPa levels

WISHE Wind-Induced Surface Heat Exchange

Abbreviations

20C Historical data from the 20th century

21C Projected data for the end of the 21th century

AR# #th IPCC Assessment report

C2001 Campins et al. (2001)

CFC Chlorofluorocarbon

CTR Numerical control simulations

FMG First Generation of Meteosat satellites

GTS Global Telecommunication System

HFC Hydrofluorocarbon

HRV High Resolution Visible

IFS Integrated Forecast System

IPCC Intergovernmental Panel on Climate Change

IR InfraRed

MED220 List of 220 cyclones that resemble a tropical cyclone in satellite images

MEDEX MEDiterranean EXperiment on cyclones that produce high impact weather

MRF Medium Range Forecast

NOFLX Numerical simulations without surface sensible and latent heat fluxes

NWP Numerical Weather Prediction

P2001 Picornell et al. (2001)

PBL Planetary Boundary Layer

PCA Principal component analysis

PC Principal components

q95ERA40 Quantile 95 for the GENPDF in ERA-40 data distribution

q99ERA40 Quantile 99 for the GENPDF in ERA-40 data distribution

RCP	Representative Concentration Pathways
TC	Tropical cyclone
UPSCALE	UK on PREACE- weather resolving Simulations of Climate for globAL Environmental risk
VIS	Visible
WV	Water vapor

Bibliography

Bibliography

- Alpert, P., Neeman, B., Shay-El, Y., 1990. Climatological analysis of Mediterranean cyclones using ECMWF data. *Tellus A* 42, 65–77.
- Bengtsson, L., Hodges, K.I., Roeckner, E., 2006. Storm tracks and climate change. *J. Clim.* 19, 3518–3543.
- Bister, M., Emanuel, K., 1998. Dissipative heating and hurricane intensity. *Meteor. Atmos. Physics* 50, 233–240.
- Bister, M., Emanuel, K., 2002. Low frequency variability of tropical cyclone potential intensity, 2, climatology for 1982-1995. *J. Geophys. Res.* 107, 4621.
- Businger, S., Reed, R., 1989. Cyclogenesis in cold air masses. *Wea. Forecasting* 20, 133–156.
- Buzzi, A., Richard, E., Romero, R., 2005. Summary report on MEDEX studies and scientific results on Mediterranean cyclones causing high impact weather. MEDEX Project .
- Buzzi, A., Tibaldi, S., 1978. Cyclogenesis in the lee of the Alps: A case study. *Q. J. R. Meteor. Soc.* 104, 271–287.
- Camargo, S., Emanuel, K., Sobel, A., 2007. Use of a genesis potential index to diagnose ENSO effects on tropical cyclone genesis. *J. Climate* 20, 4819–4834.
- Campins, J., Genovés, A., Picornell, M., Jansà, A., 2011. Climatology of Mediterranean cyclones using the ERA-40 dataset. *Int. J. Climatol.* 31, 1596–1614.
- Campins, J., Jansà, A., Genovés, A., 2006. Three-dimensional structure of Western Mediterranean cyclones. *Int. J. Climatol.* 26, 323–343.

- Catto, J., Shaffrey, L., Hodges, K., 2010. Can climate models capture the structure of extratropical cyclones? *J. Climate* 23, 1621–1635.
- Catto, J., Shaffrey, L., Hodges, K., 2011. Northern hemisphere extratropical cyclones in a warming climate in the HiGEM high-resolution climate model. *J. Climate* 24, 5336–5352.
- Cavicchia, L., von Storch, H., 2011. The simulation of the medicanes in a high-resolution regional climate model. *Clim. Dyn.* 39, 2273–2290.
- Cavicchia, L., von Storch, H., Gualdi, S., 2014a. A long-term climatology of medicanes. *Clim. Dyn.* , 1183–1195.
- Cavicchia, L., von Storch, H., Gualdi, S., 2014b. Mediterranean tropical-like cyclones in present and future climate. *J. Clim.* 27, 7493–7501.
- Charney, J., Eliassen, A., 1964. On the growth of the hurricane depression. *J. Atmos. Sci.* 21, 68–75.
- Delworth, T., Broccoli, A., Stouffer, R., Balaji, V., Beesley, J., Cooke, W., Dixon, K., Dunne, J., 2006. GFDL's CM2 global coupled climate models - Part 1: Formulation and simulation characteristics. *J. Clim.* 19. 643-674.
- Demory, M.E., Vidale, P., Roberts, M., Berrisford, P., Strachan, J., Schiemann, R., Mizielinski, M., 2014. The role of horizontal resolution in simulating drivers of the global hydrological cycle. *Clim. Dyn.* 42, 2201–2225.
- Donlon, C., Martin, M., Stark, K., Roberts-Jones, J., Fielder, E., Wimmer, W., 2012. The operational sea surface temperature and sea ice analysis (OSTIA) system. *Remote Sensing of Environment* 116, 140–158.
- Dudhia, J., 1993. A nonhydrostatic version of the Penn State/NCAR mesoscale model: Validation tests and simulation of an Atlantic cyclone and cold front. *Mon. Weather Rev.* 121, 1493–1513.
- Efimov, V., Stanichnyi, S., Shokurov, M., Yarovaya, D., 2008. Observations of a quasi-tropical cyclone over the Black Sea. *Russian Meteorology and Hydrology* 33, 233–239.
- Emanuel, K., 1986. An air-sea interaction theory for tropical cyclones. Part I: Steady-state maintenance. *J. Atmos. Sci.* 43, 585–604.

- Emanuel, K., 1987. The dependence of hurricane intensity on climate. *Nature* 326, 483–485.
- Emanuel, K., 2003. Tropical cyclones. *Annu. Rev. Earth Planet. Sci.* 31, 75–104.
- Emanuel, K., 2005a. Genesis and maintenance of Mediterranean hurricanes. *Adv. Geosc.* 2, 217–220.
- Emanuel, K., 2005b. Increasing destructiveness of tropical cyclones over the past 30 years. *Nature* 436, 686–688.
- Emanuel, K., 2006. Climate and tropical cyclone activity: A new model downscaling approach. *J. Climate* 19, 4797–4802.
- Emanuel, K., Nolan, D., 2004. Tropical cyclone activity and global climate. *Proc. of 26th Conference on Hurricanes and Tropical Meteorology*, 240–241 American Meteorological Society, Miami, FL.
- Emanuel, K., Ravela, S., Vivant, E., Risi, C., 2006. A statistical-deterministic approach to hurricane risk assessment. *Bull. Amer. Meteor. Soc.* 19, 299–314.
- Emanuel, K., Rotunno, R., 1989. Polar lows as Arctic hurricanes. *Tellus A* 41, 1–17.
- Emanuel, K., Sundararajan, R., Williams, J., 2008. Hurricanes and global warming: Results from downscaling IPCC AR4 simulations. *Bull. Amer. Meteor. Soc.* 89, 347–367.
- Ernest, J., Matson, M., 1983. A Mediterranean tropical storm? *Weather* 38, 332–337.
- Fita, L., Romero, R., Luque, A., Emanuel, K., Ramis, C., 2007. Analysis of the environments of seven Mediterranean tropical-like storms using an axisymmetric, nonhydrostatic, cloud resolving model. *Nat. Haz and Earth. Syst. Sci.* 7, 41–56.
- Gaertner, M., Jacob, D., Gil, V., Domínguez, M., Padorno, E., Sánchez, E., Castro, M., 2007. Tropical cyclones over the Mediterranean Sea in climate change simulations. *Geophys. Res. Lett.* , L14711.
- Genovés, A., Jansà, A., 1991. The use of potential vorticity maps in monitoring shallow and deep cyclogenesis in the Western Mediterranean. *WMO/TD* 420, 55–65.
- Gordon, H., Rotstayn, L., McGregor, J., Dix, M., Kowalczyk, E., O’Farrell, S., 2002. The CSIRO Mk3 Climate System Model. *Tech. Pap.* 60, CSIRO Atmospheric Research,

BIBLIOGRAPHY

- Aspendale, Victoria, Australia. , 134 ppCSIRO Atmospheric Research, Aspendale, Victoria, Australia.
- Gray, W., 1968. Global view of the origin of tropical disturbances and storms. *Mon. Wea. Rev.* 96, 669–700.
- Greeves, C., Pope, V., Stratton, R., Martin, G., 2007. Representation of Northern hemisphere winter storm tracks in climate models. *Clim. Dyn.* 28, 683–702.
- Grell, G., Dudhia, J., Stauffer, D., 1995. A description of the fifth-generation Penn State/NCAR mesoscale model (MM5). NCAR Tech. Note NCAR/TN-398+STR .
- Hart, R., 2003. A cyclone phase space derived from thermal wind and thermal asymmetry. *Mon. Wea. Rev.* 131, 585–616.
- Hasumi, H., Emori, S., 2004. K-1 Coupled GCM (MIROC) description K-1 Tech. Rep. Cent. for Clim. Syst. Res., Univ of Tokyo, Tokyo 1, pp. 34.
- Henderson-Sellers, A., Zhang, H., Berz, G., Emanuel, K., Gray, W., Landsea, C., Holland, G., Lighthill, J., Shieh, S.L., Webster, P., McGuffie, K., 1998. Tropical cyclones and global climate change: A post-IPCC assessment. *Bull. Amer. Meteor. Soc.* 79, 9–38.
- Hodges, K., 1994. A general method for tracking analysis and its applicaton to meteorological data. *Mon. Weather Rev.* 122, 2573–2586.
- Hodges, K., 1995. Feature tracking on the unit sphere. *Mon. Weather Rev.* 123, 3458–3465.
- Hodges, K., 1999. Adaptative constrains for feature tracking. *Mon. Weather Rev.* 127, 1362–1373.
- Homar, V., Romero, R., Stensrud, D., Ramis, C., Alonso, S., 2003. Numerical diagnosis of a small, quasi-tropical cyclone over the western Mediterranean: dynamical vs. boundary factors. *Q. J. R. Meteorol. Soc.* 129, 1469–1490.
- Hong, S., Pan, H., 1996. Nonlocal boundary layer vertical diffusion in a medium-range forecast model. *Mon. Weather Rev.* 124, 2322–2339.
- Hoskins, B., Hodges, K., 2002. New perspectives on the Northern Hemisphere Winter Storm Tracks. *J. Atmos. Sci.* 59, 1041–1061.

- IPCC, 2007. Climate change 2007: The physical science basis. contribution of working group i to the fourth assessment report of the intergovernmental panel on climate change. Solomon, S., D. Qin, M. Manning, Z. Chen, M. Marquis, K. B. Averyt, M. Tignor and H. L. Miller (eds) .
- IPCC, 2013. Climate change 2013: The physical science basis. contribution of working group i to the fifth assessment report of the intergovernmental panel on climate change. Stocker, T.F. and Qin, D. and Plattner, G.-K. and Tignor, M. and Allen, S.K. and Boschung, J. and Nauels, A. and Xia, Y. and Bex, V. and Midgley, P.M. (eds) .
- Jansà, A., 2003. Miniciclons a la mediterrània. IX Jornades de Meteorologia Eduard Fontserè, Associació Catalana de Meteorologia (ACAM), Barcelona , ISBN: 84-930328-6-7, 75-85.
- Jansà, A., Genovés, A., Picornell, M., Campins, J., R. Riosalido, O.C., 2001. Western mediterranean cyclones and heavy rain. part 2: Statistical approach. Meteorol. Appl. 8, 43-56.
- Kain, J., Fritsch, J., 1990. A one-dimensional entraining/detraining plume model and its application in convective parametrization. J. Atmos. Sci. 47, 2784-2802.
- Knutson, T., Mcbride, J., Chan, J., Emanuel, K., Holland, G., Landsea, C., Held, I., Kossin, J., Srivastava, A., Sugi, M., 2010. Tropical cyclones and climate change. Nat. Geosci 3, 157-163.
- Knutson, T., Toleya, R., 2004. Impact of co2-induced warming on simulated hurricane intensity and precipitation: Sensitive to the choice of climate model and convective parameterization. J. Clim. 17, 3477-3485.
- Lighthill, J., Holland, G., Gray, W., Landsea, C., Craig, G., Evans, J., Kurihara, Y., Guard, C., 1994. Global climate change and tropical cyclones. Bull. Amer. Meteor. Soc. 75, 2147-2157.
- Lionello, P., Boldrin, U., Giorgi, F., 2008. Future changes in cyclone climatology over europe as inferred from a regional climate simulation. Clim. Dyn. 30, 657-671.
- Martín, A., Romero, R., Homar, V., Luque, A., Alonso, S., Rigo, T., Llasat, M., 2007. Sensitivities of flash flood event over catalonia: A numerical analysis. Mon. Wea. Rev. 2, 651-669.

BIBLIOGRAPHY

- Mayençon, R., 1984. Warm core cyclones in the mediterranean. *Mariners Weather Log* 28, 6–9.
- Miglietta, M., A. Moscatello, D.C., Mannarini, G., Lacorata, G., Rotunno, R., 2011. Numerical analysis of a mediterranean 'hurricane' over south-eastern italy: Sensitivity experiments to sea surface temperature. *Atmos. Res.* 101, 412–426.
- Miller, B., 1958. On the maximum intensity of hurricanes. *J. Atmos. Sci.* 15, 184–195.
- Mizielinski, M.S., Roberts, M.J., Vidale, P.L., Schiemann, R., Demory, M., Strachan, J., Edwards, T., Stephens, A., Lawrence, B.N., Pritchard, M., Chiu, P., Iwi, A., Churchill, J., del Cano Novales, C., Kettleborough, J., Roseblade, W., Selwood, P., Foster, M., Glover, M., Malcolm, A., 2014. High-resolution global climate modelling: the upscale project, a large-simulation campaign. *Geosci. Model Dev* 7, 1629–1640.
- Nakicenovic, N.e.a., 2000. Emissions scenarios. A special report of working group III of the Intergovernmental Panel on Climate Change. Cambridge University Press , 599 pp.
- Nykjaer, L., 2009. Mediterranean sea surface warming 1985-2006. *Clim. Res.* 39, 11–17.
- Ooyama, K., 1964. A dynamical model for the study of tropical cyclone development. *Geophys. Int.* 4, 187–198.
- Palmén, E., 1948. On the formation and structure of tropical cyclones. *Geophysica* 3, 26–38.
- Pettersen, S., 1956. *Weather Analysis and Forecasting*. Mac Graw Hills Book Company .
- Picornell, M., Campins, J., Jansà, A., 2014. Detection and thermal description of medicanes from numerical simulation. *Nat. Hazards Earth Syst. Sci.* , 1059–1070.
- Picornell, M., Jansà, A., Genovés, A., Campins, J., 2001. Automated database of mesocyclones from the Hirlam(INM)-0.5 analyses in the western Mediterranean. *Int. J. Climatol.* , 335–354.
- Pytharoulis, I., Craig, G., Ballard, S., 1999. Study of the hurricane-like Mediterranean cyclone of January 1995. *Phys. Chem. Earth (B)* 24, 627–632.
- Pytharoulis, I., Craig, G., Ballard, S., 2000. The hurricane-like Mediterranean cyclone of January 1995. *Meteorol. Appl.* 7, 261–279.

- Reale, O., Atlas, R., 2001. Tropical cyclone-like vortices in the extratropics: observational evidence and synoptic analysis. *Weather Forecast* 16, 7–34.
- Reiter, E., 1975. Handbook for forecasters in the Mediterranean. Part 1: General description of the meteorological processes. Naval Environmental Research Facility, Monterey, California .
- Roberts, M., Vidale, P., Mizieliński, M., Demory, M.E., Schiemann, R., Strachan, J., Hodges, K., Bell, R., Camp, J., 2015. Tropical cyclones in the upscale ensemble of high-resolution global climate models. *J. Climate* 28, 574–596.
- Roeckner, E., Bäuml, G., Bonaventura, L., Brokopf, R., Esch, M., Giorgetta, M., Hagemann, S., Kirchner, I., Kornblüeh, L., Manzini, E., Rhodin, A., Schlese, U., Schulzweida, U., Tompkins, A., 2003. The atmospheric general circulation model ECHAM5, Part I: Model description. Max-Planck-Institute für Meteorologie , 127 pp.
- Romero, R., Emanuel, K., 2006. Space-time probability density of Mediterranean hurricane genesis in the light of an empirical tropical index. 5a Assembleia Luso-Espanhola de Geodesia e Geofisica .
- Romero, R., Emanuel, K., 2013. Mediane risk in a changing climate. *Journal of Geophysical Research: Atmospheres* 118, 5992–6001.
- Speranza, A., Buzzi, A., Trevisan, A., Malguzzi, P., 1985. A theory of deep cyclogenesis in the lee of the Alps. Part I: Modifications of baroclinic instability by localized topography. *J. Atmos. Sci.* 42, 1521–1535.
- Strachan, J., V.P.L.H.K.R.M., Demory, M.E., 2013. Investigating global tropical cyclone activity with a hierarchy of AGCMs: the role of model resolution. *Journal of Climate* 26, 7966–7980.
- Sumner, G., Romero, R., Homar, V., Ramis, C., Alonso, S., Zorita, E., 2003. An estimate of the effects of climatic change on the rainfall of Mediterranean Spain by the late 21st century. *Clim. Dyn.* 20, 789–805.
- Tous, M., Romero, R., 2013. Meteorological environments associated with mediane development. *Int. J. Climatol.* 33, 1–14.

BIBLIOGRAPHY

- Tous, M., Romero, R., Ramis, R., 2013. Surface heat fluxes influence on medicane trajectories and intensification. *Atmos. Res.* 123, 400–411.
- Trenberth, K., 2005. Uncertainty in hurricanes and global warming. *Science* 308, 1753–1754.
- Walsh, K., Giorgi, F., Coppola, E., 2014. Mediterranean warm-core cyclones in a warmer world. *Clim. Dyn.* 42, 1053–1066.
- Webster, P., Holland, G., Curry, J., Chang, H.R., 2005. Changes in tropical cyclone number, duration and intensity in a warming environment. *Science* 309, 1844–1846.
- Wernli, H., Schwierz, C., 2006. Surface cyclones in the ERA-40 dataset (1958-2001). Part I: novel identification method and global climatology. *J. Atmos. Sci.* 63, 2486–2507.
- Zappa, G., Shaffrey, L., Hodges, K., 2013. The ability of CMIP5 models to simulate north atlantic extratropical cyclones. *J. Climate* 26, 5379–5396.
- Zappa, G., Shaffrey, L., Hodges, K., 2014. Can polar lows be objectively identified and tracked in the ECMWF operational analysis and the ERA-Interim reanalysis? *Mon. Wea. Rev.* 142, 2596–2608.

